

AL-FARABI KAZAKH NATIONAL UNIVERSITY

FACULTY OF PHYSICS AND TECHNOLOGY

**ASKAROVA A.S., BOLEGENOVA S.A.,
BOLEGENOVA S.A.**

**3D SIMULATION OF REACTIVE FLOTATIONS
IN COMBUSTION CHAMBERS**

STUDENT TRAINING MANUAL

Almaty 2018

UDC 532.5:532.135

*Recommended for publication by the Scientific Council
of the Faculty of Physics and Technology
and RISO of Al-Farabi Kazakh National University*

A u t h o r s:

Askarova A.S., Bolegenova S.A., Bolegenova S.A.

R e v i e w e r s:

*Doctor of technical sciences, professor A.B. Ustimenko
Doctor of physics and mathematics, professor M.E. Abishev*

3D simulation of reactive flows in combustion chambers. Student Training Manual. /A.S.Askarova, S.A.Bolegenova, Bolegenova S.A. Almaty: Al-Farabi KazNU, 2018. – p.158.

The manual is devoted to the 3-dimensional computer simulation of heat and mass transfer processes in the combustion of Ekibastuz coal in the steam boilers furnaces, describes physical and mathematical models of the task in hand, as well as methods for solving equations describing the three-dimensional process of convective heat and mass transfer during solid fuel combustion in a pulverized one, taking into account radiative transport and multiphasal nature of the medium.

The manual is primarily intended for master's students of the Department of Thermophysics, Standardization and Metrology, but it can also be helpful for students, postgraduate and PhD students.

© Al-Farabi KazNU, 2018.

TABLE OF CONTENTS

Introduction.....	4
1 Basic equations and description of their solution method	10
1.1 Simulation of two-phase flotation.....	13
1.2 Heat exchange by emission.....	14
1.3 Transfer Equations Solution method.....	25
1.4 Obtaining difference equations using control volume approach.....	27
1.5 Pressure calculation.....	36
1.6 Initial and boundary conditions.....	38
1.7 Simulation of chemical reactions.....	46
2 Heat and mass transfer during the combustion of pulverized coal in a simulator with tangential feed.....	56
2.1 Basic characteristics of the model.....	58
2.2 Analysis of main results.....	66
3 Analysis of heat and mass transfer processes in solid fuel combustion in industrial boilers using the example of Pavlodar TPP.....	80
3.1 Initial data for simulation of Ekibastuz coal combustion (boiler BKZ - 420).....	80
3.2 Numerical study results.....	83
3.3 Results of the study of the effect of operating parameters on heat and mass transfer in the combustion chamber.....	96
4 Simulation of optimal combustion modes for pulverized coal fuel using the example of Ekibastuz GRES.....	104
4.1 About the problem of reduction of nitrogen oxides NO _x	104
4.2 Characteristics of furnace chamber of PK-39 boiler	108
4.3 Results of numerical experiment.....	115
References.....	134

INTRODUCTION

The relevance of simulation of convective heat and mass transfer processes in reactive environments in combustion chambers and the growing attention of the world public to such studies can be explained by the fact that with the growth of industrial production there has been a heavy increase in the amount of pollutants entering the biosphere.

Many countries, including Kazakhstan, have faced the task of regulating the quality of the environment in connection with damage to nature caused by human activities.

In the cities of Kazakhstan, atmospheric air is polluted with many harmful ingredients; this problem is especially pressing for the city of Almaty, where high level of pollution is contributed to by total emissions from motor transport, industrial enterprises, and unique geographical conditions of the city. Among the thermal power sources, the main share of emissions falls on large sources of district heat supply: CHPP, GRES of different levels, district plants houses, etc.

About 30% of the produced fuel is used for the production of electricity in our republic, more than 40% goes to the production of heat, or almost 3/4 of fuel is used for these purposes. Participation of energy companies in environmental pollution by fuel combustion products and solid wastes is significant, and these primarily include power plants that operate on solid fuels and are the main source of air, water and soil pollution.

Heat-and-power engineering of Kazakhstan is focused on the use of high-ash coals, mainly the Ekibastuz-basin, where low-cost coals are mined by the open-pit mining. As a result of the adopted technology for the extraction of high ash coals from Ekibastuz deposit and their use without prior enrichment, the natural environment experiences significant anthropogenic impact. Most of the coal, for example from Ekibastuz, is of

low quality due to high ash content. Ash is a mixture of minerals that are in a loose condition or associated with fuel. These non-combustible minerals are primarily composed of alkali and alkaline earth metal salts, silicon, iron, aluminum oxides, and calcium and magnesium sulfates. The presence of ash in the fuel adversely affects the quality of the fuel, because it reduces the amount of heat per unit mass of fuel. The smallest solids of ash are captured by the flue gas stream and carried away from the furnace, forming fly ash, which pollutes, and sometimes floods, the convective heating surface, reducing heat exchange. Ash content of domestic coals reaches 10-55%. Accordingly, dust content of flue gases also changes, reaching 60-70 g/m³ for high-ash coals.

The use of such coal is associated with a number of difficulties, such as unstable combustion, slagging problems, as well as protection of the atmosphere from ash, carbon monoxide (CO), nitrogen oxides (*NO* and *NO*₂), sulfur oxides (*SO*₂ and *SO*₃), hydrocarbons, compounds vanadium (mainly vanadium pentoxide), etc. However, it is known that Ekibastuz coal has such advantages as a low tendency to spontaneous combustion, a low sulfur S content, and boiler units operating on this coal have a high efficiency in pulverized coal combustion.

Analysis of steam generators operation using Ekibastuz coals shows that high ash content of fuel poses a number of additional requirements for the design of combustion and burner devices and has a significant effect on its combustion patterns in furnaces.

As is noted in the monograph of B.K. Aliyarov [1] by the beginning of the 1970's there were practically no detailed data on the ignition and burning out of the Ekibastuz coal flare, according to the objective laws of heat exchange in boiler units operating on these coals. The available results were obtained on different types of boiler units, at different times, by different

authors and have a limited nature. It became necessary to conduct a detailed theoretical and experimental study of the peculiar characteristics of burning of Ekibastuz coal in the furnace of a modern powerful steam generator.

While in the past in the energy sector only energy production was in the foreground, today it is necessary to comply with strict emission standards and at the same time use the equipment efficiently. It is extremely important to develop a process of "clean" coal combustion with the minimum possible emission of harmful substances, and therefore all design and operating parameters of such a process should be optimized.

To reduce the emission of harmful substances, primary measures are applied, such as a special fire mode that suppresses generation of harmful substances in the flame. There are also secondary measures, such as connection of the emission gas control system. Development of new ways to reduce emissions of harmful substances using these primary and secondary measures with the help of physical models, on the one hand, involves large costs related to physical experiment, on the other hand, this development can only provide suggestions to solve partial problems, as physical simulation of all the parallel processes in the combustion chamber and in smoke duct on scaled-down units is essentially impossible. This problem can only be solved on the basis of systematic analysis, physical and chemical modeling. In this connection, the numerical experiment becomes one of the most cost-effective and convenient methods for detailed analysis and a deeper understanding of complex physical and chemical phenomena taking place in the furnace units [2-4].

To apply mathematical simulation, it is necessary to have sufficiently accurate and informative content about regularities of occurrence of physical and chemical phenomena in conditions close to full-scale, as well as physical and kinetic param-

ters that can be obtained from experiments. The numerical experiment includes the following steps:

- formulation of the physical model of the phenomenon;
- refinement and formulation of the mathematical model (equations and boundary conditions), adequately describing the physical process we are studying;
- development of a numerical method and algorithm for solving problems or choosing a known method;
- development of a program or software package for solving the problem and processing results on a computer or choosing a well-known problem-oriented software package;
- debugging the selected software package and testing;
- solving a specific physical problem, analyzing and processing the results;
- comparison of the obtained results with physical experiment data obtained on full-size objects or on their scaled-down models, which will make it possible to make conclusion on the relevance of the mathematical model we have chosen to the real physical process under consideration and the need for some adjustment of the physical (mathematical) model or improvement of the numerical method and program;
- practical application of the results of computing experiment and optimization.

A rigorous mathematical description of all the processes taking place in steam generators, furnaces and reactors, together with modern computational algorithms using supercomputers, allow solving these problems for specific installations. Conducting numerical experiments with a purposeful change of these or other parameters proved to be more effective than labor-intensive and energy-intensive field experiments and allows one to flexibly intervene in the process at any stage of it, and in changing the design features of the apparatus without considerable costs. Using computer simulation, a wide

analysis of all characteristics of the future boiler can be made within a short time, which will save time and money, unlike construction of the current model, individual technical solutions can be tried out (camera configuration, layout and design of burner units), and environmental problems of emissions of harmful combustion products addressed.

A number of monographs [5-13] and reviews [14-18] are devoted to the problems of mathematical modeling of heat and mass transfer processes in the reacting media. In simulating processes in chemically reacting flows, simplified schemes are applied in a number of cases [19-29] or, which is very widely used in heating engineering to calculate free and wall jets and flows, the problem is solved in the boundary layer approximation [30-50]. Much attention is paid to the development of perfect models [51-58], for more accurate numerical experiments.

Analysis of works devoted to the combustion of solid fuels in combustion chambers of power plants has shown that they are mostly carried out on the assumption of one-dimensionality or two-dimensionality of motion, and in cases where three-dimensional transfer equations are used, only aerodynamics of the flow are considered. The energy crisis and environmental problems require effective management of the fuels combustion in boiler plants with the necessary impact on various parameters using a computer and predicting the impact result. Such optimization of processes occurring in combustion chambers has long been used in advanced economies of Europe and it can be carried out more efficiently using three-dimensional simulation.

Significant experience in optimizing the combustion of solid fuels in order to reduce the emission of harmful substances and increase the efficiency of power plants has been accumulated in Germany [59-69]. However, it should be noted that coal, which is used by German colleagues in power plants and, accordingly, in numerical simulation has very different charac-

teristics, for example, very low ash content (about several percent) compared to Kazakhstani coal (40-50%).

This manual presents the results of computing experiments on 3-dimensional computer simulations of heat and mass transfer processes in the combustion of Ekibastuz coal in steam boilers furnaces. Computing experiments were carried out both on the fire model of the boiler furnace unit with tangential fuel supply and in combustion chambers of operating boilers with vortex burners: BKZ-420 at Pavlodar CHPP and PK-39 Erma-kovskaya GRES. The obtained results will allow optimizing fuel combustion process with respect to efficiency and minimization of harmful emissions and creating cost-efficient power plants efficiently using "clean" coal.

Physical and mathematical models of the problem are described below, as well as methods for solving equations describing three-dimensional process of convective heat and mass transfer during combustion of solid fuel in a pulverized state, taking into account radiation transfer and multiphase nature of the medium.

1 BASIC EQUATIONS AND DESCRIPTION OF THEIR SOLUTION METHOD

Burning of a pulverized-coal torch under real conditions represents a physicochemical process that is complex for mathematical analysis. In furnace units designed to burn sputtered fuels in the air flow and flue gases, a number of interrelated phenomena occur: complex aerodynamics, the combustion of coal dust under conditions of changing gas temperature and concentration of chemical components therein, radiant heat exchange of the flare with the fencing surfaces of the furnace unit.

Simultaneously, the processes of formation of carbon, nitrogen and sulfur oxides, corrosive and carcinogenic substances take place; the mineral part of the fuel is converted.

The mathematical model for the description of reacting flows in combustion devices is a system of nonlinear partial differential equations consisting of the continuity equations, the motion of a viscous medium, the propagation of heat and diffusion for the components of the reaction mixture and reaction products, the equation of state and equations of chemical kinetics determining the intensity of nonlinear sources of energy and matter. In this case, unlike boundary layer equations, the solution of these equations requires set-up of boundary conditions at all boundaries of the region under review.

Numerical simulation of solid fuel combustion in a pulverized state was carried out on the basis of three-dimensional transport equations taking into account chemical reactions. In the general case of a 3-dimensional fluid motion with variable physical properties, the velocity, temperature, and concentration field is described by a differential equations system:

$$\frac{\partial \rho}{\partial t} = -\frac{\partial}{\partial x_i}(\rho u_i) \quad (1)$$

$$\frac{\partial}{\partial t}(\rho u_i) = -\frac{\partial}{\partial x_j}(\rho u_i u_j) + \frac{\partial}{\partial x_j}(\tau_{i,j}) - \frac{\partial p}{\partial x_j} + \rho f_i \quad (2)$$

$$\frac{\partial}{\partial t}(\rho h) = -\frac{\partial}{\partial x_i}(\rho u_i h) - \frac{\partial q_i^{res}}{\partial x_j} + \frac{\partial p}{\partial \tau} + u_i \frac{\partial p}{\partial x_i} + \tau_{ij} \frac{\partial u_j}{\partial x_i} + s_q \quad (3)$$

$$\frac{\partial}{\partial t}(\rho c_\beta) = -\frac{\partial}{\partial x_i}(\rho c_\beta u_i) + \frac{\partial \tilde{q}_i}{\partial x_i} + R_\beta, \quad (4)$$

where $i=1, 2, 3$; $j=1, 2, 3$; $\beta=1, 2, 3, \dots, N$.

To close them and simulate turbulent viscosity, we use k- ε turbulence model. The standard k- ε turbulence model includes two differential equations: the equation of transfer of the kinetic energy density of turbulence and the equation for dissipation rate of turbulent kinetic energy:

$$\frac{\partial}{\partial t}(\bar{\rho}k) = -\frac{\partial}{\partial x_i}(\overline{\rho u_i k}) + \frac{\partial}{\partial x_i} \left[\frac{\mu_{eff}}{\sigma_k} \frac{\partial k}{\partial x_i} \right] + n - \bar{\rho} \varepsilon \quad (5)$$

$$\frac{\partial}{\partial t}(\bar{\rho} \varepsilon) = -\frac{\partial}{\partial x_i}(\overline{\rho u_i \varepsilon}) + \frac{\partial}{\partial x_i} \left[\frac{\mu_{eff}}{\sigma_\varepsilon} \frac{\partial \varepsilon}{\partial x_i} \right] + c_{\varepsilon 1} \frac{\varepsilon}{k} n - c_{\varepsilon 2} \bar{\rho} \frac{\varepsilon^2}{k} \quad (6)$$

$$\text{where } n = \left[\mu_i \left(\frac{\partial \bar{u}_i}{\partial x_j} + \frac{\partial \bar{u}_j}{\partial x_i} \right) - \frac{2}{3} \bar{\rho} k \delta_{i,j} \right] \frac{\partial \bar{u}_i}{\partial x_j}, \quad (7)$$

and also the model correlation for turbulent viscosity:
 $\mu_t = c_\mu \rho k^2 / \varepsilon$.

A correlation connecting the density of the medium with temperature and pressure must be added to the above system of equations, for which we shall use characteristic curve for ideal gases.

When developing methods for the numerical solution of equations of the type (1-7), the main one is the description that is sufficiently accurate for the practical purposes of the fields of the unknown quantities, calculation of the main operating characteristics of heat and mass exchange processes in the real range of technical (technological) parameters in the geometric configurations that occur in practice) and their satisfactory coincidence with the experimental data obtained at full-scale sites. Currently, problem-oriented software packages for the entire class of problems of continuum mechanics are created [70-77].

To carry out the computing experiment, a computer software package was used for the programs of 3D simulation of coal combustion in combustion chambers of steam boilers FLOREAN [78-83]. This package is based on the solution of conservative equations for a gas-fuel mixture by a finite volume method. It includes a sub-model balance of momentum, energy, SIMPLE-method of pressure adjustment, k- ε turbulence model, a 6-stream model for calculating heat transfer by radiation, the balance equation for the matter components.

The selected software package allows us to calculate the velocity components - u, v, w, temperature T, pressure P, concentration of combustion products and other characteristics of the solid fuel combustion process in the pulverized state throughout the combustion space. For the transition from the specific enthalpy $h = c_p T$ to gas temperature in the computational pro-

gram, there is a procedure for calculating heat capacity of a mixture of gases and fuel. Dependence of the heat capacity of individual components (CO_2 , N_2 , air, water vapor and ash) on temperature is presented in the form of polynomials [84]. There is also a procedure for calculating dust/gas mixture density.

FLOREAN computer software package for the calculation of 3-dimensional turbulent flows of reacting media, which is verified in detail on a large number of experiments in laboratory conditions and in large furnace units, does not require huge computational costs. When the goal is to solve a specific type of reacting flotation problem, the best method to use is one that was well tested and adjusted. Let us dwell on the method for solving the above equations and on the main points of the FLOREAN software package mathematical model.

1.1 Two-phase floatation simulation

In floatations with a large number of particles, a solid medium can have a reverse effect on convective and diffusion transfer. However, the presence of solids in carbon monoxide from installations with combustion of coal dust is so insignificant (except for the region near the burners) that the effect of the second phase is neglected in calculations [85-87]. Then the combustion of solid fuel in combustion chambers can be represented as follows: the flame is a two-phase gas-dispersed system, and the effect of the solid phase on aerodynamics of the flow is insignificant [13].

In this paper, this assumption is used to reduce computational costs and transfer processes in the flame region are simulated roughly. Thus, for example, the point concentration of a solid matter is determined using the balance equations for a monodisperse solid with an average particle diameter. To de-

termine density of the mixture, we proceed from a homogeneous model, when velocities of solid particles are assumed to be equal to the local gas velocity, in some cases we will take into account the heat exchange between solid particles and gas by radiation. The solid phase effect on the turbulent exchange coefficients can be quite simply taken into account using the following empirical correlation:

$$\partial_{P,eff} = \frac{\mu_{P,eff}}{\sigma_{P,turb}} \quad (8)$$

Then for the turbulent viscosity with allowance for solid particles, we can use the following formula [88]:

$$\mu_{P,eff} = \mu_{G,eff} (1 + \rho_P / \rho_G)^{-1/2}, \quad (9)$$

which shows that an increase in the partial density of solid particles results in a decrease in the turbulent exchange. For the turbulent Schmidt-Prandtl number, taking into account the particles, the following numerical value was selected [88]: $\sigma_{P,eff} = 0.7$.

1.2 Heat transfer by radiation

When considering reacting flows in furnace units, it is necessary to take into account heat exchange by thermal radiation, which occurs due to energy transfer in the form of electromagnetic waves between two mutually radiating surfaces. In the process of heat exchange, a double energy conversion takes place: heat energy into the radiant energy on a body surface radiating heat, and of radiant energy into thermal energy on the surface of the body absorbing the radiant heat flux.

The radiant heat exchange phenomena play an important part in the working processes of various industrial devices, primarily combustion units and furnaces. In a steam boiler, heat is transferred from the fuel combustion products to the steel walls of boiling and screen tubes by radiation and convection, and through steel walls of the pipes it is transferred to water by thermal conductivity.

To simulate technical currents in the temperature range from 500K to 2000K, only the exchange of radiation in the infrared part of the spectrum and in the visible light region is important [89]. Although the integral equations of radiant energy exchange are known, their application to solving practical problems is extremely difficult. The radiation energy is characterized by the spectral intensity I_v [90]:

$$I_v = \lim_{dA, d\Omega, dv, d\tau \rightarrow 0} \frac{dE_v}{\cos \Theta dA d\Omega dv dt} \quad (10)$$

This quantity describes the radiation energy flux over dt time from the dA site in the dv frequency range, in the $d\Omega$ solid angle and in the direction determined by Θ angle cone between the normal to the plane and radiance beam.

In the emitting, absorbing and scattering medium, the intensity of radiation weakens due to absorption and scattering and amplifies due to the energy of radiation coming from the surrounding medium. In the general case, the radiation energy balance equation can be written as follows:

$$\begin{aligned} \frac{1}{c} \frac{\partial I_v}{\partial t} = & + \frac{\partial I_v}{\partial s} - (K_{a,v} + K_{s,v}) I_v + \\ & + K_{a,v} I_{b,v} + \frac{K_{s,v}}{4\pi} \int_{\Omega^*} P_v(\Omega^* \rightarrow \Omega) I_v(\Omega) d\Omega^* \end{aligned} \quad (11)$$

In this equation:

$\frac{1}{c} \frac{\partial I_\nu}{\partial t}$ - change by intensity time;

$\frac{\partial I_\nu}{\partial s}$ - change in intensity along an infinitely small ds element;

$-(K_{a,\nu} + K_{s,\nu})I_\nu$ - weakening of intensity due to absorption and dispersion;

$K_{a,\nu}I_{b,\nu}$ - increase in intensity along the segment due to self-emission in the direction of radiation;

$\frac{K_{s,\nu}}{4\pi} \int_{\Omega^*} P_\nu(\Omega^* \rightarrow \Omega) I_\nu(\Omega) d\Omega^*$ - increase in intensity due to the influx of radiation energy from all directions.

Let the thermodynamic equilibrium come and the heat transfer process by radiation is quasi-stationary. In this case, emission and absorption coefficients are equal, and because of the high light velocity, the intensity variation with time can be neglected. Let us also assume that all the surfaces and volumes participating in heat transfer are considered gray radiators, which will allow further simplification of the radiation transfer equation. For a gray volumetric radiator, we can write the following:

$$I_b = \int_{\nu=0}^{\infty} (K_{a,\nu} + K_{s,\nu}) I_{b,\nu} d\nu = (K_a + K_b) I_b, \quad (12)$$

where I_b is the intensity of black radiator, K_a and K_s are integral absorption and scattering coefficients. For the intensity

of black radiation according to Planck's law, we have the following:

$$I_b = \int_{\nu=0}^{\infty} I_{b,\nu} d\nu = \frac{\sigma T^4}{\pi} \quad (13)$$

To determine the S_q source term S_q in the energy equation (3), it is necessary to integrate equation (11) over the solid angle. Then for gray radiation and isotropic scattering from (11) we obtain the following:

$$\int_{\Omega=4\pi} \frac{\partial I}{\partial x} d\Omega = +(K_a + K_s) \int_{\Omega=4\pi} I_b d\Omega + K_s \int_{\Omega=4\pi} I d\Omega \quad (14)$$

According to [91], the radiation scatter in equation (14) does not contribute to the source term of the energy balance equation (3). Let us write the radiation balance equations (14) for gray radiation and isotropic scattering in the Cartesian coordinate system [92]:

$$\xi \frac{\partial I}{\partial x_1} + \psi \frac{\partial I}{\partial x_2} + \phi \frac{\partial I}{\partial x_3} = K_a I + \frac{\sigma}{\pi} T^4, \quad (15)$$

where $\xi = \sin \Theta \cos \phi$, $\psi = \sin \Theta \sin \phi$, $\phi = \cos \phi$.

When determining the boundary conditions, equations are required to describe the surfaces and volumes of radiation. Solids are impenetrable for radiation and emit radiation into a half-space above the surface. The dependence of the radiation emitted by solids from the direction is described by the Lambert cosine law. The radiation emitted by gray radiating surface does not depend on the direction:

$$q_S^I = \int_{2\pi} I \cos \Theta d\Omega = \pi I = \varepsilon \sigma T^4 \quad (16)$$

If instead of the surface the volume of the liquid radiates, heat flux is equal to the following:

$$q_S^{II} = \int_V \int_{4\pi} (K_a + K_s) I_b d\Omega dV \quad (17)$$

Integral absorption coefficient depends on the properties of the liquid and temperature. The radiation transfer equation (11) is an integrodifferential equation. Models for solving this equation can be divided into three groups: statistical models, zonal methods and flow models [92].

In statistical models (Monte Carlo models), the trajectory of individual rays in space is traced. The initial direction of rays, their interaction with matter is determined with the help of random numbers, which are defined in such a way that in the statistical sense the physical laws are fulfilled. The course of each ray is traced until its original energy is absorbed by the medium or the beam does not leave the system.

Naturally, the accuracy of the method depends on the number of traced rays. The Monte Carlo method is considered a method capable of giving an exact solution for equation (11). Its disadvantages are as follows: a large expenditure of computer time; the algorithm for solving the radiation transport equations differs significantly from the method for solving heat and mass transfer equations [93-94].

In zonal methods, the solution region is divided into a finite number of volumes and zones bounding the surface. Constant conditions are assumed within the zone and volume. The exchange of radiation energy between the zones is described by

radiative exchange factors, which are determined by numerical integration of the differential equation. The exchange coefficients determine the radiation energy balance for each volume. This leads to a nonlinear algebraic system of equations. When considering radiation transfer in a medium with a temperature-dependent absorption coefficient at each time step, it is necessary to re-determine the radiative exchange coefficients. Zonal methods, like the Monte Carlo method, are considered to be methods that can provide an exact solution to the radiation transfer equation [95]. The disadvantage is the high cost of the computer main memory.

The flow model contains various assumptions about distribution of radiation fluxes along the direction. According to this model, equation (11) is integrated over solid angles for which the flows are assumed to be independent of the direction. As a result, the integrodifferential equation (11) comes down to a system of coupled differential equations. These solution methods were developed for astrophysics problems and later applied in fluid thermodynamics. So, the Schuster, Schwarzschild, Eddington and Schuster-Hamakar methods used in astrophysics with the division of a solid angle into two parts were used to calculate heat transfer in the furnace units [96]. In works [97-98], two-flow methods were developed in a four-flow model, which is used for axisymmetric geometry problems. For three-dimensional Cartesian geometry in six-flow models [99], the radiation flux is divided into six parts in coordinate directions. Flows in different directions for these models are bound to temperature only.

In the present paper, a more advanced six-flow model was used to calculate heat transfer by radiation, proposed [100]. According to this model, the radiation energy flux distribution in the corresponding regions is approximated by means of power series and spherical functions.

To determine the source term in the energy balance, the absorbed radiation energy of all the individual rays passing through the control volume is summed. Using this method, heat transfer in the furnace flame was considered in [101]. Advantages of this method include, first of all, insignificant computer time expenditure, as well as similarity of the algorithm with the methods for solving basic heat and mass transfer equations. The intensity distribution along various directions is approximated using power series along the solid angle [100]:

$$I = A_x(\vec{i}\Omega) + A_y(\vec{j}\Omega) + A_z(\vec{k}\Omega) + B_x(\vec{i}\Omega)^2 + B_y(\vec{j}\Omega)^2 + B_z(\vec{k}\Omega)^2 + \dots \quad (18)$$

The A_i and B_i coefficients of this expansion, like two-current Schwarzschild model, are associated with radiation intensities:

$$A_i = \frac{1}{2}(I_i^+ - I_i^-) \quad (19)$$

$$B_i = \frac{1}{2}(I_i^+ + I_i^-) \quad (20)$$

Here I_i^+ and I_i^- are the radiation intensities integrated over the wavelengths in $\pm x$, $\pm y$ and $\pm z$ directions. We add the polynomial (18) to the radiation transfer equation (11), and integrate it over the solid angle $\Omega_i = 2\pi$. Integration leads to a system consisting of three equations and six unknown quantities [100]:

$$\frac{\partial B_i(b_{i,j})}{\partial x_i} = -K_a A_i, \quad (21)$$

$$\text{where } b_{i,j} = \frac{\pi}{2} \begin{pmatrix} 1 & 1/2 & 1/2 \\ 1/2 & 1 & 1/2 \\ 1/2 & 1/2 & 1 \end{pmatrix} \quad (22)$$

If further we integrate the radiation transfer equation with the adopted intensity distribution (18) over infinitely small angles, the bisector of which lies on the positive and negative coordinate axes, we obtain the following correlation:

$$\frac{\partial A_i}{\partial x_i} = -K_a B_i + \frac{K_a}{\pi} \sigma T^4 \quad (23)$$

Substituting (23) into (21), we obtain the following differential equations system of the six-flow model:

$$\frac{\partial}{\partial x_i} \left(\frac{1}{K_a} \frac{\partial}{\partial x_i} b_{i,j} B_i \right) = +K_a B_i - \frac{K_a}{\pi} \sigma T^4 \quad (24)$$

This model was used in work [102] in case of variable integration angles, which are related to the intensity distribution in three coordinate directions. The $b_{i,j}$ coefficients are determined by the following matrix:

$$b_{i,j} = \frac{1}{2} \begin{pmatrix} 1+x_i^{n^2} & \frac{1-x_i^{n^2}}{2} & \frac{1-x_i^{n^2}}{2} \\ \frac{1-x_i^{n^2}}{2} & 1+x_i^{n^2} & \frac{1-x_i^{n^2}}{2} \\ \frac{1-x_i^{n^2}}{2} & \frac{1-x_i^{n^2}}{2} & 1+x_i^{n^2} \end{pmatrix}$$

(25)

$x_i^{n^2}$ parameters depend on the intensity of the guiding radiation and are determined by the following correlation:

$$x_i^{\odot\odot 2} = \gamma \frac{B_i}{\sqrt{B_1^2 + B_2^2 + B_3^2}}, \text{ where } \gamma=0.1$$

(26)

The source term associated with radiant flows in the energy balance (3) is obtained by integrating the total intensity along the solid angle $\Omega=4\pi$. In accordance with equation (16) we have the following:

$$q = \frac{4\pi}{3} \left(\frac{\partial A_1}{\partial x_1} + \frac{\partial A_2}{\partial x_2} + \frac{\partial A_3}{\partial x_3} \right) \quad (27)$$

The main influence by radiation on heat exchange is exerted by water vapor and carbon dioxide due to their high concentration in the combustion chamber, and such components as sulfur dioxide or ammonia make a small contribution to heat exchange by radiation, as their concentration is negligible. The dispersion of the radiation energy for gases in the region of thermal radiation can be neglected. Water vapor and carbon dioxide emit and absorb thermal radiation in limited wave-

length regions. To calculate the heat exchange by radiation using a six-flow model, it is necessary to take into account that the emissivity of a gas mixture consists of the emitting powers of components and depends on temperature, wavelength and partial pressure. In a mixture for which there is overlapping of emission bands of different components, the emissivity must be reduced by means of a correction term. The nature of the radiation, effective radiation ranges, diagrams, and methods for calculating emissivity are described in [103].

The influence of partial pressure of water vapor and dioxide is taken into account in work [104]. Here, to simplify the radiation model, it is assumed that the emission bands of both gases completely overlap, and mass factors and specific absorption coefficients depend on the gas temperature. Then for the absorption coefficient we have the following correlation:

$$K_{a,G} = a_{G,CO_2} k_{CO_2}^* p_{CO_2} + a_{G,H_2O} k_{H_2O}^* p_{H_2O} \quad (28)$$

The model constants are given in Table 1 according to [104].

Table 1

Model Constants		
Component	$k_{\beta}^*, 1/mbar$	$a_{G,\beta}$
CO ₂	$85.0 T_G^{-1/3}$	$0.275-8.4 \cdot 10^{-5} T_G$
H ₂ O	$1100 T_G^{-0.82}$	$7.2 T_G^{-0.4}$

In gases containing solids, the effect of particles on heat exchange by radiation can be several times greater than the effect of water vapor and carbon dioxide. The processes occurring during the emission of particles differ from the gas radiation

processes: in a particle cloud, radiation is partially scattered on the surface of individual particles and is partially absorbed. However, it is necessary to take into account the processes of reflection, diffraction and refraction, and the fact that the properties of the particles cloud radiation are affected by their magnitude and shape, which change in the burnout process, and the wavelength [92].

Analytical determination of the absorption and scattering coefficients is impossible (for example, because optical properties are unknown for coal dust).

In this paper, by analogy with gas emission, the following correlation is chosen for them, which takes into account the attenuation of the intensity due to the presence of coal dust [94]:

$$I = (K_{P,a} + K_S)I_o \quad (29)$$

Absorption is proportional to the surface of all particles. For simplicity, it is assumed that the particle cloud consists of gray radiating balls with different diameters, and then the scattering and absorption coefficients of the particles are determined as follows:

$$K_{P,a} = X_a n_P \sum_{n=1}^l d_{n,P}^2 \frac{\pi}{4} \quad (30)$$

$$K_S = X_S n_P \sum_{n=1}^l d_{n,P}^2 \frac{\pi}{4} \quad (31)$$

X_a and X_s take into account properties of gray radiation and are called absorption and scattering factors, which for gray ra-

diation are bound by the following formula: $X_s = 1 - X_a$. The values of absorption and scattering factors are given in work [94]. If we assume that the particle cloud consists of particles of the same diameter and density, this simplifies determination of the absorption and scattering coefficients:

$$K_{P,a} = X_a \frac{6\rho_G x_P}{4\rho_p d_p} \quad (32)$$

The averaged value of the absorption factor is $X_a = 0.85$. Where there is a thermodynamic equilibrium between gas and solid particles, emission of suspension is described by combining the emissions of dust and gas:

$$K_a = K_{a,P} + K_{a,G} \quad (33)$$

X_a and X_s take into account properties of gray radiation and are called absorption and scattering factors, which for gray radiation are bound by the following formula: $X_s = 1 - X_a$. Work [94] cites the absorption and dispersion factors values.

1.3 The method of solving transport equations

Equations (1-6) with the corresponding boundary conditions form a closed system of equations, which we write down in the following generalized form:

$$\frac{\partial}{\partial t}(\rho\Phi) = -\frac{\partial}{\partial x_i}(\rho u_i \Phi) + \frac{\partial}{\partial x_i}(\partial_\phi \frac{\partial \Phi}{\partial x_i}) + S_\phi \quad (34)$$

This system of equations has no analytical solution and can only be solved numerically. Solution method for such equations was proposed by Patankar and is described in detail in his works [27, 105-106]. In order to solve these transfer equations,

it is necessary to know such properties of gas-fuel mixture as thermal conductivity, specific enthalpy, heat capacity, the dependence of which in the form of polynomials on temperature is presented in work [85]. The liquid density is determined and concentrations for various relative values are recalculated according to R. Leitner [107].

The system of transfer equations (34) is a system of second-order differential nonlinear equations. For their numerical solution, the entire design area is divided by a difference mesh into discrete points or volumes, a continuous field of variables is replaced by discrete values at grid nodes, and the derivatives entering differential equations are replaced by their approximate expressions through the difference of values of the grid nodes functions. As a result, we obtain a system of nonlinear algebraic equations, the number of which is equal to the number of grid nodes. There are various methods for obtaining difference equations [54]:

- Taylor series expansion for grid nodes;
- use of polynomial approximation;
- use of local analytical solutions of differential equations for individual control volumes;
- variational calculus or Galerkin's methods (finite element methods);
- control volume approach.

Approximation of differentials in all methods results in an error (the difference between analytical and numerical solution), which heavily depends on discretization method and the size of the grid. However, discretization methods should not only have a small error, yet be stable. The methods of high accuracy order formally give small errors, but are prone to instability. For three-dimensional simulation of complex turbulent flows with chemical reactions, it is necessary to use fairly simple, reliable and stable methods. The systems obtained by the

difference equations must be solved with little computer memory and time expenditure. Many of the discretization methods described in the literature has a high order of accuracy, but on coarse grids and with large grid Reynolds numbers it proves to be unstable.

Thus, in work [108], a comparison of the finite-difference method and discretization method using spline interpolation and fourth and sixth-order Hermite polynomials for flows in isothermal boundary layer was carried out. The work shows the advantages of finite-difference methods: simplicity, efficiency, cost-effectiveness, utility, etc.

A model of a turbulent diffusion flame using the finite element method was proposed in work [109]. The finite element method allows simple modeling of geometrically complex flow modes. In this paper, we compared the results and computer time expenditures for the finite-difference method and the finite element method. The computer time expenditures for the finite element method were 50% higher. For three-dimensional problems of convective heat and mass transfer, the main disadvantages in using the finite element method are large computer time and memory expenditures. For such tasks, the control volume method, which is physical in its essence and most vividly describes the process of numerical simulation itself, is considered to be the most suitable one [105, 110-114].

1.4 Obtaining difference equations by control volume method

The method of obtaining difference equations using the control volume method is that for each cell in the computational range, the physical conservation laws and differential equations that describe these conservation laws (transfer equations) are used, and integrate over the volume of each cell. Then the fol-

lowing integro-differential equation is valid for the Φ variable balance equation:

$$\iiint_V \frac{\partial}{\partial t} \rho \Phi dV = \iint_A \left(-(\rho \Phi u_i) + \partial_{tm} \frac{\partial \Phi}{\partial x_i} \right) \vec{n} dA_{no} + \iiint_V S_{tm} dV \quad (35)$$

The surface integral on the right-hand side (35) describes the convective and diffusive transfer of the desired Φ variable through the A surface of the cell. The volume integral on the right-hand side describes the variation of the Φ variable in the V volume due to the source term. To integrate the integro-differential equation (35), we adopt the following assumptions:

- as the values of the Φ variable and the properties of the substances, the mean value of the cell is used;
- flows through the cells boundaries are also determined by mean values over the areas of the corresponding surfaces. The average by area and by volume is considered equal.

Then, for the control volume in the Cartesian coordinate system (see Fig. 1), from equation (35) we obtain the following equation:

$$\begin{aligned}
\frac{\partial}{\partial t}(\rho\Phi)_p \Delta x \Delta y \Delta z = & \left[(\rho\Phi u_1)_w - (\rho\Phi u_1)_e \right] \Delta y \Delta z + \\
& + \left[(\rho\Phi u_2)_s - (\rho\Phi u_2)_n \right] \Delta x \Delta z + \left[(\rho\Phi u_3)_b - (\rho\Phi u_3)_t \right] \Delta x \Delta y - \\
& - \left[\left(\partial_{TM} \frac{\partial \Phi}{\partial x_1} \right)_w - \left(\partial_{TM} \frac{\partial \Phi}{\partial x_1} \right)_e \right] \Delta y \Delta z - \\
& - \left[\left(\partial_{TM} \frac{\partial \Phi}{\partial x_2} \right)_s - \left(\partial_{TM} \frac{\partial \Phi}{\partial x_2} \right)_n \right] \Delta y \Delta z - \\
& - \left[\left(\partial_{TM} \frac{\partial \Phi}{\partial x_3} \right)_b - \left(\partial_{TM} \frac{\partial \Phi}{\partial x_3} \right)_t \right] \Delta y \Delta z + S_{TM} \Delta x \Delta y \Delta z
\end{aligned} \tag{36}$$

Analysis of this equation shows that along with the values at the center of the control volume (point p), the variables and their derivatives at the boundaries of the reference volume (points e , w , b , t , s , n) are required. These values should be determined by interpolation. The choice of the interpolation method affects approximation errors and stability of the method.

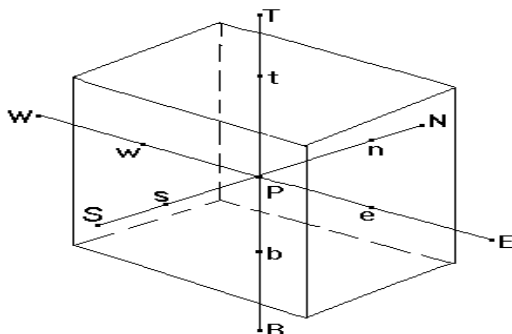


Figure 1 – Control Volume

In technical currents, when convective transfer predominates over a diffusion one, the approximations of convective

terms cause great difficulties. High-order methods become unstable for large Reynolds numbers, and methods of the first order of accuracy have a significant "scheme" or "approximate" viscosity and distort the results of the numerical calculation.

"Scheme" viscosity, or as it is also called "numerical" diffusion, as is well known, arises by using asymmetric differences to approximate convective terms in the transfer equations, and this leads to the appearance of an additional summand in the difference equation. Then numerical solution of this equation will correspond to the process of transfer of the Φ quantity in a medium with an additional fictitious transfer coefficient, i.e. as if with a distorted transfer coefficient. The magnitude of this distortion can be reduced by decreasing the spatial Δx_i interval between the grid nodes. However, for technical processes, when absolute speed value is significantly greater, the distortion of the transfer coefficient may be much larger than the actual value.

In this case, an important stability criterion is the "grid" Reynolds number $Re = \frac{\Delta x_i u_i \rho}{\mu_{eff}}$, formed by a reference volume dimensions and saying that "numerical" diffusion and instability increase with the width of the grid.

An estimate of the "numerical" diffusion coefficient for rotating two-dimensional flows with a uniform grid can be obtained with the help of the following formula proposed in [110]:

$$\partial_f \approx \frac{\sqrt{2}}{4} \rho \sin\left(\frac{4}{\pi} + \Theta\right) |\vec{u}| \Delta x \sin 2\Theta, \quad (37)$$

where: Θ is the angle between the velocity vector and the mesh (grid) line; $|\vec{u}|$ is the vector module velocity. An equation

analysis (37) shows that the numerical diffusion reaches its maximum value if the flow line crosses the grid line at an angle of 45° .

Patankar's paper [105] describes the approximation schemes often used in fluid mechanics: unwind differences schemes and central difference; hybrid scheme, etc. He has shown that the unwind differences are unlimitedly stable, but they have the first order of accuracy and are rather coarse.

The scheme with central differences is formally more accurate, but for $Re > 2$ it is unstable. Therefore, it is necessary to use a very small grid, which results in a large computer memory and time expenditure. In hybrid schemes, the central differences are used up to the critical Reynolds number and the unwind difference at large grid Reynolds numbers. Such schemes provide a smaller approximation error and are unlimitedly stable [111].

The analysis shows that when comparing the results of these three approximation methods with the experimental data, they all give about the same error. But it should be noted that higher order methods require about 3 times more time than unwind differences. Therefore, in mathematical simulation of complex physical processes, the most appropriate is the use of simple and stable approximation schemes.

For reasons of stability and the saving of computer time, in this paper, the unwind differences are used to solve the system of transfer equations. Due to the choice of a sufficiently fine grid in those regions where strong gradients of the sought ϕ value are expected and there is a large angle between the flux lines of this value and the grid, it is possible to reduce the effect of "numerical" diffusion. For convective terms in the x direction, the unwind differences lead to the following formulas:

$$\begin{aligned}
(\rho u_1 \Phi)|_e &= (\rho u_1)|_e \Phi_{f'} && \text{with } u_1 > 0.0 \\
(38) \quad (\rho u_1 \Phi)|_e &= (\rho u_1)|_e \Phi_P && \text{with } u_1 < 0.0
\end{aligned}$$

Formulas for the remaining cell boundaries are similar.

To approximate diffusion a flow, a second-order accuracy method is used, which here does not cause any stability problem. For the x direction, for example, we have the following (see Fig. 1):

$$(39) \quad \partial_{\text{TM}} \left. \frac{\partial \Phi}{\partial x} \right|_e = \partial_{\text{TM}, HB} \frac{\Phi_{f'} - \Phi_m}{x_{1,E} - x_{1,P}}$$

The source term in the balance equation is integrated over the control volume. If the source is a function of a variable $S_{\text{TM}} = f(\Phi)$, it is linearized:

$$(40) \quad S_{\text{TM}} = S_{\text{TM}}^{RS} - S_{\text{TM}}^{AP} \Phi_P.$$

The linearization of the source term is described in detail in [105].

The approximation method of time derivatives also affects the accuracy of the solution. In three-dimensional problems, due to lack of memory, an approximation is used with no more than two layers in time. One can use the forward and backward differences. Forward differences result in an explicit equation solution method:

$$\left. \frac{\partial \rho \Phi}{\partial t} \right|^n \approx \frac{\rho \Phi^{n+1} - \rho \Phi^n}{\Delta t} = RS(\Phi^n)$$

(41)

However, the time step is subject to strict stability criteria:

$$\Delta t_{\max} \langle \text{Min} \left\{ \frac{\Delta x_i}{|u_i|} \right\} \rangle ,$$

(42)

$$\Delta t_{\max} \langle \text{Min} \left\{ \frac{1}{2 \text{Re}} \frac{\Delta x^2 \Delta y^2 \Delta z^2}{\Delta x^2 + \Delta y^2 + \Delta z^2} \right\} \rangle$$

(43)

The fulfillment of stability conditions (42-43) in practice often leads to unjustified reduction of Δt step for the achievement of high accuracy. In backwards approximation using time derivative of the differences, leads to an implicit method:

$$\left. \frac{\partial \rho \Phi}{\partial t} \right|^{n+1} \approx \frac{\Phi \rho^{n+1} - \Phi \rho^n}{\Delta t} = RS(\Phi^{n+1})$$

(44)

To solve the system of equations (44), iterative solution methods must be used. Implicit schemes are certainly sustainable; as time step for an implicit scheme can theoretically be arbitrary. But the high stability of such schemes leads to the complication of the algebraic side of the problem, since in this case it is necessary to solve a system of related algebraic equations. This is especially true for the multidimensional and non-

linear equations of the problem that we have set, which, as a rule, are solved using the iteration method.

In this paper, the system of equations (34) is solved with the help of a perfect implicit method. The system of algebraic equations for the difference equation of the control volume (36) looks as follows:

$$a_p^{\text{TM}} = \sum_{n=E,W,N,S,T,B} a_n \Phi_n + S_{\text{TM}}^{\text{RS}} \Delta x \Delta y \Delta z, \quad (45)$$

where the coefficients of the ϕ_n variable at six adjacent points of the control volume are determined by the following formulas:

$$a_E = \left(\text{AMAX} (0.0; -(\rho u)|_e) + \frac{\partial_{\text{TM},Eb}}{\Delta x_e} \right) A|_e \quad (46)$$

$$a_W = \left(\text{AMAX} (0.0; -(\rho u)|_w) + \frac{\partial_{\text{TM},W}}{\Delta x_w} \right) A|_w \quad (47)$$

$$a_N = \left(\text{AMAX} (0.0; -(\rho v)|_n) + \frac{\partial_{\text{TM},n}}{\Delta y_n} \right) A|_n \quad (48)$$

$$a_S = \left(\text{AMAX} (0.0; -(\rho v)|_s) + \frac{\partial_{\text{TM},s}}{\Delta y_s} \right) A|_s \quad (49)$$

$$a_T = \left(\text{AMAX} (0.0; -(\rho w)|_t) + \frac{\partial_{\text{TM},t}}{\Delta y_t} \right) A|_t \quad (50)$$

$$a_B = \left(\text{AMAX} (0.0; -(\rho w)|_b) + \frac{\partial_{\text{TM},b}}{\Delta y_b} \right) A|_b \quad (51)$$

These coefficients in turn determine the a_p coefficients in the center of the control volume:

$$a_p = a_E + a_W + a_N + a_S + a_T + a_B + S_{TM}^{Am} \Delta x \Delta y \Delta z \quad (52)$$

Here, for the source term, according to equation (40), we have the following formula:

$$S_{TM}^{AP} = (S_{TM}^{LS} + \rho^0 \Phi^0) \quad (53)$$

As a result of approximation of the equations system (34), we obtained an algebraic equation (45) for each control volume and each desired Φ_n variable. The coefficients of this equation are functions of the Φ_n variables and are simultaneously directly or indirectly related to variable in other equations. Thus, we have obtained a nonlinear, connected (non-autonomous) system of algebraic equations. No direct method for solving this system of equations is possible because of the large computer time expenditure.

The system of equations can be linearized, and transfer equation for each variable can be solved separately, using iteration methods. There are many different iterative methods for solving the system of algebraic equations (45). It is well-known that the degree of convergence of the iterative methods is greater the better the relation between elementary volumes is taken into account during the solution of the equations. However, it should be taken into account that the higher the relationship between variables is, the higher the numerical cost of the calculation.

When simulating technical flows by the control volume method, simple and cost-effective methods for solving systems

of algebraic equations are often used, such as sweep methods [85, 105]. For the linearization of equations, the coefficients of the variables can be determined using the quantities from the previous iterations, where the corresponding quantities are kept constant during the solution of the linearized system of equations.

The calculated values are used at the next iteration to determine the coefficients [77].

where: $60 < y_* < 500$,

$$P(\sigma_h / \sigma_{h,turb}) = 9.24[(\sigma_h / \sigma_{h,turb})^{3/4} - 1][1 + 0.28e^{(-0.007\sigma_h / \sigma_{h,turb})}]$$

Boundary conditions for the transfer equation of the concentration of components

Input: c_β is the value of the component concentration,

Output: $\left. \frac{\partial c_\beta}{\partial x_i} \right|_{no} = 0$, line of symmetry: $\left. \frac{\partial c_\beta}{\partial x_i} \right|_{no} = 0$, on the sur-

face: $\left. \frac{\partial c_\beta}{\partial x_i} \right|_{no} = 0$

1.5 Pressure calculation

To solve the momentum transfer equation, it is necessary to know the pressure distribution. However, in the system of ϕ transfer equations (34) there is no equation that explicitly determines the pressure. Therefore, pressure is indirectly determined through the relationship between the equation of continuity and the equation of motion. Using certain pressure distribution, we can determine the velocity field from the motion equation. However, pressure distribution in the flow region needs to be adjusted in such a way that for the velocity fields satisfying the equation of motion, the equation of continuity

was fulfilled simultaneously. If the pressure is incorrectly selected, we get the so-called "defect" of the masses for the reference volume. Therefore, further adjustment of the pressure and a new calculation of the velocities is needed. The velocities and pressures are corrected with the help of the following formulas [54]:

$$p = p^* + \Delta\hat{p}, \quad u_i = u_i^* + \Delta\hat{u} \quad (54)$$

Correction to pressure $\Delta\hat{p}$ is determined from the following formula:

$$\Delta\hat{p} = -\frac{\Delta\overset{\circ}{m}\beta}{2\Delta t\left((1/\Delta x^2) + (1/\Delta y^2) + (1/\Delta z^2)\right)}, \quad (55)$$

where: $\Delta\overset{\circ}{m}$ is the mass defect, β -relaxation parameter. Using the $\Delta\hat{p}$ adjustment in control volume and velocity on its edges is adjusted as follows:

$$p = p^* + \Delta\hat{p}, \quad u_i = u_i^* + \frac{\Delta t}{\Delta x_i} \Delta\hat{p}, \quad u_{i-1} = u_{i-1}^* - \frac{\Delta t}{\Delta x_i} \Delta\hat{p} \quad (56)$$

However, the equations for the velocity and pressure components are solved completely separately. The pressure adjustment and solution of the momentum transfer equation must be repeated until the mass defect in all control volumes reaches the required limit or is less than a certain predetermined value. This iteration method of pressure adjustment, which is called the SIMPLE method, was proposed by Patankar and is described in detail in [105].

1.6 Initial and boundary conditions

To solve non-stationary transfer equations (34), it is necessary to specify initial and boundary conditions. Solution of the Navier-Stokes equations requires formulation of boundary conditions at all boundaries of the region under consideration. Errors in the choice of boundary conditions can result in a physically meaningless result or in instability of a finite-difference scheme and can become a source of large computational costs and errors.

To solve the equations describing convective heat and mass transfer, it is sometimes difficult to formulate the boundary conditions to make them simple for calculation and physically identical. Therefore, in numerical modeling, "wall laws" are often used, when the concept of a viscous sublayer is used to calculate the boundary values of the desired variables, which corresponds to a greater accuracy in the specification of the boundary conditions.

Let us formulate the initial and boundary conditions for our problem:

a) **Initial conditions.** The initial values (at $t=0$) of u , v , w and P variables are usually chosen to be zero in the entire solution region. Sometimes, as initial values, the previously obtained convergent solutions are used.

b) **Boundary conditions.** The boundaries of the design area in the combustion chambers can be solid walls and free surfaces. Free surfaces are the inlet (fuel and oxidizer supply points), exit from the combustion chamber and the plane of symmetry. The formulation of the boundary conditions at the input and output causes great difficulties for such problems.

The distribution of all input and output variables is known in very few cases. In fluid dynamics, the Neumann conditions (second kind conditions) are usually used when normal derivative at the boundaries and the Dirichlet conditions (first kind

conditions) are fixed when the values of the variables on the boundary are set. Based on the type of boundary conditions used, it is necessary to determine the convective and diffusion flows through the cells surface located at the boundaries of computational domain.

In order to reduce the influence of the choice of boundary conditions at the inlet and outlet, these boundaries should be as far removed as possible from the region of interest [77]. During iterations, additional control volumes located outside the calculation area are often used to specify the difference boundary conditions. Let us write down the boundary conditions for the solution of the motion equation. For the motion equation, the values of velocity components or normal and tangential velocity gradients must be fixed at the boundaries. For this problem, we choose the following boundary conditions:

Input: - u_i – input velocity values

$$\text{Output: } - \frac{\partial u_i}{\partial x_i} \Big|_{no} = 0$$

(57)

The last condition (57) is considered to be more stringent than the "soft" boundary conditions $\frac{\partial^2 u_i}{\partial x_i^2} \Big|_{no} = 0$, used in [13, 28].

$$\text{Symmetry plane: } u_i \Big|_{no} = 0, \frac{\partial u_i}{\partial x_i} \Big|_{no} = 0,$$

(58)

$$\text{Rigid surface: } u_i|_{no}=0, \quad \frac{\partial u_i}{\partial x_i} \Big|_{no}=0, \quad u_i|_{ta}=0$$

This is explained by the fact that a viscous sublayer emerges near the walls, where physical viscosity cannot be neglected, and the assumption of the equality of turbulent and physical viscosities means that we have sort of overestimated the value of the tangential stress near the walls, and this in turn leads to the greatest error in the calculations in this region.

The correct specification of the boundary conditions on the wall can be made, for example, by taking into account the viscous sublayer, the flow in which is quasi-laminar, since turbulent pulsations penetrate it from the outer part of the flow and decay under the influence of molecular viscosity as it approaches the surface [13].

For laminar flows, a linear velocity distribution is often used between the nearest point to the wall and the wall:

$$\frac{\partial u_i}{\partial x_j} \Big|_{ta} = \frac{u_{i,wp}|_{ta}}{\Delta x_{w,p}} \quad (59)$$

Then for the frictional stress on the wall we have the following:

$$\tau_w = \mu \frac{u_{i,wp}|_{ta}}{\Delta x_{wp}} \quad (60)$$

For turbulent flows, it was proposed in [146] to introduce in the equation (60) an adjustable factor $0 < f < 1$ or to take into account the attenuant [145]. In work [13], the refinement of the calculation was obtained by using transient formulas describing

the change in the effective viscosity from a turbulent in the flow core to a laminar one near the walls. In simulating turbulence using the k-ε model, the empirical wall functions proposed in [147-148] are used to determine the turbulent momentum flux on the wall:

$$\tau_w = \frac{\rho C_\mu^{0.25} k_{WP}^{0.5} \kappa}{\ln[EEy_*]} u_{i,WP} \Big|_{ta} \quad (61)$$

The value of the Karman constant $\kappa = 0.41$ was obtained experimentally, and the constant $EE=5.5$ for hydraulic smooth walls. To correct for pressure, Neumann-type conditions are used at all boundaries of the calculated region:

$$\Delta \hat{p} \Big|_{boundary} = 0 \quad (62)$$

Boundary conditions for the solution of energy equation. Input: $h = c_p T$ - the flow temperature at the input is set

$$\text{Output: } \frac{\partial h}{\partial x_i} \Big|_{no} = 0 \quad (63)$$

$$\text{Symmetry plane: } \frac{\partial h}{\partial x_i} \Big|_{no} = 0, \quad \frac{\partial h}{\partial x_i} \Big|_{ta} = 0 \quad (64)$$

Different types of boundary conditions for temperature can be set on solid walls. For adiabatic walls, the heat flux q_w is zero and in this case the boundary conditions are used as in the

symmetry plane. In case of heat exchange between the wall and the liquid, it is possible to set the wall temperature or the heat flux. If α convective heat transfer coefficient is experimentally or analytically determined, the following condition can be used:

$$q_W = \alpha(T_{WP} - T_W) \quad (65)$$

Convective heat exchange between a liquid and a wall with a set temperature is determined by the flow in the wall region. If $y_* \leq 60$ condition is fulfilled, the heat flux is determined by the following formula:

$$q_W = \lambda \frac{T_{WP} - T_W}{\Delta x_{WP}} \quad (66)$$

Let us write down the boundary conditions for the k- ε turbulence model. Since in very rare cases the real distribution of k and ε at the input is known, an estimation of their values is usually performed. It is often assumed that there is a completely developed flow with isotropic turbulence at the inlet. Then kinetic energy of turbulence k can be estimated from the degree of turbulence T_u :

$$T_u = \frac{(u'^2)^{1/2}}{\bar{u}}, \quad (67)$$

which in the input sections of technical flows varies from 5 to 20% [150].

Then for the kinetic energy of turbulence at the inlet we have the following:

$$k_{input} = \frac{3}{2} (\bar{u}_{i,input} T_u)^2 \quad (68)$$

To estimate the degree of dissipation of ε turbulent energy on the input, in general, there are no experimental data. However, in flows with fully developed isotropic turbulence, production and dissipation of the kinetic energy of turbulence are in equilibrium. In work [151] the following formula is given for the energy dissipation at the input:

$$\varepsilon_{input} = C_\mu^{0.75} \frac{k^{3/2}}{L_m} \quad (69)$$

where L_m is the mixing length, which is determined by the following relationship: $L_m = 0.03 (4S/P)$. Here, S is the area, P is the perimeter of the control volume at the inlet (for our task - these are the cells into which the burner outlet is divided).

$$\text{Output: } \left. \frac{\partial k}{\partial x_i} \right|_{no} = 0, \quad \left. \frac{\partial \varepsilon}{\partial x_i} \right|_{no} = 0 \quad (70)$$

$$\text{Symmetry plane: } \left. \frac{\partial k}{\partial x_i} \right|_{no} = 0, \quad \left. \frac{\partial \varepsilon}{\partial x_i} \right|_{no} = 0 \quad (71)$$

As for the solid boundary conditions, it should be noted that in the near-wall region the k - ε model loses its applicability. To

obtain the boundary conditions on the wall for k and ε , it is assumed that the flow in this region is one-dimensional and occurs without a pressure gradient. From considerations of similarity, it is not difficult to obtain [149] for a laminar boundary layer:

$$\frac{u_i|_{ta}}{u_*} = U^+ = y_* \quad (72)$$

and for a turbulent boundary layer:

$$\frac{u_i|_{ta}}{u_*} = U^* = \frac{1}{\kappa} \ln[y_* EE] \quad (73)$$

Here, the dynamic velocity u_* and the dimensionless distance y_* are determined by the following formulas:

$$y_* = \frac{u_* \Delta x_{i,WP} \rho}{\mu}, \quad u_* = \sqrt{\frac{\tau_w}{\rho}} \quad (74)$$

With a local equilibrium between production and dissipation of the turbulence energy, we have the following [147-148, 77, 152]:

$$u_*^2 = k_{WP} C_\mu^{1/2} \quad (75)$$

From equations (74) and (75) we obtain the following:

$$\tau_w = \frac{\rho C_\mu^{0.25} k_{WP}^{0.5} \kappa}{\ln[EEy_*]} u_{i,WP}|_{ta}$$

(76)

Equation (76) is true for the range of $60 \leq y_* \leq 500$.

For smaller dimensionless distances $y_* < 60$, the flow can be considered laminar and the following formula can be used:

$$\tau_w = \mu \frac{\Delta u_i|_{ta}}{\Delta x_w P}$$

(77)

To determine the dissipation energy in equation (69), it is assumed that the scale of length L_m varies linearly as distance from the wall changes, then for ε_{wp} we are going to have the following:

$$\varepsilon_{WP} = C_\mu^{3/4} \frac{k_{WP}^{3/2}}{\kappa x_{i,WP}}$$

(78)

In the equation of turbulence kinetic energy transfer (5), the source term $S_k = \Pi - \rho \varepsilon$ is also modeled with the help of wall-adjacent functions. For Π in equation (7), instead of the tangential velocities derivatives, the frictional stress is used according to (76) or (77). Since gradients of turbulent energy dissipation degree are especially large near the walls, it is possible to use

the averaged control volume value here: $\rho\varepsilon = \frac{1}{x_{i,WP}} \int_0^{x_{i,WP}} \rho\varepsilon dx_i$,

where ε is determined through (78)

When using the k- ε turbulence model, heat exchange is calculated using wall-adjacent (empirical) functions [153]:

$$q_w = \frac{c_p(T_w - T_{WP})(\tau_w / \rho)^{0.5}}{\sigma_{h,\mp} \text{Pr}^{\pm} \left[\frac{1}{\kappa} \ln[EEy_*] + P(\sigma_h / \sigma_{h,\mp} \text{Pr}^{\pm}) \right]} \quad (79)$$

where: $60 < y_* < 500$,

$$P(\sigma_h / \sigma_{h,turb}) = 9.24[(\sigma_h / \sigma_{h,turb})^{3/4} - 1][1 + 0.28e^{(-0.007\sigma_h / \sigma_{h,turb})}]$$

The boundary conditions for the components concentration transfer equation

Income: c_β - component concentration value,

$$\text{Input: } \left. \frac{\partial c_\beta}{\partial x_i} \right|_{no} = 0, \text{ symmetry axis: } \left. \frac{\partial c_\beta}{\partial x_i} \right|_{no} = 0, \text{ on the surface: } \left. \frac{\partial c_\beta}{\partial x_i} \right|_{no} = 0$$

1.7 Simulation of chemical reactions

The model of chemical reactions determines for the reaction flows the source term R_β , related to the rate of chemical reaction $\dot{\omega}_\beta$ in equation (4). The accuracy of the combustion process description is determined by the accuracy of knowledge about the kinetics of chemical reactions in the flame. The speed of reactions is greatly influenced by local distribution of the reacting components and temperature. In turbulent flows,

these values undergo fluctuations, and the values of these pulsations depend on the degree of local turbulence.

Simulation of parallel transfer processes and the influence of fluctuations in temperature and concentration thereon cause a lot of difficulties. The most poorly studied aspect of combustion is the kinetics of chemical processes in the furnace flame.

Many combustion theories and models are based on a simplified chemical mechanism that reduces all chemical processes in the flame to a single reaction with effective kinetic parameters. Combustion is a process of rapid and complete oxidation of a burning substance (coal) with oxygen, which occurs at a high temperature and is accompanied by the release of heat. In the furnace units of boiler plants only the most widely used oxidizer is used, which is atmospheric air, 21% in volume or 23,2% in mass of which is oxygen.

The main one is coke residue combustion stage, the intensity of which determines the intensity of fuel combustion. The heat of combustion of the coke residue is the main part of the heat of combustion of the combustible mass, and the stage of its combustion is the longest of all stages and can take up to 90% of the total time required to burn coal. The combustion process is affected by a number of factors, such as furnace structure, concentration of oxygen in the air supplied for combustion, pressure at which combustion occurs, and others.

A detailed simulation of all the reactions taking place (including all intermediate reactions) because of the large computational costs or lack of information on all the intermediate reactions is only possible in simple cases, such as, for example, in the combustion of carbon monoxide. For the processes simulated in this paper, simplified models are used, which only take into account the key components reactions.

Using integral reaction model in the work is based on the fact that most chemical reactions occur in several stages (steps), with the slowest reaction stage determining the rate of

the entire reaction. A multitude of multistage reactions can be modeled using regularities of single-stage reactions, while kinetic data are determined by the slowest reaction stage. The coal dust combustion model used in this work takes into account integral oxidation reactions of fuel components to stable final reaction products. In this case, intermediate reactions, as well as the formation and change of unstable intermediates, are not taken into account.

Many chemical reactions occurring in combustion chambers can be described using the integral reaction model for limited temperature and concentration regions only. Generation of harmful substances and reduction of their release can only be simulated using reaction-kinetic models that are valid for a wide range of temperatures and concentrations. The basis of reaction-kinetic model is the corresponding reaction mechanism, which includes a description of the molecular course of reaction between components, taking into account unstable intermediate products.

For many elementary reactions in the literature there are values of reaction rate constants. These values are not derived from physical laws, but are determined experimentally and moreover with large errors. In order to ensure that calculations results are consistent with the measured data, empirical reaction rate constants are often used in the development of reaction-kinetic models.

The simplest case of a chemical reaction is the reaction between two A and B components of the same phase. Over time change of AB product concentration can be described by the following equation:

$$\dot{\omega}_\beta = \frac{dc_{AB}}{dt} = k(T)c_A c_B$$

(80)

This change in product concentration is determined by concentrations of reagents and k reaction constant, which takes into account temperature dependence and reactivity of the substance components. According to the Arrhenius law [115], the rate constant is determined by the following formula:

$$k(T) = k_0 e^{-E/RT},$$

(81)

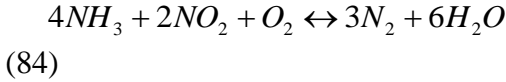
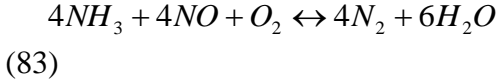
where k_0 coefficient and energy E activation are the kinetic constants determined experimentally. This empirical law is often written in the following form [116-117]:

$$k(T) = k_0 T^n e^{-E/RT}$$

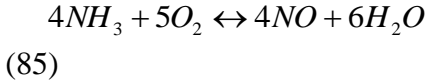
(82)

Generation of nitrogen oxides from nitrogen-containing fuel substances can be approximated by a simplified process scheme, according to which decomposition of these substances occurs primarily during combustion of volatiles to active atomic nitrogen, which is then partially recombined into molecular nitrogen ($N+N \rightarrow N_2$) and partially oxidized to nitrogen oxides mixture ($mN+O_2 \rightarrow mNO_x$).

The concentration of generated molecular nitrogen and a mixture of nitrogen oxides in flue gases is found by solving equations (80-82) of homogeneous kinetics [118]. Nitrogen and water vapor predominate up to a temperature of approximately 1300K, i.e. carbon monoxide is reduced. The reactions taking place in the ternary mixture: ammonia-carbon monoxide-oxygen can be represented as follows:



If temperature is too high or if oxygen content in the flue gases is too high, unwanted reactions may occur. For example, at a temperature above 1300K, ammonia is oxidized to nitric oxide:



Equations (83)-(85) describe integral reactions from stable reagents to stable final products, neglecting intermediate reactions in which free radicals, such as for example OH, H or O, are involved, in the first place. Different combinations of possible reaction paths are the basis of various models [107, 119, 120-128]. The choice of one of them is primarily connected with the capabilities of the existing computer. The criteria for choosing model are the minimal number of reactions and participating components with simultaneous accuracy of the calculations performed and a satisfactory agreement with experimental data.

In this paper we use the model of work [119], which requires insignificant computational costs. In addition, this model was verified in detail on a large number of experiments in laboratory conditions and in large furnace units [59-61, 67-68, 77, 107, 129, etc.]. This model takes into account the 31 elementary reactions for NO_x-model involving 15 substances, the reaction of the volatiles with the generation of water, hydrogen, oxide and carbon dioxide, methane, as well as the conversion

reaction of primary volatiles released from coal in the gas phase, all the way to final products (CO, CO₂, H₂O, H₂, O, H). Reactions and their kinetic data are given in [77, 119]. The change in the concentration of components with time is described by a system of ordinary differential equations of the type (80). When choosing a numerical method for solving a system of differential equations, it is necessary to take into account the "rigidity" of this system, i.e. presence in the solution of a wide range of time scales for various reactions:

$$\max \left[\frac{\hat{\alpha}_\beta}{\hat{\alpha}_n} \right] / \min \left[\frac{\hat{\alpha}_\beta}{\hat{\alpha}_n} \right] \gg 1$$

To solve this rigid equations system, Gear method is used in this work from the well-known NAG mathematical software package [77].

The ignition and combustion of coal can be divided into processes for the exit and ignition of volatiles and combustion of the coke remaining after pyrolysis. These processes can be modeled with the help of reaction-kinetic equations. Combustion model should exclusively describe local heat generation as a result of combustion and the effect of combustion products on heat transfer. Therefore, when selecting pyrolysis and combustion models, we decide against using bulky systems with a large number of components.

Starting at 570⁰K, volatile hydrocarbons, hydrogen and carbon monoxide emanate from the raw coal with an increase in temperature. The amount and composition of pyrolysis products depends very strongly on the type of coal, the temperature and coal powder heating rate. A typical temperature for a flare in pulverized-coal furnaces is 1500-1900K, while coal dust heating rate is 10⁴-10⁵K/s. At such a high heating rate, the reaction pyrolysis maximum shifts to higher temperatures. Models

that describe the experimentally proven relationships between composition and quantity of pyrolysis products, heating rate and temperature, using the appropriate number of reactions and equations, are presented in works [130-135]. The change in carbon concentration over time in one-stage pyrolysis model is described using an ordinary differential equation of the first order:

$$\frac{dc}{dt} = -k_{pyr}c \quad (86)$$

With initial conditions: at $t=0$ $c = c_0$

When solving kinetic equations, initial data are usually taken from data on the composition of stable products obtained as a result of processing experiments on mass spectrometric sounding of a flame. The pyrolysis rate constant in this case is assumed to be constant, as, for example, in work [136]. Temperature dependence of the pyrolysis rate is modeled using the modified Arrhenius law (82):

$$k_{pyr} = k_{0pyr} T^n e^{-E_{pyr}/RT}$$

Below in Table 2 kinetic data are given for different types of coal, obtained experimentally.

Table 2

Kinetic data for various grades of coal

$k_{pyr} = k_{0pyr} T^n e^{-E_{pyr}/RT}$		Description			
No	Coal	k_{0p-r} , 1/s	n	E_{pyr} , kJ/mol	Author
1	Black coal	$1.50 \cdot 10^5$	0	74	[137]
2	Black coal	$2.08 \cdot 10^5$	0	92	[138]
3	Brown coal	$3.50 \cdot 10^5$	0	74	[139]

In the two-stage pyrolysis models, the volatile content is simulated using two concurrent stages, one of which relates to the low and the other to high temperatures. This paper uses a one-stage pyrolysis model, in this case, the stoichiometric coefficients of the pyrolysis reaction can be derived from the rapid analysis data, and this is very important and preferable.

Pyrolysis products, mixing with air, form a reactive mixture. The rates of combustion reactions of these gaseous products are so high that the diffusion combustion approximation is acceptable. If we do not take into account the influence of turbulent pulsations, combustion rate of volatile parts is only determined by oxygen content. But then, in order to take into account the effect of turbulent pulsations on the volatile content combustion rate, it is also necessary to solve the transfer equations, as for example, in work [140].

Consequently, combustion rate of volatiles can be related to the characteristics of the k- ε model. In areas with sufficient oxygen content and a small amount of fuel, the determining factor for the reaction rate is the concentration of volatiles:

$$\dot{\omega}_{1FL} = c_1 \bar{c}_{FL} \frac{\varepsilon}{k}$$

In the regions saturated with fuel, the reaction rate is determined by oxygen content and stoichiometry coefficient ν_{O_2FL} :

$$\dot{\omega}_{2FL} = C_2 \frac{\bar{c}_{O_2}}{\nu_{O_2FL}} \frac{\varepsilon}{k}$$

If fuel and oxygen are simultaneously present in turbulent moles, in this case the reaction rate is determined by the burning combustion products:

$$\dot{\omega}_{3FL} = C_{3FL} \frac{\bar{c}_{CO_2} + \bar{c}_{H_2O}}{v_{O_2FL} + 1} \frac{\varepsilon}{k}$$

In reality, of course, the minimum of these speeds is established: $\dot{\omega}_{FL}^* = \min(\omega_{1FL}, \omega_{2FL}, \omega_{3FL})$.

Constants in this model are provided in [141]: $c_1=4.0$, $c_2=4.0$, $c_3=2.0$

The heterogeneous reaction of combustion of solid carbon on the surface of coke particles is determined by diffusion of oxygen from the environment into the boundary layer and into the porous medium of a particle, and also by the reaction between carbon and oxygen at the surface of the particle. The slowest of these processes determines coke combustion rate. In work [136], the correlation (80) was proposed for coke reaction rate, in which, for the velocity coefficient, taking into account the effect of oxygen diffusion and reaction on the coke surface, we have the following formula:

$$k_C = \frac{k_C^{(D)} k_C^{(chem)}}{k_C^{(D)} + k_C^{(chem)}}$$

Using Fick's law for diffusion, and the assumption that the oxygen partial pressure on the surface and the slippage between gas and the particle are negligibly small, the author of work [136] obtained the following:

$$k_c^{(D)} = \frac{2\nu_c DM_c}{RT_m d_p}$$

Dependence of diffusion coefficient on temperature is given in the following form:

$$D = D_0 (T_m/T_0)^{1.75}, \quad \text{где } T_m = (T_r + T_u)/2;$$

$$T_0 = 1600 \text{ K}; \quad D_0 = 3.49 \cdot 10^{-4} \text{ m}^2/\text{s}$$

Stoichiometric coefficient ν_c takes into account the reaction taking place on the coke surface between oxygen and carbon:



The chemical reaction rate constant is modeled using the Arrhenius law:

$$k_c^{chem} = k_{0c} \exp(-E_c/RT_x)$$

For coal coke combustion we have the following values of the k_{0c} coefficient and activation energy E_c [88]:

$$k_{0c} = 204 \left[\frac{\text{kg}}{\text{m}^2 \cdot \text{s} \cdot \text{bar}^n} \right], \quad E_c = 79.4 [\text{kJ/mol}], \quad H_{uc} = 33000 \text{ kJ/kg}$$

Local changes in the concentration of oxygen, carbon dioxide and water vapor as a result of coal combustion are determined by the elemental composition of fuel and by stoichiome-

try of the reactions between hydrogen and fuel carbon and air oxygen [84, 142].

Below are the results of computing experiments, carried out using the mathematical model described in this section.

The system of equations can be linearized and transfer equation for each variable can be solved separately, using iteration methods. There are many different iterative methods for solving the algebraic equations system (45). It is known that the degree of convergence of the iterative methods is greater the better the correlation between elementary volumes is taken into account during the equations solution. However, it should be taken into account that the higher the relationship between variables, the higher is the numerical expenditures of the calculation.

When simulating technical flows using the control volume method, such simple and cost-effective methods for solving systems of algebraic equations are often used, such as sweep methods [85, 105]. For the linearization of equations, the coefficients of the variables can be determined using the quantities from the previous iterations, when the corresponding quantities are kept constant during the solution of the linearized system of equations. Calculated values are used at the next iteration to determine the coefficients [77].

Security Questions:

1. What differential equations describe the 3-dimensional motion of a fluid with variable physical properties in the general case?
2. What model of turbulence is used in the calculations?
3. What does FLOREAN computer software package represent?
4. Why is it necessary to take heat exchange into account by radiation when burning a pulverized-coal flare?
5. What models are there for solving the transport equation by radiation?
6. What are the advantages and disadvantages of each model?
7. What is the method of control volume for deriving difference equations?
8. How is the pressure determined when the coal burns in the combustion chamber?
9. What are the boundary conditions of the first and second kind?
10. What are the boundary conditions for velocities? How are the boundary conditions for the energy equation written?
11. What models exist for solving the transport equation by radiation?
12. What are the main combustion stages of coal particles?

2 HEAT AND MASS TRANSFER DURING THE COMBUSTION OF PULVERIZED COAL IN A SIMULATOR WITH TANGENTIAL FEED

2.1 Basic characteristics of the model

One of the ways of promptly obtaining the necessary data for the design and determination of optimum operating parameters of boiler units is to conduct research (both experimental and numerical) on fire models of furnaces. Finding the best constructive and layout designs that facilitate early development of powerful boiler units is no longer possible without extensive use of different models.

The use of the model in cold conditions (isothermal and non-isothermal) and under ordinary conditions makes it possible to study the influence of structural and operating parameters on the flow structure, fuel burnup and nitrogen oxides output level, to consider the issues of fuel thermal preparation, the aerodynamic structure of the vortex torch and flow in the vortex combustion chamber. The most effective is the use of modeling at the design stage of a new boiler design, when it is possible to investigate the effect of operating and design parameters on the processes occurring in the combustion chamber, and also to identify numerous bottlenecks that should be avoided in the design, setup and operation of boiler units.

In the domestic and foreign practices of simulation of processes in combustion chambers, a great deal of experience has been accumulated on the methodology for calculating and studying models of furnace and burner devices, including furnaces with a tangential arrangement of direct-fire burners. The method of fire simulation of pulverized coal furnaces has been developed at the Kazakh Research Institute of Energy and is presented in numerous works of its employees [1, 154-161].

Two types of burners are used for pulverized-coal boilers: vortex with the swirling of flows inside the burner and direct-flow burners with the swirling of flows in the furnace volume. Presently, tangential furnaces are widely used in domestic and foreign boiler industry when burning both solid and liquid fuels.

Compared with the "linear" furnaces equipped with vortex burners, tangential furnace units, as shown by domestic and foreign experience, allow to ensure more intensive heat exchange in the furnace unit, to increase the uniformity of distribution of thermal loads along the furnace perimeter, which is especially important when using all-welded gas-tight screen panels, to reduce formation of nitrogen oxides in the furnace unit, to organize the slag-free operation of the furnace, which is especially important when burning fouling coals. Despite these advantages, as well as the long and wide use of tangential furnaces, they are still considered to be the least studied. The latter considerably complicates the development and adoption of rational engineering solutions for the use of tangential furnaces for powerful boiler units on various coals.

A characteristic feature of the aerodynamics of tangential furnaces is the organization of vertically directed rotational motion of gases in the furnace, which is achieved by installing straight-flow burners at an angle to the chamber walls and tangential to the conditional circle in the center of the furnace.

Usually the diameter of this circle is assumed to be 0.1-0.3 of the depth of the furnace. Such input of flows creates inside the furnace unit a horizontal dust and gas vortex moving from the bottom upwards. As the transition from the section of the bottom tier of burners to the upper one, the intensity of the twist of the torch increases.

Consequently, the tiered powering on of burner jets results in a strong unwinding of the torch, as a result of which a completely formed velocity profile is formed at the exit from the

burner zone, typical of a strongly swirling flow. Flare rotation in such furnace improves the mixture formation, increases heat transfer rate and the efficiency of the screens, which is associated with a decrease in the size of the near-wall zone with relatively low gas temperatures, and uniform wall heating [1, 162-163].

For the combustion of solid fuels in steam boilers furnaces with high steam production, the main one is the pulverized-coal system. Coal dust is prepared in individual pulverized-coal systems, which are associated with the fuel burning process scheme. The furnace chamber is preferably made in the form of a rectangular prism filled with furnace-wall tubes. The furnaces of powerful steam boilers are made in the form of an elongated parallelepiped of rectangular, square or, more rarely, more complex, for example an octagonal section.

This section presents the results of numerical modeling of the combustion of Ekibastuz coal in a pulverized state on the steam boiler model in the form of a parallelepiped with a tangential fuel supply. The experimental setup is a combustion chamber, which has the form of a parallelepiped, which is 7.635m high, 2.1m wide and 1.55m long.

Combustion of fuel takes place in the chamber of the furnace in a suspended state, and a flare is formed in the form of a brightly shining flame. The ash formed in the fuel combustion process is carried away by the flow of outgoing flue gases, and the formed slag falls in the lower part of combustion chamber and is continuously removed in a solid or liquid state. For solid ash removal, the walls in the lower part of the combustion chamber are given a larger slope ($55-60^\circ$) and a cold slag funnel is made. The falling slag rolls down cool surfaces of the funnel into the slag-receiving device, where it is mechanically removed when cooled down. The experimental model investigated in this paper has a cold funnel below it, with a cross-

sectional area $S_B=(0,0171 \times 1,2)m^2$, through which 10% of the total air supplied to the chamber is supplied.

Flue gases carry with them solid particles of fly ash and unburnt fuel. Ash, settling on the heating surface, decreases the heat transfer, increases the resistance of flues and causes great damage to the boiler plant equipment. To reduce the harmful effect of ash high chimneys are used, which ensure its dispersion in the atmosphere. So, for example, at a pipe height of 40m, the ash is scattered at a distance of 3000m from the pipe, and at a height of 80m – at a distance of 6000m. In wet weather, ash falls out at closer distances. Consequently, an increase in the height of the chimney cannot ensure the purification of the atmosphere, so it is desirable to trap the ash before it enters the atmosphere or, more preferably, simulate the process with the lowest ash emissions.

Usually, in the numerical simulation of combustion in various technical devices, the question arises as to the method of igniting the flow. Coal dust can only ignite and burn if the temperature in the furnace is high enough. Therefore, in order to start the boiler, it is necessary to first create a corresponding temperature in the furnace unit, which is achieved by a special kind of ignition device called a muffle burner. It is a small manual furnace unit with a stationary grate, which is located under the furnace shaft in such a way that hot gases from the muffle burner exit below the dust stream. Aerial dust, passing over hot gases, ignites and continues to burn in the furnace.

Since the nature of temperature distribution in the chamber depends strongly on the boundary conditions (sources of ignition are located at the boundary), the mathematical model of these sources should, as far as possible, describe the real process more accurately. In work [47], the influence of the ignition source temperature of the on the maximum temperature of the flare was investigated, the conditions for ignition and flame

stabilization in the flare of premixed reagents were analyzed. It is shown that at $T_3 > 690\text{K}$, ignition and steady burning of the gas mixture are observed. In work [164], the dependence of combustion temperature of carbon particles on their size was found; it was determined that combustion is impossible in a certain region of particles, depending on conditions.

In some problems, the fuel mixture ignition is carried out by the oxidizer flow having a sufficient temperature for ignition [115, 165-166]. Often, the so-called "flare pilot" is used to stabilize the flame front [13]. As a mathematical model of the "pilot flare," hot spots are used at lattice sites [47], which have a high temperature level and are located on the inner edge of the burner nozzle. In the model used in this paper, a similar method of ignition of the fuel mixture is chosen and for hot spots a temperature is set that ensures stable fuel combustion.

The air required for combustion (primary) is supplied into the furnace along with the dust through the burners, which can be either circular vortex or straight-through. In the vortex burners, the dust-air mixture and the secondary air enter the furnace unit in the form of a swirling jet, and in a single-flow supply to the combustion chamber of the aerial and secondary air is carried out separately through narrow elongated slots. In addition to the primary air, additional (secondary) air is supplied to the place where the greatest combustion takes place.

The distribution of the amount of primary and secondary air depends on the type of fuel, the design of the furnace and the burner. Dusty air mixture coming from the burners in the combustion chamber forms a system of turbulent non-isothermal jets that propagate in the environment of hot combustion products. Mixing of ejected or hot gases with a dust-air flow leads to the formation of a high-heated reacting mixture and its ignition.

When fuel is burned, not all of the theoretically required air is used to burn fuel; part of it does not participate in the com-

bustion reaction as a result of insufficient mixing of air with fuel, and also because the air does not have time to come in contact with the fuel carbon and enters boiler flues in a free state. The actual amount of air necessary for complete combustion of fuel must be somewhat larger than theoretical amount; therefore combustion air is supplied to the furnace in an amount greater than theoretically required quantity. The ratio of the amount of air actually supplied to the furnace $V_{\%}$, to its theoretically necessary quantity V_0 is called the excess air factor: $\alpha_{\square} = V_{\%} / V_0$, which depends on the type of fuel burned, the method of its combustion, the design of the furnace, and is selected on the basis of experimental data. In pulverized-coal furnaces, the values of the excess air factor in the combustion chamber are optimal $\alpha_{\tau} = 1.2 \div 1.25$. For combustion of all fuel, the following amount of air will be needed: $V_B = \alpha_{\tau} V_0 B$, где $V_0 = 4,508 \text{ nm}^3/\text{kg}$ is the theoretical required volume of air per 1 kg of fuel [167], B is the total fuel consumption of the boiler plant, which in the case under consideration is 750 kg/hour. In the simulation, we used Ekibastuz coal as fuel, which has 40% ash content and high moisture content. The capacity of the boiler plant, the location of burners, their dimensions and fuel characteristics are indicated in Table 3.

Table 3

Furnace Unit Model Characteristics

N	Description of values	Dimension	Values
1	2	3	4
1	Capacity B	kg/hour	750.0
2	Fuel - (Ekibastuz coal). W Fuel composition	%	7.0
	A	%	40.9
	S	%	0.8
	C	%	41.1
	H	%	2.8
	O	%	6.6
	N	%	0.8
	Volatile content, FL	Mj/kg	30
	Calorific value, Q_H	nm^3/kg	15.87
	Theoretical air volume		4.2
3	Excess air ratio at the furnace outlet	α_T	1.2
4	Air temperature (secondary)	$^{\circ}\text{C}$	300
5	Coal-air mixture temperature	$^{\circ}\text{C}$	100
6	First tier of burners. Number of burners in the tier	units	4
	Layout	tangent.	
	Solid fuel consumption per burner	kg/hour	70.3
	Excess air factor per burner	α_T	1.01
	Primary air velocity at the burner outlet	m/s	8
	Secondary air speed at the burner outlet	m/s	12
	Burner height	mm	200
	Burner width	mm	80
7	Second tier of burners. All data are identical to that of the first tier burners		

Table 3 (continued)

1	2	3	4
8	Third tier burners. Number of burners in the tier. Layout Solid fuel consumption per burner Primary air speed Secondary air speed Burner height Burner width	Unit tangent. kg/h m/s m/s mm mm	4 35.625 8 12 100 60
9	Teritary air		
9.1	I - input (4 th tier). Number of nozzles Z Layout	unit tangential	4
	Air velocity at the nozzle outlet	m/s	25
	Nozzle diameter	mm	34
9.2	II- input (5 th tier). All data is identical to input II.		
9.3	III- input (6 th tier). Number of nozzles Z Layout Air velocity at the nozzle outlet Nozzle diameter	unit tangential m/s mm	4 30 58
10	Gas stage (7 th tier) Recirculation stage r Excess air factor in recirculation gases Recirculation gas temperature t_{rp} Total consumption of products of recycling and gas Number of gas stage nozzles Layout Air velocity at the nozzle outlet Gas stage nozzle diameter	α_{rp} $^{\circ}C$ unit m/s mm mm	0.08 1.3 250 0.1915 4 tangent. 25 50

The experimental model has 12 burners, which are located four on each of the first three tiers of the chamber. Dimensions of burners of the first two tiers: $(0.2 \times 0.08) \text{m}^2$, and third tier burners: $(0.1 \times 0.060) \text{m}^2$. To supply the remaining air, the boiler has on its side walls four more tiers of holes: tiers 4, 5 - nozzle diameter of 0.034 m, tier 6 - 0.058m, tier 7 - 0.05m. We used a tangential fuel supply (see Fig.2). A separate supply of the air mixture and secondary air was carried out, as provided for in the full-scale furnace model [168].

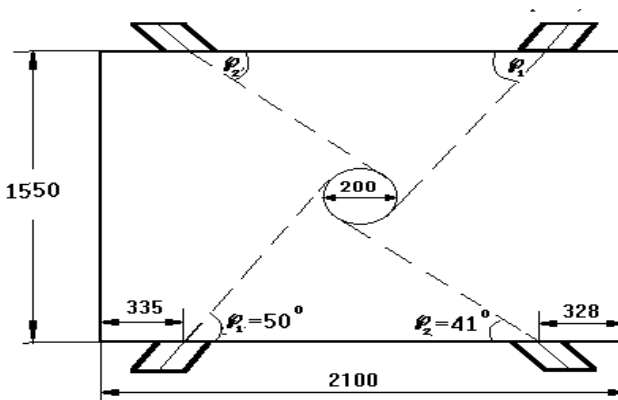
2.2 Analysis of main results

Computer modeling of the problem of combustion of Eki-bastuz coal, which has a large ash content (up to 40%) and high moisture content was carried out on the basis of three-dimensional momentum transfer equations, as well as energy and concentration transfer equations, taking into account chemical reactions under appropriate boundary conditions. In the calculations, a grid of $14 \times 17 \times 27$ was used. Combustion of volatile constituents was modeled in the approximation of instantaneous mixing. In the calculation of particle radiation, pyrolysis and combustion of coke, the assumption of thermodynamic equilibrium with the gas phase was used.

The results of a numerical coal combustion experiment in a particulate form are provided below. During the experimental work on the model, due to slagging of the measuring probes, it is not possible to thoroughly study aerodynamics of the nonisothermal flow. Numerical modeling of nonisothermal flows in combustion chambers allows this to be done in full measure.

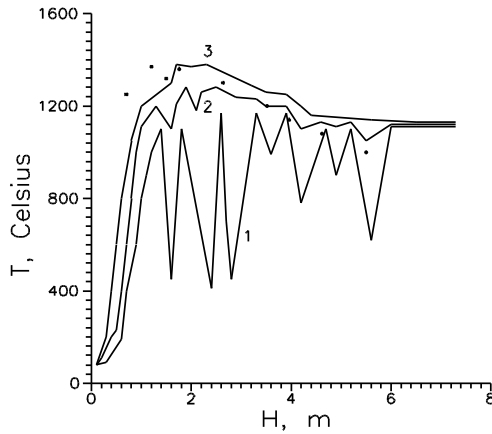
Figure 3 shows distribution of the calculated maximum, minimum and average horizontal flow temperature of the burning flow along the height of the boiler. The flare temperature in the pulverized coal fired furnace passes through a maximum and decreases when it leaves it due to the absorption of a large

amount of heat by the boiler tubes of the furnace walls. It can be seen that the zone of maximum temperatures is localized at the level of the second tier burners. With the increase of z coordinate (in Fig. 3 and hereinafter it is the height H), all three temperature profiles equalize and reach the level of $T \sim 1200^{\circ}\text{C}$. The first three minima on the lower curve are associated with the low temperature of the fuel air mixture entering the burners of the first three tiers. The maximum temperatures zone is somewhat stretched out, which is due to the supply of tertiary air on the fourth, fifth and sixth tiers. If we did not supply tertiary air, the maximum temperatures would be localized at the level of the last tier of burners.



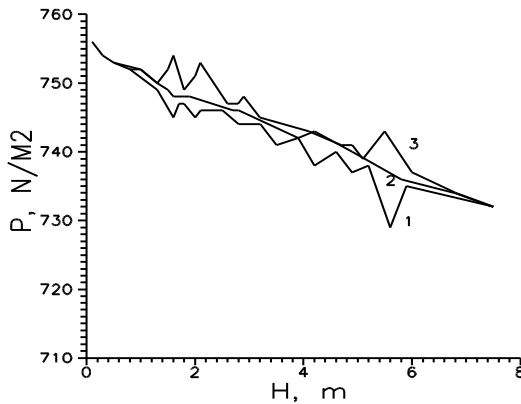
(values are provided in millimeters)

Figure 2 - Configuration of burners in the first three tiers with the supply of solid fuel



1-minimum, 2-average, 3-maximum in the cross-sectional values; line-simulation, * - experiment

Figure 3 - Comparison of the calculated and experimental distribution of temperature over the height of combustion chamber

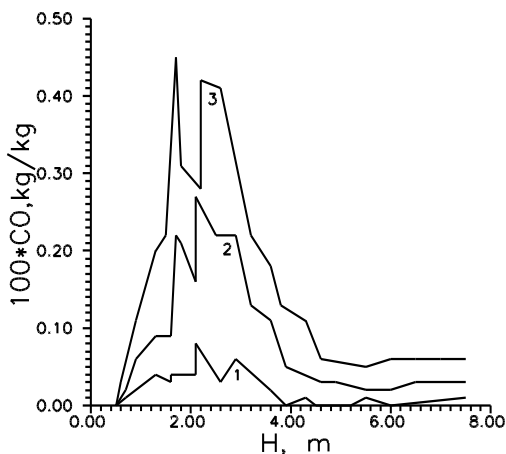


1-minimum, 2-average, 3-maximum in the cross section

Figure 4 - Pressure distribution over height of the combustion chamber

Figure 3 also shows the experimental distribution of the average temperature over the furnace height. The comparison implies that the calculated temperature value is somewhat exaggerated at the output, which obviously has to do with the supply of a tertiary blast; the experiment provides a faster flare ignition.

In normally operating furnaces a slight suction is set, which at the end of the furnace does not exceed 2-3 mmAq. Consequently, within the furnace, the pressure changes by no more than 0,02-0,03%. Figure 4 shows the estimated distribution of the maximum, average and minimum values (along the cross-section of the boiler) of the pressure P along the combustion chamber. The pressure decreases as you move toward the exit from the boiler plant. True pressure can be determined by the following formula $P_{\text{нст}} = P + 10^5 (\Pi\text{a})$.



1-minimum, 2-average, 3-maximum value in cross-section

Figure 5 - Distribution of carbon monoxide concentration CO along the height of the combustion chamber

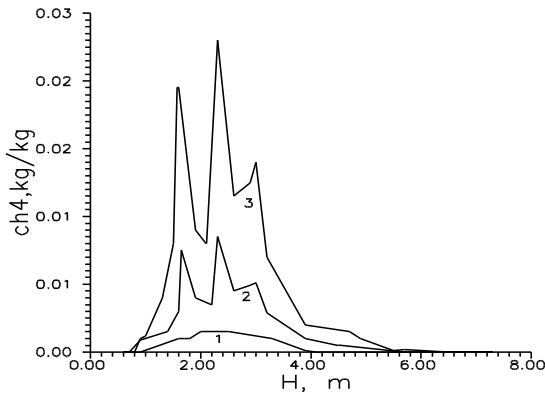
Combustion in the furnace must be as complete as possible with minimal losses from the chemical (lack of incoming air into the boiler furnace, low temperature in the furnace, improper distribution of air therein, insufficient volume of furnace space) and mechanical (failure and carry-over of small particles of unburnt fuel into boiler flues) incompleteness of combustion. For full fuel combustion in the furnace unit it is necessary to simulate the appropriate conditions: sufficient oxygen for burning volatile combustibles, the corresponding temperature in the furnace (carbon does not react at low temperatures), sufficient hold-up time of combustible particles in the furnace, and good mixing of fuel with air.

In the combustion process, a number of chemical reactions occur between the fuel (coal) and the oxidant (oxygen), resulting in the concentration of CO , CH_4 , CO_2 , O_2 , H_2O , etc. The distribution of these concentrations over the height of combustion chamber is shown in Fig. 85-91. In case of incomplete combustion, flammable gases appear additionally in the composition of gases leaving the furnace: hydrocarbons, carbon monoxide CO , methane CH_4 , and sometimes pure hydrogen H , and with excessive excess of air, unburnt volatile combustibles and particles of solid fuel are carried away from the furnace. Therefore, when burning fuel, it is necessary to reduce incompleteness of combustion to a minimum. As a rule, the boiler unit works either with complete combustion, or with minor chemical incompleteness of combustion.

Figures 5-6 give the distribution curves of the maximum, minimum, and average cross-sectional concentrations of carbon monoxide and methane in the chamber height. These curves reach the maximum in the region of the burners location (tiers I-III), where CO and CH generation actually occurs in the course of chemical reactions between solid fuels and oxidants. Knowing the content of carbon monoxide in the exhaust flue

gases, determine the loss from incompleteness of combustion. Usually, the loss is 3-7%, depending on the type of fuel, and with a large shortage of air can be up to 25% or more.

For example, 1% of carbon monoxide in the flue gases corresponds to approximately 6-7% of heat loss of the fuel consumed. It can be seen from the graphs that the calculated values of CO and CH₄ concentrations at the outlet correspond to a minimum of incomplete combustion: at the boiler outlet, the CO concentration is lower than the maximum allowable concentration, while CH₄ concentration is practically zero.

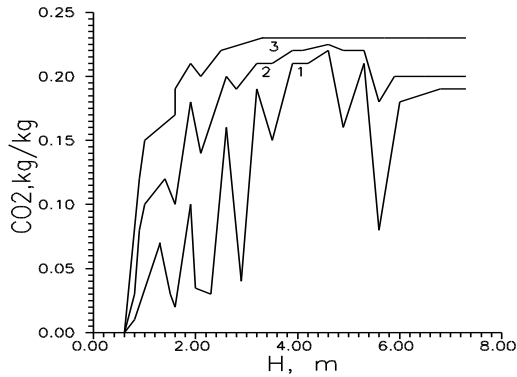


1-minimum, 2-average,
3-maximum value in the cross section

Figure 6 - Distribution of methane CH₄ concentration in the height of the combustion chamber

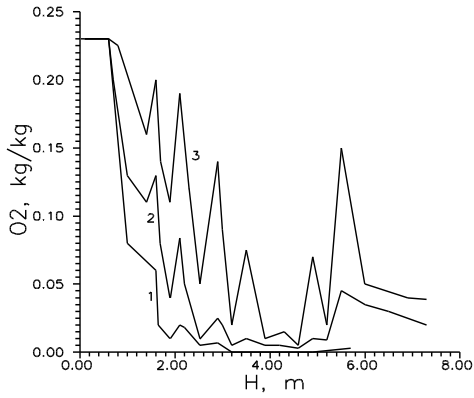
With the most cost-efficient operation of the boiler unit, the carbon dioxide content in the flue gases, depending on the type of top fuel, should be 13-15%. With a large excess of air, the content of carbon dioxide due to dilution with air in combus-

tion products can be reduced to 3-5%, but the loss of heat with outgoing gases will increase sharply. Figure 7 shows concentration distribution of carbon dioxide CO_2 along the channel height from which it can be seen that its concentration at the outlet is completely in line with standards and experimental values.



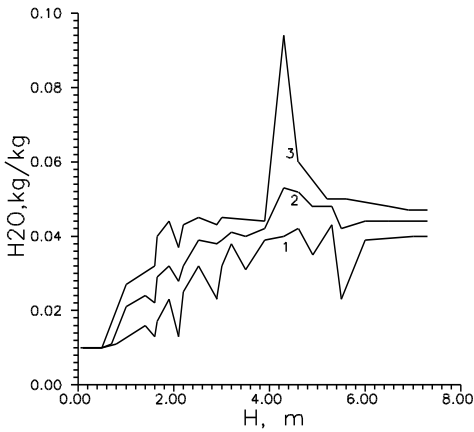
1-minimal, 2-average, 3-maximum value at cross-section

Figure 7 - Distribution of CO_2 carbon dioxide concentration by chamber height



1-minimum, 2-average, 3-maximum value in cross-section meanings

Figure 8 - Distribution of O₂ concentration throughout combustion chamber height

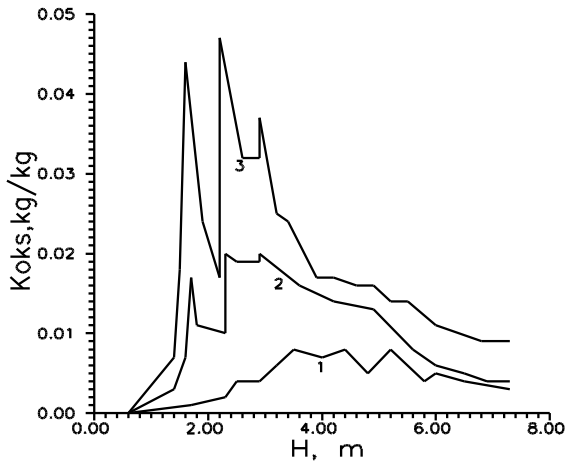


1-minimum, 2-average, 3-maximum value in the cross section

Figure 9 - Distribution of H₂O concentration throughout combustion chamber height

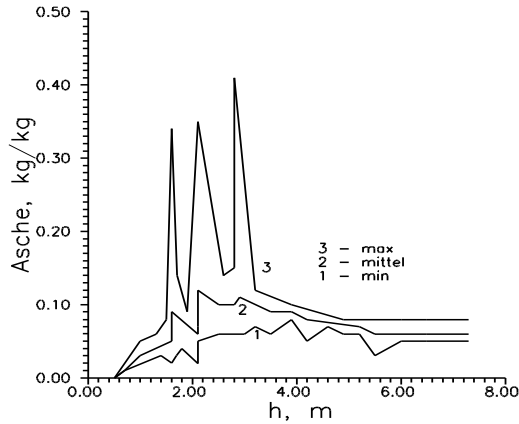
With complete combustion of fuel, flue gases contain nitrogen N_2 , oxygen O_2 (Fig. 8), carbon dioxide CO_2 , water vapor H_2O (Fig. 9), and in the presence of combustible sulfur in the fuel, which is sulfur dioxide SO_2 .

Fig. 10-11 show the change in the concentration of coke and ash (Asche) as it moves up combustion chamber. Naturally, it reaches its maximum in places where pulverized coal is supplied, coke residue is burned and ash is formed, i.e. where there are I-III tiers' burners of the boiler plant. At the coke output, we have small values, which indicates a minimum loss from mechanical incompleteness of combustion.



1-minimum, 2-average, 3-maximum value in cross-section

Figure 10 - Coke concentration distribution throughout combustion chamber height

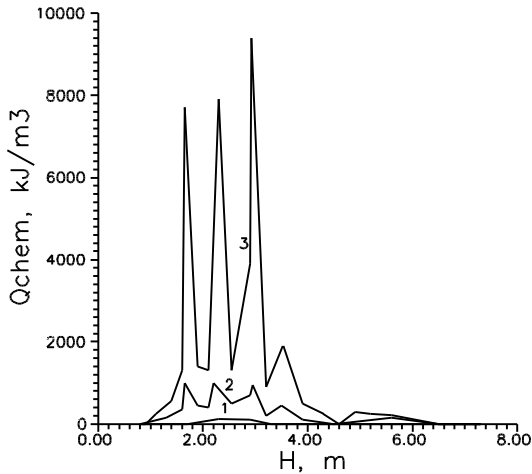


1-minimum, 2-average, 3-maximum values in cross-section

Figure 11 - Distribution of ash concentration (Asche) throughout combustion chamber height

Distribution of Q_{chem} energy released as a result of fuel combustion is shown in Fig. 12. This value reaches its maximum where coal combustion directly takes place, i.e. in places of fuel supply (burners of the first three tiers).

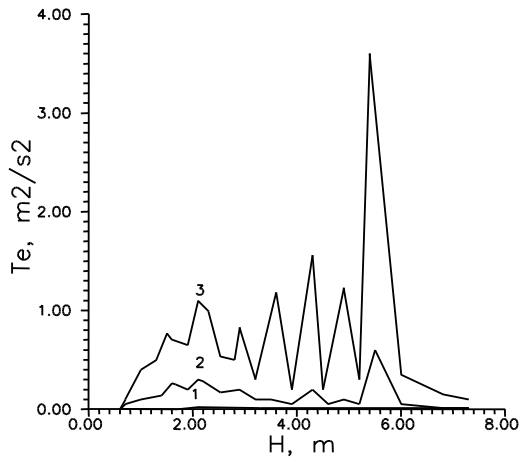
Figure 13 shows distribution of the kinetic energy of turbulence T_e in the boiler plant, which has the maximum values at the points of fuel supply and primary, secondary, tertiary air (seven tiers of holes and seven maxima on the distribution curve T_e), where the flow speed and disturbances are the highest.



1-minimum, 2-average, 3-maximum values

Figure 12- Distribution of Q_{chem} chemical energy throughout combustion chamber height

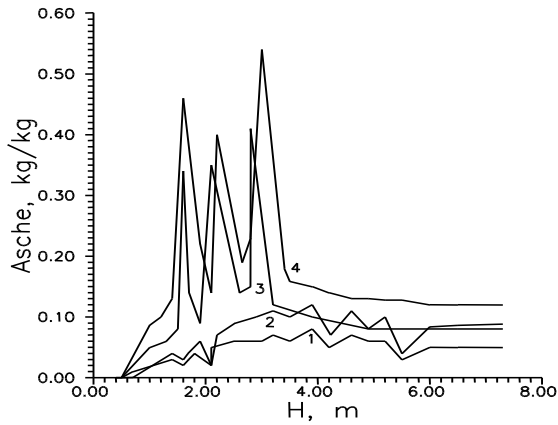
In the real operating conditions of the boiler, situations are created where an emergency stop of the mills is necessary. In this paper, a situation of a shutdown of pulverized-coal system was simulated, when the second stage of the burners is closed. To maintain the boiler's fuel load and boiler output, the second tier fuel is distributed between the remaining uncovered burners. As a result of solving this problem, this paper provides a detailed description of the fields of velocity, temperature and concentration of all coal combustion products: CO , CO_2 , CH_4 , H_2O , O_2 , coke, ash, etc., both for the nominal conditions and for closing of the corresponding burners.



1-minimum, 2-average, 3-maximum values

Figure 13 - Distribution of kinetic energy of turbulence T_e over the chamber height

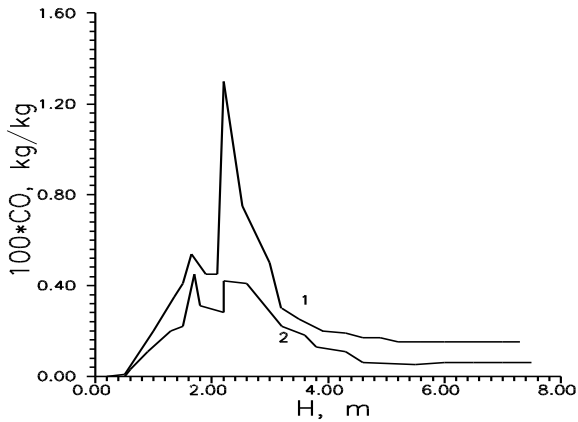
Figures 14-15 show some results of such studies: maximum and minimum ash concentrations (Asche) and maximum concentrations of carbon monoxide (CO) along the furnace space for two coal combustion modes. One mode, when the furnace is at full power, i.e. all burners are open and fuel is supplied through them. Another mode, when one of the tiers of burners is closed.



1, 2-minimum, 3, 4-maximum values,
 1, 3 - all burners are open, 2, 4- second tier burners are closed

Figure 14- Distribution of ash concentration for two operating modes of the furnace

From the analysis of the numerical experiment results, it can be concluded that the model studied in this section works steadily and can be recommended for computer simulation of such flows. The obtained results will allow to optimize the process of burning solid fuel and give the corresponding concept of energy generation with the minimum amount of harmful substances.



1, 2-maximum values, 2 - all burners are open,
1 - second tier burners are closed

Figure 15- Distribution of carbon monoxide concentration for two operating modes of the furnace

Test Questions:

1. What is a tangential furnace unit?
2. What is their advantage compared to furnaces equipped with vortex burners?
3. How can harmful effect of ash be reduced?
4. What is a muffle burner?
5. How is the excess air factor calculated?
6. Where is the maximum temperature zone located in combustion chamber?
7. What substances are formed as a result of fuel combustion?
8. How does the different operation mode of the burners affect the combustion of pulverized coal fuel?

3 ANALYSIS OF HEAT AND MASS TRANSFER PROCESSES IN SOLID FUEL COMBUSTION IN INDUSTRIAL BOILERS USING THE EXAMPLE OF PAVLODAR TPP

3.1 Initial data for simulation of Ekibastuz coal combustion (boiler BKZ - 420)

High ash content of Ekibastuz coal reduces the stability of flame ignition, while flame core is displaced to the exit from combustion chamber, and the outlet temperature is increased, which in turn leads to undesirable effects, for example, to increase nitrogen oxide emissions, to temperature deterioration of steam-heating devices. Recently, new highly efficient combustion devices designed to work on cheap low-grade coals have been widely developed. The boiler plant operation depends on many factors, including the design of the burner units and their arrangement [169-174]

This section considers the issues of aerodynamics, heat and mass transfer using the example of the BKZ-420-140 boiler plant at Pavlodar CHP. Boilers of this type had a different configuration of burners: a single-stage with a bilateral layout of straight-blow burners with tangential fuel supply and a two-stage burner when vortex burners are arranged on one side wall of the boiler. Each of these burners' arrangements, which to some extent depend on the boiler's performance, has its disadvantages and advantages. However, experience in operating boilers with different burner configurations and analysis of operation of furnaces for boilers burning Ekibastuz coal have shown that a more promising layout seems to be the opposed arrangement of the vortex burners, which ensures high stability of the combustion process [1, 154-156, 158, 162, 175].

The furnace chamber of the BKZ-420 boiler has the appearance shown in Fig. 16. Pulverized fuel is supplied to the com-

bustion chamber through the burners by a stream of air. For this purpose, combustion chamber is equipped with 12 turbulent burners located along the same line on the side walls of the boiler, 6 burners opposite of each other. BKZ-420 boiler is the main boiler for many CHPPs. There are 300 MW 16 boiler units and 9 500 MW boiler units with such furnaces [1] in Kazakhstan. In order to increase gas velocity in the upper part of the furnace unit, and thus reduce contamination of screens, the side walls of the chamber draw together upwards.

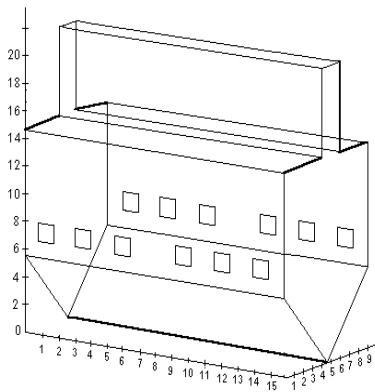


Figure 16 – Furnace chamber diagram
(BKZ-420-140 boiler plant)

The boiler's capacity is 67 347 kg/h. Then the air flow through each burner can be determined by the following formula:

$$V_i = \alpha_r V_0 B_i = 1.05 \times 4.508 \times 5612.25 = 26565 \text{ nm}^3/\text{hour},$$

where $\alpha=1.05$ is the excess air factor in the burner, $V_o=4.508 \text{ nm}^3/\text{kg}$ is the theoretical required air volume for combustion of 1 kg of fuel. Air supply speed from the bottom is determined

from the condition that the blow is 10% of the total amount of air blown into the combustion chamber. Technical characteristics of the BKZ-420-140 boiler and the initial data for modeling and optimization of Ekibastuz coal combustion process are given in Table 4, and composition of coal - in Table 6. In numerical calculations, a grid of 33x14x28 was used, which amounts to 12 936 reference volumes.

Table 4

Characteristics of the combustion chamber of BKZ420 boiler

Value Name	Designation	Dimension	Value
1. Fuel consumption	B	kg/hour	67 347
2. Fuel consumption through a burner	B_i	kg/hour	5612.25
3. Fuel calorific value	Q_N^P	kCal/kg	4050
4. Boiler capacity	Q	kw	31 9196
5. Furnace depth	A	m	9,024
6. Furnace width	B	m	15,744
7. Furnace height	H	m	20,9
8. Number of burner tiers	$n_{\text{яп}}$	unit	1
9. Number of burners	Z_{Γ}	unit	12
10. Burner diameter	D_{Γ}	m	1.05
11. Coal-air temperature	t_a	$^{\circ}\text{C}$	110
12. Air temperature in the burners	t_b	$^{\circ}\text{C}$	350
13. Excess air ratio in burners	α_{Γ}		1.05
14. Air velocity at the burner outlet	V_{Γ}	nm/s m/s	8.531 19.468
15 Speed of the circumferential velocity component in the burner	V_{φ}	nm/s m/s	6.8 15.518

Table 5

Fuel Characteristic

	EKIBASTUZ COAL								
Composition and characteristics of fuel	W ^P	A ^P	S ^P	C ^P	H ^P	O ^P	N ^P	V ^P	Q ^P _H /10 ⁴ (kJ/kg)
Contents (%)	8.0	36.8	0.8	44.2	2.9	6.5	0.8	30	1.697

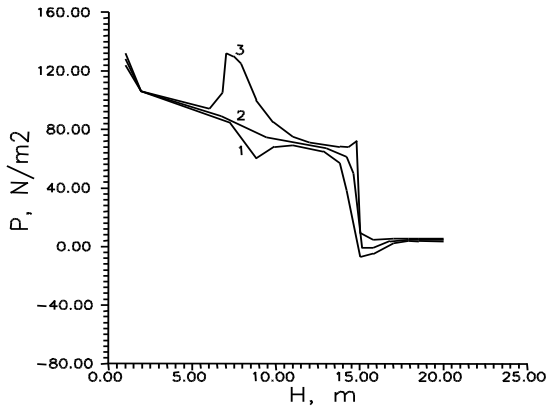
3.2 Numerical study results

The results of the numerical experiment are shown in Figs. 17-46. Swirl jets that supply fuel through counter-nozzles of burners located in the (X, Y) plane at $z = 7.81\text{m}$ create a volumetric vortex flow in the middle part of the furnace with an outlet to the directed "channel" flow between the adjacent side walls in the upper part of the furnace at $Z = 14.650\text{m}$. The velocities around the corners are small, except for the lower edge of the funnel $Z = 0$, $Y = 4.512\text{m}$, through which cold air is sucked.

Below the plane of the burners, $3 < Z < 7.81\text{m}$, the flow from the burners along with the air sucked from the lower edge of the funnel to create counter vortices with high velocities down in the (X, Y) plane and small circumferential velocities in the (Y, Z) plane. Under these vortices in the bottom region of the chamber (in its funnel at $0 < Z < 3\text{m}$), one can see the flow upwards near the (X, Z) symmetry plane at $Y = 4.512\text{ m}$. Thus, the maximal convective transfer in the considered chamber design is observed in the plane of the fuel mixture supply and in the symmetry plane along the depth of the furnace. This nature of the velocity field determines the established picture in the chamber volume: the maximum combustion is observed in its central part.

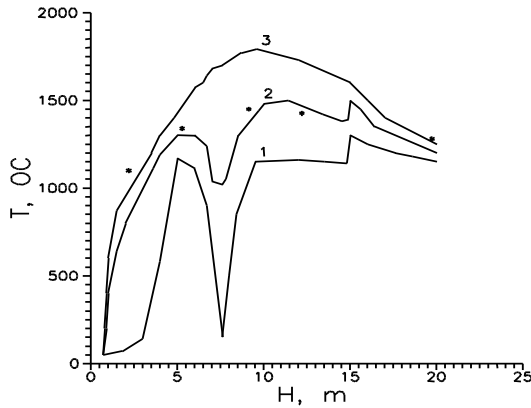
Fig. 17-28 provides the profiles of the maximum, minimum and average cross-section (X, Y) values of the values calculated for each value of $Z = \text{const}$. Thus, Fig. 17, where distribution of such values for the pressure over the boiler height is given, a sharp increase in the pressure in the fuel and oxidizer supply area and a gradual increase in pressure along the way to the exit from the boiler plant can be seen. True pressure is: $P_w = P + 10^5$ (Pa).

Figure 18 shows distribution of the maximum, minimum and average cross-sectional (X, Y) theoretical and experimental temperature throughout boiler height. The minima on all the curves are related to the low temperature of the air and fuel mixture entering this area of the combustion chamber through the burners. Comparison shows good compliance with experimental data. The temperature at the furnace outlet is about 1200°C , and the greatest differences in the calculated values from the experimental values are observed in the core flame region. The gas at the top of the furnace is higher than the estimated temperature level, as noted in the monograph [1], with impeded conditions for igniting the Ekibastuz coal flare due to its high ash content and deteriorated heat exchange in the furnace, which is possibly determined by screen contamination caused by it being covered with an ash bed.



1-minimum, 2-average, 3-maximum values

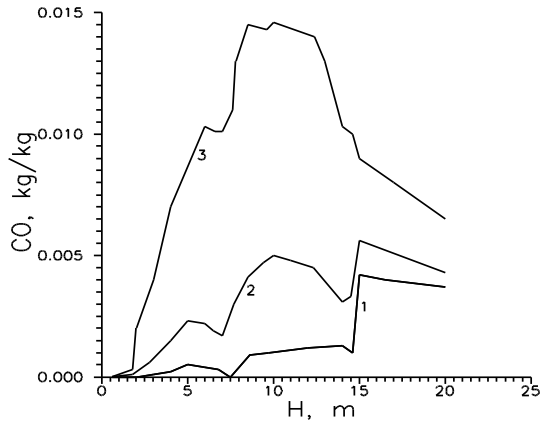
Figure 17- Distribution of pressure throughout the combustion chamber height



1-minimum, 2-average, 3-maximum values;
line-calculation, *-experiment

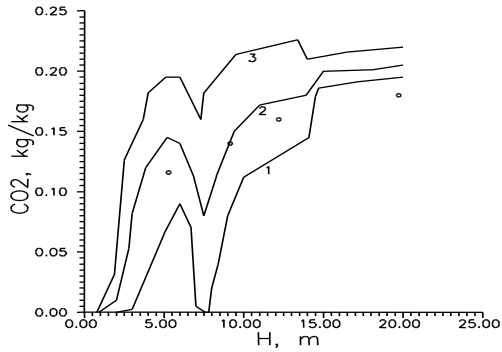
Figure 18 - Temperature distribution throughout the combustion chamber height

Distributions of the maximum, minimum and average values for the carbon dioxide concentration (X, Y) CO₂ (carbon dioxide), CO (carbon monoxide), oxygen O₂ and methane CH₄ throughout the height of combustion chamber are shown in Figures 19-20. The maximum reached by CO (Fig. 19) and CH₄ (Fig. 20) curves is in the area of the burners' location, where the formation of carbon monoxide occurs in the course of chemical reactions between the fuel and the oxidant. In the output of the boiler plant, CO₂ concentration is approximately 19% at a rate of 16-18%, (Figure 20), the CO concentration is about 0.4%, methane CH₄ is 0.2%, which is below the permissible limit. The maximum O₂ values in Figure 21 correspond to air supply through the cold funnel (H = 0) and through the burners.



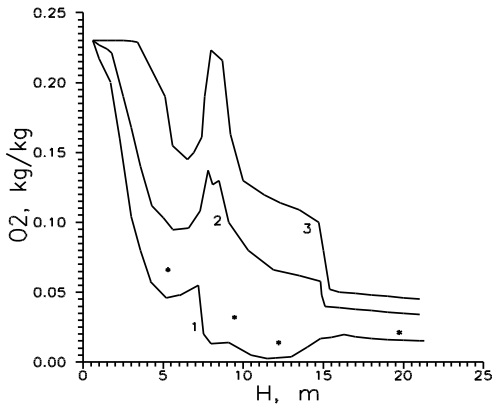
1-minimum, 2-average, 3-maximum values

Figure 19 - Distribution of CO concentration throughout the combustion chamber height



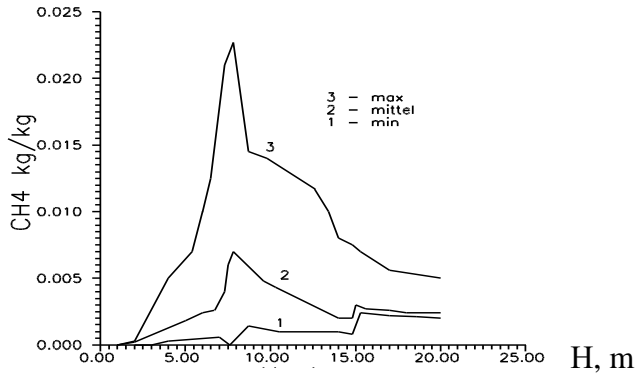
1-minimum, 2-average, 3-maximum values;
line-calculation, *-experiment

Figure 20 - Distribution of CO₂ concentration throughout the combustion chamber height



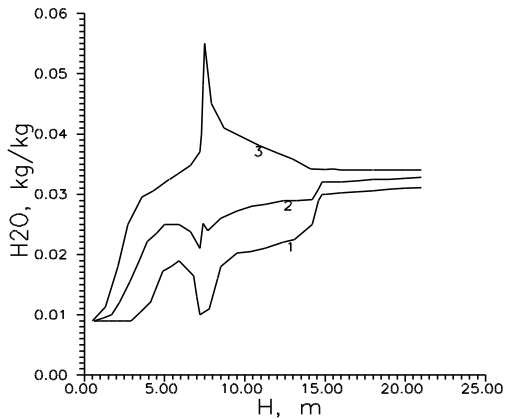
1-minimum, 2-average, 3-maximum values;
line-calculation, *-experiment

Figure 21 - Distribution of O₂ concentration along the combustion chamber



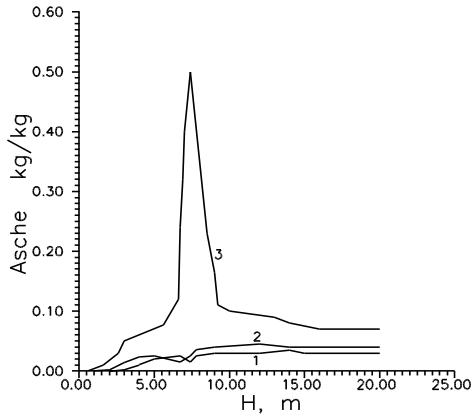
1-minimum, 2-average, 3-maximum values;

Figure 22 - Distribution of methane CH₄ concentration throughout the combustion chamber height



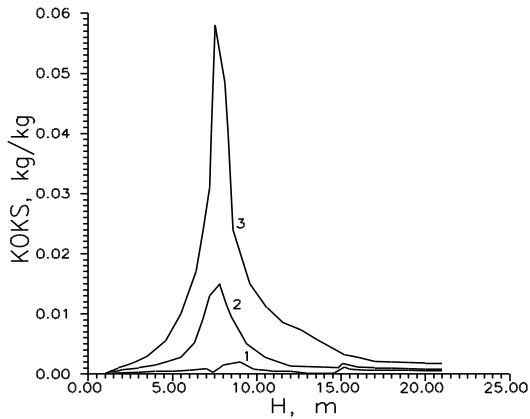
1-minimum, 2-average, 3-maximum values

Figure 23 - Distribution of H₂O concentration throughout the combustion chamber height



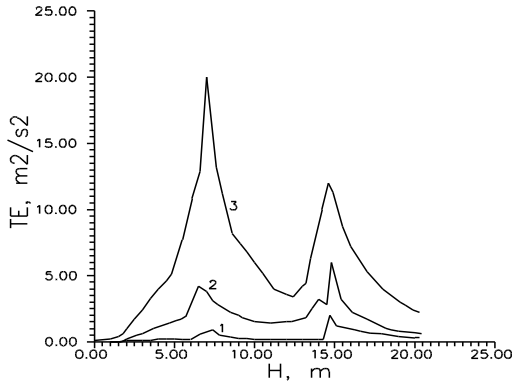
1-minimum, 2-average, 3-maximum values

Figure 24 - Distribution of ash concentration throughout the combustion chamber height



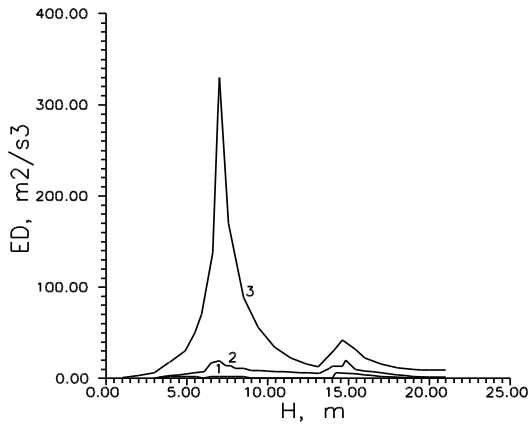
1-minimum, 2-average, 3-maximum values

Figure 25 - Coke concentration distribution throughout the combustion chamber height



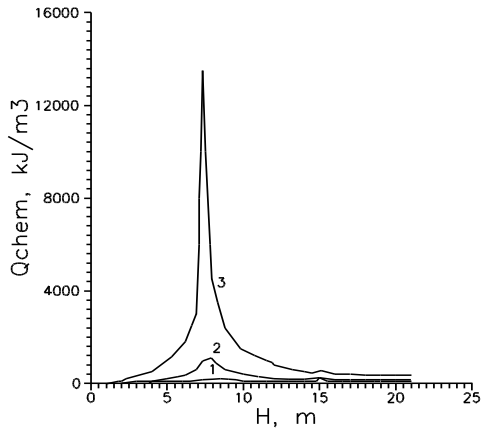
1-minimum, 2-average, 3-maximum values

Figure 26 - Distribution of kinetic energy turbulence throughout the combustion chamber height



1-minimum, 2-average, 3-maximum values

Figure 27 - Distribution of energy dissipation throughout the combustion chamber height



1-minimum, 2-average, 3-maximum values

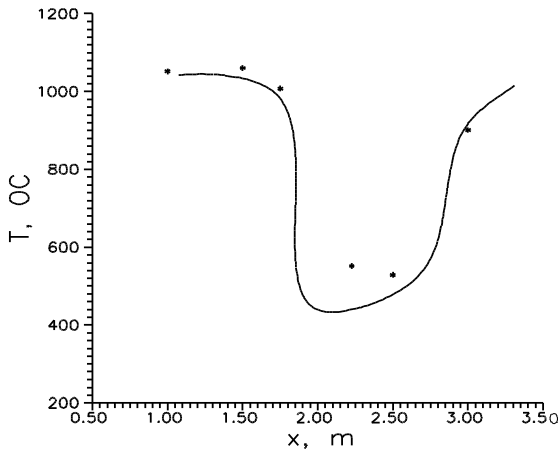
Figure 28 - Distribution of Q_{chem} chemical energy throughout the combustion chamber height

Analysis of the graphs shown in Fig. 23-28 shows that the most abrupt changes that all the curves undergo in these figures take place in the locations of the burners, through which both fuel and air are supplied. It is in this area of the combustion chamber that the core of the flame is located, where the most intense chemical reactions occur between the fuel carbon and the oxygen of the oxidant, with the generation of both CO_2 and CO , H_2O (Fig.23), ash (Fig. 24), coke (Fig. 24), with the highest emission of heat Q_{chem} (Fig. 28) and the highest level of turbulence (Fig. 26, Fig. 27).

It is obvious that the greatest discrepancy with experiment (Fig. 18, 20-21) is observed in the area of ignition and combustion of volatile substances. One of the main reasons for this is determination of combustion rate of gases using a one-stage pyrolysis model, which uses a number of kinetic constants for the entire temperature range. However, it should be noted that

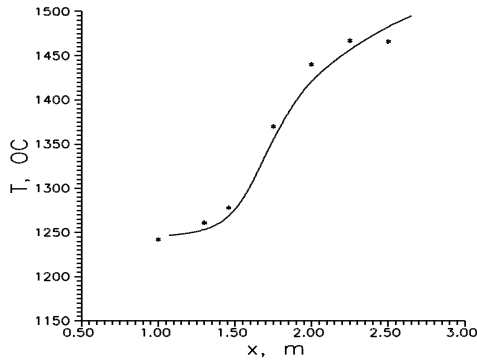
the change in the pyrolysis parameters and combustion model does not have a significant effect on the simulation results [67]. The results of calculation here are quite in line with the experimental measurements. Thus, we can conclude that the version of the mathematical model that we use is suitable for the calculation of the formation of harmful substances and can be used to calculate the currents in furnaces of operating boiler units.

Fig. 29-30 show the temperature distributions along the first two burners along the x axis, for two values of the y coordinate (0.54m and 4.6m in the depth of the furnace) in the section of the boiler at the burners level of the ($z = 7.5$ m). The sharp drop in temperature (Fig. 29) on the curve at $y = 0.54$ m (near the burner nozzle) takes place in the area where cold air mixture enters and then sharply reaches a maximum in the area of combustion space between the burners.



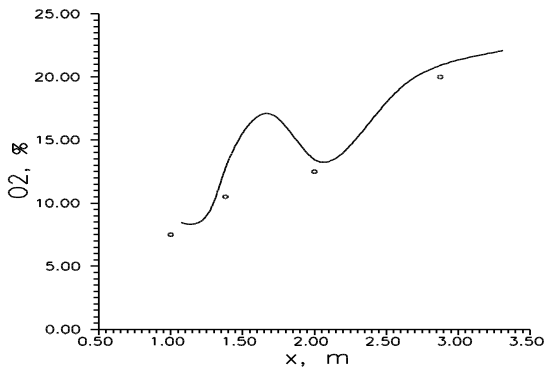
In-depth section of chamber $y=0.54$ m
line - theory, *-experiment

Figure 29 - Temperature distribution across the width of the chamber in the area of the first two burners



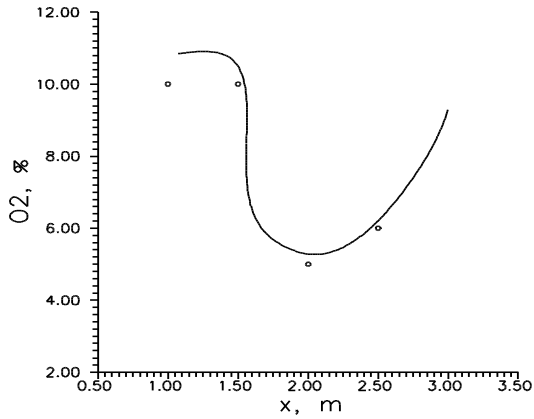
In-depth section of chamber $y=0.54\text{m}$
 line - theory, *-experiment

Figure 30 - Temperature distribution across the width of the chamber in the area of the first two burners



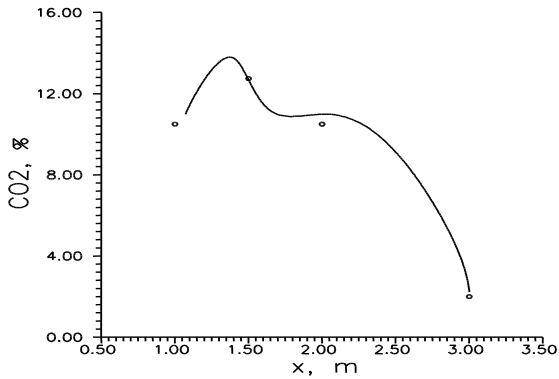
In-depth section of chamber $y=0.54\text{m}$
 line - theory, *-experiment

Figure 31 – O₂ concentration distribution throughout the chamber width in the area of the first two burners



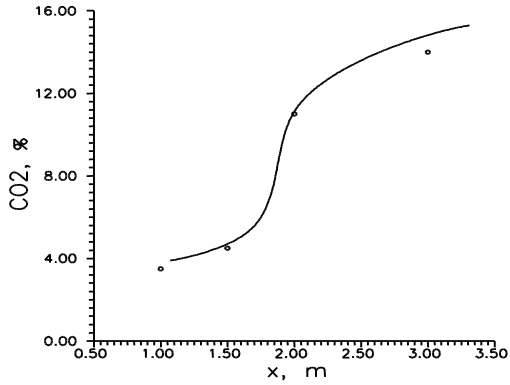
In-depth section of chamber $y=4.6\text{m}$
line - theory, *-experiment

Figure 32 – O₂ concentration distribution throughout the chamber width in the area of the first two burners



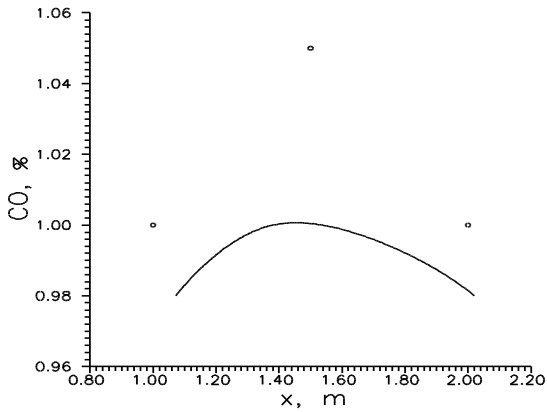
In-depth section of chamber $y=0.54\text{m}$
line - theory, *-experiment

Figure 33 – CO₂ concentration distribution throughout the chamber width in the area of the first two burners



In-depth section of chamber $y=4.6\text{m}$
line - theory, *-experiment

Figure 34 – CO₂ concentration distribution throughout the chamber width in the area of the first two burners



In-depth section of chamber $y=4.6\text{m}$
line - theory, *-experiment

Figure 35 – CO concentration distribution throughout the chamber width in the area of the first two burners

Figure 30 shows the temperature curve at the furnace axis, i.e. at a distance $y = 4.6$ m into the furnace depth. Here, far from the nozzle section of the burner, the curve has a different temperature character, namely, the temperature on the jet axis increases as it moves to the center of the combustion chamber (see diagram in Fig. 37). The experimental data presented in Fig. 29-30, obtained directly from the Pavlodar CHPP, indicate a good agreement with the calculated data of the computing experiment.

This also fully applies to the calculation results of concentrations of O_2 , CO_2 and CO in the above sections of the combustion chamber (Fig. 31-35). Near the burner hood, the greatest changes in temperature and concentrations of O_2 , CO_2 and CO are observed. The difference in the results of numerical simulation and experimental data does not exceed one percent. This implies sufficient reliability of our proposed mathematical model describing convective heat and mass transfer when burning solid fuel in a particulate form in the combustion chambers of boiler plants and a program for calculating the turbulent characteristics of this process. Calculated values of T , O_2 , CO_2 and CO in the cross section located in the range of the chamber burner position ($Z = 7.5$ m) were determined using the diagrams presented in Fig. 17-36.

3.3 Results of the study of the effect of operating parameters on heat and mass transfer in the combustion chamber

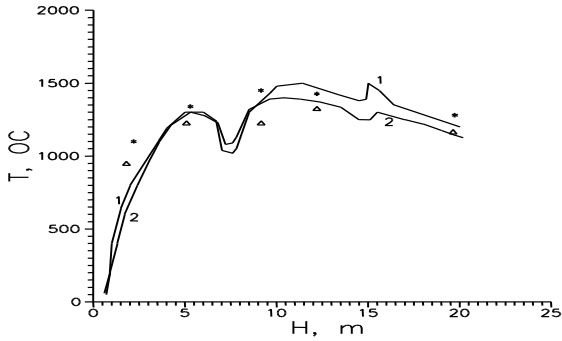
When boilers operate, it is often necessary to turn off part of the burners due to the shutdown of the pulverized-coal system. In this work, this situation was modeled (hereinafter referred to as "emergency") in order to see how the ignition conditions have changed. However, the results of a numerical experiment will offer an optimal mode of shutting down the burners and

supplying air therein, which would not affect conditions of ignition and burning out of the flare.

For example, Figures 36-42 present distribution of the average temperature T across the cross section and concentrations of O_2 , CO and CO_2 along the furnace for two modes of operation: the basic mode, when all the burners are working (full load of the fuel boiler according to Table 1), and, say, "emergency" mode, when for one reason or another it is necessary to disconnect the burners 1, 3, 5.

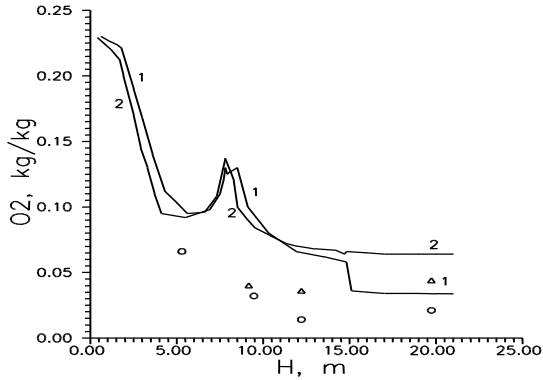
Despite the fact that coal is not supplied to these burners, 30% of the previously supplied air is supplied to them in the computing experiment. It is customary to do this on full-sized boilers in order to prevent burnout of the outlet part of the burners. The qualitative nature of temperature distribution and concentrations of O_2 , CO and CO_2 does not change for these two modes.

However, it should be noted that if the flare ignition did not affect the boiler loading mode, the burner shutdown resulted in a general decrease in the temperature level in the furnace unit, which led to a decrease in the temperature at the outlet from the combustion space by $73^{\circ}C$ (curve 2 in Fig. 36). It can also be noted that the comparison with the experimental data provides a greater difference for the temperature distribution in the "emergency" mode.



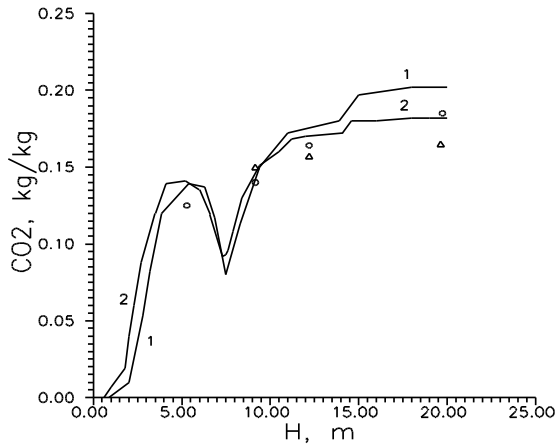
1, *-all burners are in operation; 2, Δ -burners 1,3,5 are closed, line - theory, Δ -experiment

Figure 36 - Mean temperature T distribution along the combustion chamber for two boiler load options



1, o - all burners are in operation; 2, Δ - burners 1,3,5 are closed, line - theory, o, Δ - experiment

Figure 37 - Distribution of O_2 concentration throughout the combustion chamber height for two boiler load options

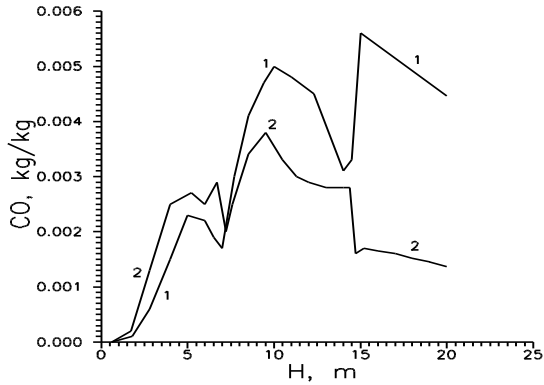


1, o - all burners are in operation; 2, Δ - burners 1, 3, 5 are closed, line - theory, o, Δ - experiment

Figure 37 - Distribution of CO₂ concentration throughout the

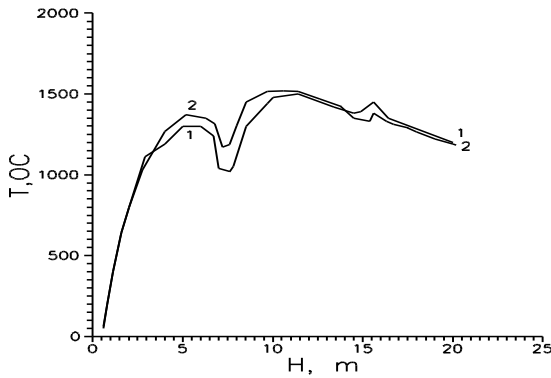
combustion chamber height for two boiler load options

As for O₂ concentration, switching off the burners for fuel, which means a reduction in the boiler load, should lead to an increase in the air excess ratio, and consequently also to an increase in the oxygen concentration (curve 2 in Figure 37) at the furnace outlet. This is confirmed by both experimental and calculated data presented in this figure. On the contrary, for obvious reasons the decrease in fuel supply reduced the CO concentration (curve 2 in Fig. 39) and CO₂ (curve 2 in Figure 38), the latter being verified by experiments on the operating boiler, both generally for combustion space, and at the outlet.



1- all burners are in operation; 2 - burners 1, 3, 5 are closed

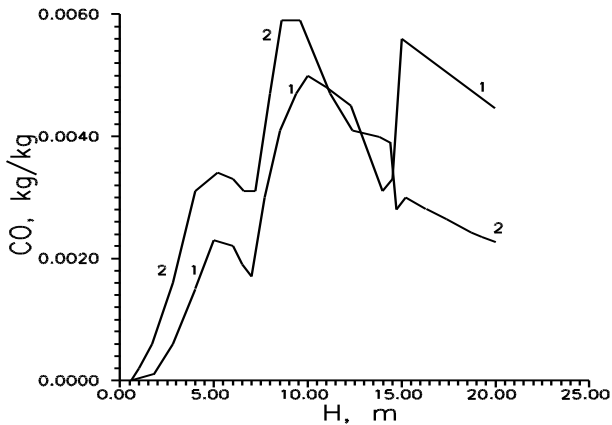
Figure 39 - Distribution of CO₂ concentration throughout the combustion chamber height for two boiler load options



1- all burners are in operation; 2 – fuel from burners 1, 3, 5 was transferred to burners 2, 4 and 6

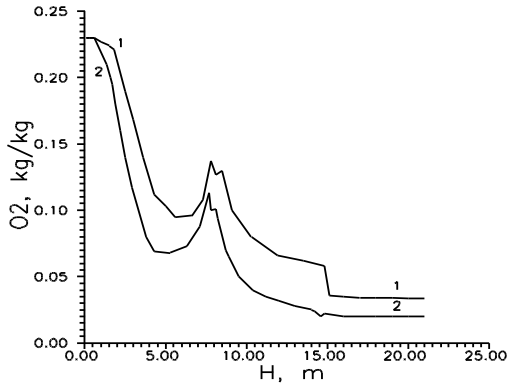
Figure 40 - T temperature distribution for two modes of boiler operation at its nominal load

In Fig. 40-42 presents results of simulation of production situation when the boiler is operating in nominal mode, but fuel in the burners is distributed unevenly: burners 1, 3, 5 are closed to fuel, which is transferred to burners 2,4,6. In this option we have an undesirable eccentricity of fire in the fuel chamber. The above figures make a comparison with the basic version, determined by the data in Table 6, when all the boiler burners are operating. Analysis of the graphs presented in Fig. 40-42 showed that the greatest difference in temperature for the two options (curve 1-basic, curve 2-fuel eccentricity Fig. 40) is observed in the body of flame, and it is almost the same at the boiler outlet. In turn, output CO concentrations (curve 2 in Fig. 41) and O₂ (curve 2 in Fig. 42) decrease in comparison with the base mode, although they behave differently inside combustion chamber: CO concentration is greater and O₂ is less than their values in the base mode (curves 1).



1- all burners are in operation; 2 – fuel from burners 1, 3, 5 was transferred to burners 2, 4 and 6

Figure 41 - CO concentration distribution for two boiler operation modes at its nominal load



1- all burners are in operation; 2 – fuel from burners 1, 3, 5 was transferred to burners 2, 4 and 6

Figure 42 – O₂ concentration distribution for two boiler operation modes at its nominal load

All the experimental data given in this section were obtained in field experiments conducted directly by the staff of the KazNIIenergiki at the operating boiler BKZ-420-140 of Pavlodar CHPP and are presented in their works [1, 176-180]. Unfortunately, it was impossible to compare all the process characteristics of convective heat and mass transfer taking into account combustion and chemical reactions obtained at this boiler as a result of the computing experiment conducted in the present paper. Lack of experimental data on some characteristics of the combustion process is due to inability to obtain them practically.

In this sense, the importance and convenience of numerical modeling of complex phenomena that occur in combustion chambers are quite obvious. As a result of the computing experiment at BKZ-420-140 boiler, an extensive databank of various characteristics of combustion process was obtained in this

paper, including aerodynamics, temperature, pressure, concentrations field of both gas and solid composition of combustion products, turbulent characteristics (kinetic energy of turbulence and energy dissipation), energy released by chemical reactions for various loads and modes of operation.

Analysis of the results obtained in this section showed that, except for the region of ignition and combustion, the discrepancy between the calculated and measured temperature and concentration distributions at the CHPP is quite acceptable. Although the neglect of two-phase effects and simulation of pulverized coal as a monodisperse phase presents a rough simplification for regions with a high solid fuel loading (burner hood region and core flame), the nature of the distribution of velocities, temperature, pressure and concentrations is nevertheless simulated quite well. The results obtained will undoubtedly help optimize the combustion of fuels relative to efficiency and minimization of harmful emissions and create power plants using "clean" and efficient coal.

Control Questions:

1. What is a BKZ -420 boiler?
2. How many burners does combustion chamber of BKZ-420 boiler has? How are they arranged?
3. How to determine air flow rate through the burner?
4. What are the dimensions of the furnace chamber of the BKZ-420 boiler?
5. What is the composition of Ekibastuz coal?
6. How are the pressure and temperature in the combustion chamber distributed?
7. What is the "emergency mode" in the operation of combustion chamber?
8. How does the burner shutdown affect the temperature in the combustion chamber?

4 SIMULATION OF OPTIMAL COMBUSTION MODES FOR PULVERIZED COAL FUEL USING THE EXAMPLE OF EKIBASTUZ GRES [181-186]

4.1 About the problem of reduction of nitrogen oxides NO_x

While protection of the atmosphere against PM emissions has been successful, it is much more difficult to deal with gas pollutants, and especially with NO₂ and SO₂. This is because before 1950-1960, research and work on the protection of the atmosphere from TPP emissions were carried out for solid pollutants and sulfur dioxide, and a number of TPPs were created subject to compliance with the MPC only for these pollutants. In our country, a requirement has been adopted, according to which total concentration of nitrogen oxides, sulfur and carbon monoxide was determined from the following condition:

$$\frac{C_{SO_2}}{\text{ПДК}_{SO_2}} + \frac{C_{NO_x}}{\text{ПДК}_{NO_x}} + \frac{C_{CO}}{\text{ПДК}_{CO}} \leq 1$$

Carbon monoxide appears as a result of an incomplete oxidation reaction of slag carbon and volatile coal particles evaporating. Generation of carbon monoxide depends on the temperature and oxygen concentration in the reaction zone and can therefore be reduced by an increased excess of air and high temperatures. However, this in turn results in an increase in the formation of nitrogen oxides NO_x.

Nitrogen oxides, the maximum permissible concentration of which is 6 times lower than for sulfur dioxide, are now they are recognized to be the most toxic pollutants of the atmosphere. It is believed that the emissions of nitrogen oxides (NO_x= NO + NO₂), generated during combustion, contribute to the oxidation of atmospheric precipitation, photochemical air pollution and

depletion of the ozone layer. Nitric oxide (NO), which is more than 90% of the total amount of its oxides emitted by the combustion devices, is oxidized further in the atmosphere to NO₂. Thus, one of the urgent tasks in the development of new and operation of existing combustion devices is to reduce the concentration of nitrogen oxides in combustion products.

Basically, there are two sources of formation of nitrogen oxides during combustion of hydrocarbon fuels. First of all, they are formed due to fuel nitrogen oxidation (up to 90%). This is the so-called "fuel NO_x". This reaction can be affected by oxygen concentration and temperature in the reaction zone, the time of gas residence in the high-temperature zone. At temperatures above 1300°C, oxidation of nitrogen in the air takes place - "thermal NO_x" [187].

The regularities in the formation of air NO_x in the combustion of gas mixtures were studied most extensively by Ya.B. Zeldovich and others [118]. It was shown that the reaction of generation of nitrogen oxide from nitrogen and air oxygen has a thermal nature and activation energy of this reaction is very high $E=129000$ kcal/mol. To date, there are many studies on the mechanism of generation of "fuel" NO_x [155, 167, 188-217].

Thus, the author of works [155, 188-189] showed that when coal is burned, fuel nitrogen is distributed between volatiles and coke. Part of the nitrogen subsists in coke due to carbon in fly ash to the very end of the furnace. The proportion of nitrogen oxides generated from coke is relatively small and amounts to about 20%. For the most part fuel nitrogen oxides are generated from fuel nitrogen volatiles. The mechanism of this process is understudied, but it is known that was in a complex reaction, the fuel nitrogen released during pyrolysis is oxidized or reduced, and NO_x generation process proceeds simultaneously with the process of its reduction to N₂.

It was noted in [167] that no further NO oxidation occurs during movement along the gas path of the boiler. After it exits chimney into the atmosphere, the main part of NO over a relatively short period of time under the exposure to oxygen from the surrounding air passes into NO₂ according to the following reaction: $2\text{NO} + \text{O}_2 \rightarrow 2\text{NO}_2 + 188 \text{ J/mol}$. Based on the experimentally established fact that atomic nitrogen is generated in the reaction zone at high temperatures, whose amount is several times greater than the amount of atomic oxygen produced as a result of thermal dissociation of atmospheric oxygen, the following nitrogen oxides generation mechanism can be represented as follows: $\text{O} + \text{N}_2 \leftrightarrow \text{NO} + \text{N}$; $\text{N} + \text{O}_2 \leftrightarrow \text{NO} + \text{O}$. However, atomic oxygen is generated in a significant amount in the intermediate stages of the combustion reaction of hydrocarbons and carbon dioxide. Figure 43 shows the conversion scheme for nitrogen-containing compounds adopted during coal combustion [194-195].

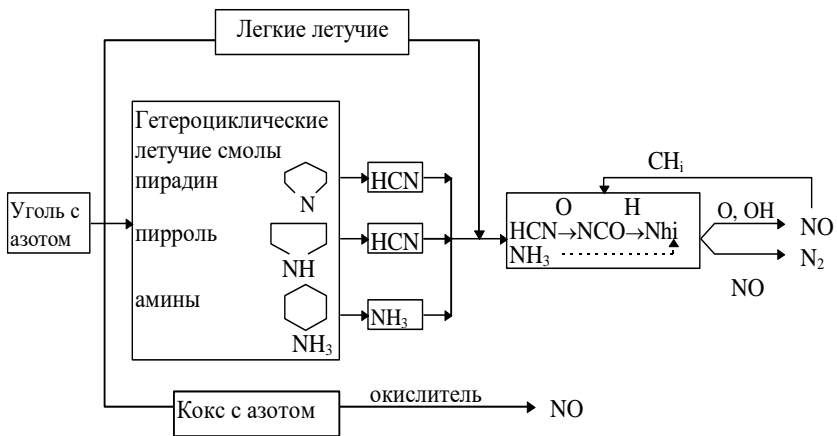


Figure 43 - Scheme of transformation of nitrogen-containing compounds during coal combustion

Various methods for suppressing the generation of nitrogen oxides during combustion have been developed and it has been shown that there are two methods to reduce NO_x emissions: by changing the burning technology and by cleaning gases after combustion. Changes in combustion technology include the use of burners with low NO_x emissions, staged fuel combustion, preparation of low-grade coals for combustion, recirculation of flue gases, etc.

Preparation of fuel for combustion is based on the intensification of combustion of low-grade coals in steam generators using partial or complete gasification of fuel. One of the progressive methods is the method of pulse initiation of pulverized coal streams combustion by AC plasma jets, associated with the thermochemical preparation of high ash content coals and plasma processing of low-grade energy coals. Works [217-224] are devoted to such studies.

It was shown in work [217] that recirculation of gases and a decrease in the temperature of core flame, where the main source of NO_x is air nitrogen, are ineffective if the main source of NO_x is fuel nitrogen. Two-stage combustion is one of the effective ways of burning NO_x , where the burner operates with a reduced air excess (or even with lack of air), and the missing part of the combustion air is supplied behind the zone of generation of most of NO_x .

This causes a decrease in the ignition zone of the flare oxygen concentration and mass transfer rate in the gas phase due to a decrease in secondary air velocities at the burner outlet.

The authors of work [191] argue that the widely used method of suppressing nitrogen oxides during combustion of gaseous fuels by introducing recirculation of flue gases into the ignition zone proves to be ineffective when burning solid fuels. Staged combustion seems to be more promising, and it can be arranged in various ways. For example, fuel redistribution in

tiers or rows of burners. Such a scheme is used in furnaces with corner burners [192] and is recommended in a circular furnace [190, 193]. Or it is possible to arrange staged combustion by applying a reduced air excess to all the main burners and injecting the missing air upstream of the flare. Based on the analysis of the work presented above, it can be concluded that staged combustion is one of the most effective ways to reduce "fuel NO_x " in the combustion of solid fuels as in flaring high-ash coals, the bulk of NO_x (up to 80%) is generated at the initial flare section, i.e. in the volatiles outlet and ignition zone. Therefore, the main condition for reducing the rate of NO_x generation reaction is a decrease in the oxygen concentration in this zone. In addition, collision of opposite flares enhances heat and mass transfer and intensifies the combustion process.

4.2 Characteristics of furnace chamber of PK-39 boiler

This section presents the results of simulations of convective heat and mass transfer in the staged combustion of pulverized coal fuel. The entire computing experiment was performed for the PK-39 boiler to a 300MW block 0, with a steam output of 475 t/h. Boiler is installed at Aksu power station (formerly Ermakovskaya GRES). Fig. 44 is an overall diagram of the combustion chamber of this boiler. The boiler top is equipped with 12 swirl three-channel burners.

The burners are arranged opposite to each other in two tiers of 6 burners each and have two sizes that ensure different air ratio therein: bottom tier $\alpha_r=1.4$, upper tier $\alpha_r=0.9$. Fuel in tiers is distributed equally (nominal mode for the base version), the cold funnel slot has the following dimensions: (0.836 x 5.50) m², height of the funnel: 5.335m.

A detailed description of the boiler characteristics, its dimensions, number and location of burners, productivity, air

temperature, air mixtures and walls, etc., as well as coal data used for numerical simulation, are presented in Table 6.

To intensify the ignition, air is supplied to the chamber in such a way that the oxygen contained therein reacts gradually. Usually, for this purpose, all air is divided into primary, supplied in a mixture with coal dust, and to the secondary, supplied separately from the primary through the same burners or, less often, apart from them. Part of the primary air is used to dry fuel in the pulverized-coal system. Consequently, primary air is used for three purposes: as a drying agent, for transporting dust into the furnace and as one of the reagents of the flame fuel.

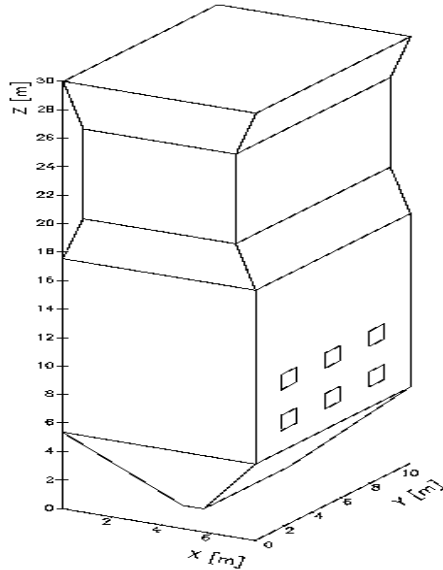


Figure 44 – General layout of combustion chamber

Data on the recommended proportion of primary air that were obtained from the experience of long-term boilers operation are given in [167]. The greater the reactivity of the fuel is,

the more volatile combustibles it has in it, and the more perfect is the burner and furnace devices and the better is combustion process, the larger the proportion of primary air should be taken. Work [227], where the effect of oxygen content on the ignition of a vortex flare is considered, shows that a decrease in the oxygen content in secondary air significantly worsens the flame ignition conditions, while length of the core flame increases and the maximum temperature decreases. Table No. 6 shows the rates of primary and secondary air supply by tiers for the boiler plant under consideration. For numerical simulation we used a 16x33x41 grid, which is 21 648 control volumes (see Figure 45).

The basic conditions for the correct arrangement of the combustion process are determined to a certain extent by aerodynamics of the furnace space, which in turn depends on the shape and dimensions of combustion chamber, as well as on the design, operating modes and layout of burners.

A distinguishing characteristic of flows in a vortex flame with strong whirling is the occurrence of a counterflow in the near-axis region of the jet near the nozzle (Fig. 46). As is well known, presence of a reverse currents zone of flue gases, similar to a wake behind a poorly streamlined body, plays a major role in the flame stabilization phenomena (see, for example, [166], as heat content of these gases determines the warm-up of the fuel, the release of volatiles and their ignition.

The farther from the burner mouth the formation of a zone of axial reverse currents will begin, the greater will be the probability that high-temperature flue gases will enter it. In this case, not the entire jet is warmed-up, but only the layers that are located near the boundary of the axial reverse currents zone. Heat from combustion of volatile and fine coke residue fraction in this region goes towards warm up of adjacent layers of the fuel-air mixture, etc.

Table 6

Characteristics of combustion chamber of PK-39 boiler

№	Description, characteristic and dimensions	Designation	Величина
1.	Fuel consumption rate per boiler, kg/h	B	87 500
2.	Fuel consumption rate per burner, kg/h	$B_{\Gamma} = B/Z$	7291.1
3.	Fuel - Ekibastuz coal, Coal composition, %	W^P A^P S^P C^P H^P O^P N^P	7.0 40.9 0.8 41.1 2.8 6.6 0.8
4.	Calorific value, MJ/kg	Q_H^P	15.87
5.	Volatile content, %	V^F	30.0
6.	Coal particles diameter, $m \cdot 10^{-6}$	d_{par}	30.0
7.	Excess air factor at the furnace outlet	α_{Γ}	1.25
8.	Excess air factor at the burners	α_{Γ}	1.15
9.	Air inflow into combustion chamber	$\Delta\alpha$	0.1
10.	Air mix temperature, $^{\circ}\text{C}(\text{K})$	T_a	150(423)
11.	Secondary air temperature, $^{\circ}\text{C}(\text{K})$	T_2	327(600)
12.	Tertiary air temperature, $^{\circ}\text{C}(\text{K})$	T_3	327(600)
13.	Wall temperature, $^{\circ}\text{C}(\text{K})$	T_w	600(873)

Table 6 (continued)

1	2	3	4
14.	Type of burners used	vortex	
15.	Number of burner, unit	n_B	12
16.	Number of tiers,	n	2
17.	Furnace height, m	$z(H)$	29.985
18.	Furnace width, m	y	10.76
19.	Furnace depth, m	x	7.762
20.	Primary air velocity (air-fuel mixture) of the bottom tier burners, m/s	W_1	15.0
21.	Secondary air velocity of the bottom tier burners, m/s	W_2	28.0
22.	Tertiary air velocity (air-fuel mixture) of the bottom tier burners, m/s	W_3	26.0
23.	Central air velocity (air-fuel mixture) of the bottom tier burners, m/s	W_0	10.0
24.	Primary air velocity (air-fuel mixture) of the upper tier burners, m/s	W_1	15.0
25.	Secondary air velocity of the upper tier burners, m/s	W_2	23.0
26.	Tertiary air velocity (air-fuel mixture) of the upper tier burners, m/s	W_3	23.0
27.	Central air velocity (air-fuel mixture) of the upper tier burners, m/s	W_0	10.0
28.	Size of the bottom tier burners. m	\emptyset	1.2
29.	Size of the upper tier burners. m	\emptyset	1.05

Vortex burners, based on their operating principle, can be considered individual. In the furnaces in which they are used, flame ignition and the burnout process are mainly organized with the help of the burners themselves and, to a lesser extent, by their layout in the furnace. Therefore, operation of the furnace, in particular at the initial section, can be experimentally investigated at a testing facility with a single burner.

Obtaining the aerodynamic characteristics of an individual flame and the flow of gases in combustion chamber makes it possible to estimate with a sufficient degree of approximation the efficiency of the combustion process organization and use this data in numerical simulation. And since in the level section of the flare (2-3 burner diameters) it can burn up to about 90% of the fuel, in mathematical simulation of convective heat and mass transfer processes in combustion chambers, it is very important to correctly set the initial and boundary conditions on the velocity that would correspond to the combustion scheme adopted for the boiler.

In numerical simulation to determine boundary conditions for the velocity at the output section of the burner we used profiles obtained on isothermal and firing stands with a vortex three-channel burner [181, 228]. Figure 47 shows these profiles of the velocity vector components (u , v , w), referred to W_0 (average consumption velocity) and obtained during experimental studies of aerodynamic structure of isothermal flare on the model (scale 1:20) of the PK- 39-II.

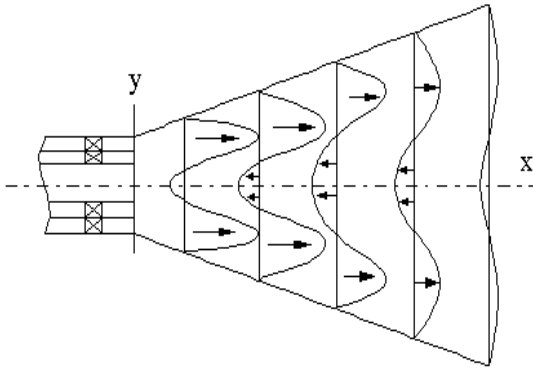
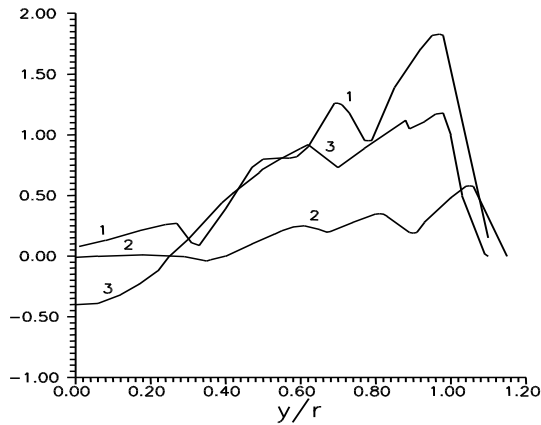


Figure 46 - Flow pattern in the vortex burner flame

When carrying out computing experiment, as in the previous sections, the effect of chemical reactions on velocity and temperature fields was only taken into account for integral models of chemical reactions. When considering reaction-kinetic models, the velocity and temperature fields were preliminarily calculated, which determine the convective and diffusion fluxes. After this, the equations for components of substances were solved.

The equations for the components were solved separately from the definition of the velocity and temperature fields with constants at each iteration by turbulent and convective transport factors. The source terms in these equations are determined from the solution by Gear method of a nonlinear system of ordinary differential equations describing changes in the concentrations of the corresponding components.



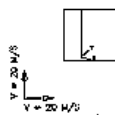
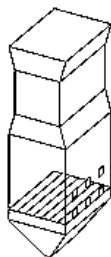
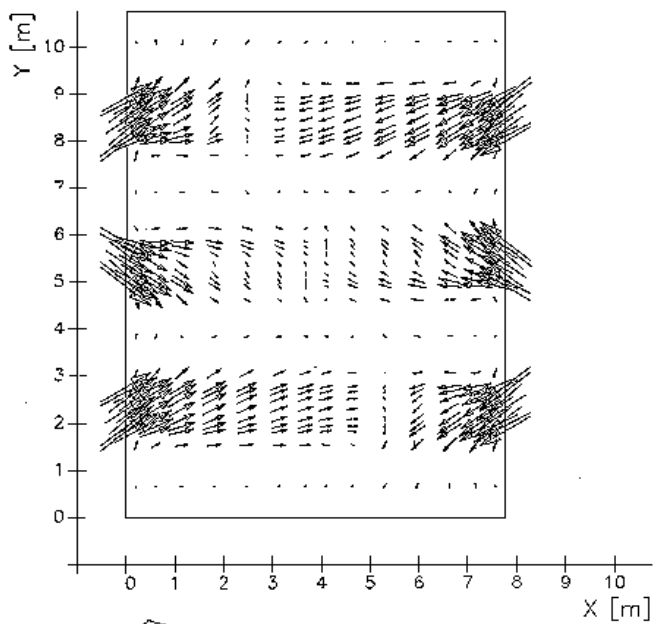
1-u, 2-v, 3-w

Figure 47 - Experimental dimensionless profiles of u, v, w components of the velocity vector at the burner outlet

Below are the results of numerical simulation of the burning process of high-ash Kazakhstan coal from Ekibastuz coal basin in the furnace of PK-39-II steam boiler of the Aksu Electric Power Station.

4.3 Results of numerical experiment

Figure 48 shows full velocity vectors in the transverse and longitudinal sections of the boiler. In the cross section, which falls on the lower stage burners ($H = 6.84$ m), it is shown how the air mixture is fed, and the longitudinal section of the chamber ($y = 1.83$) allows you to see how it flows through the furnace tiers. A rough decomposition of the computational domain, conducted with the aim of saving core memory, leads to the appearance of mild backward current regions.



Schnittebene K=10 (Z=6.84m)

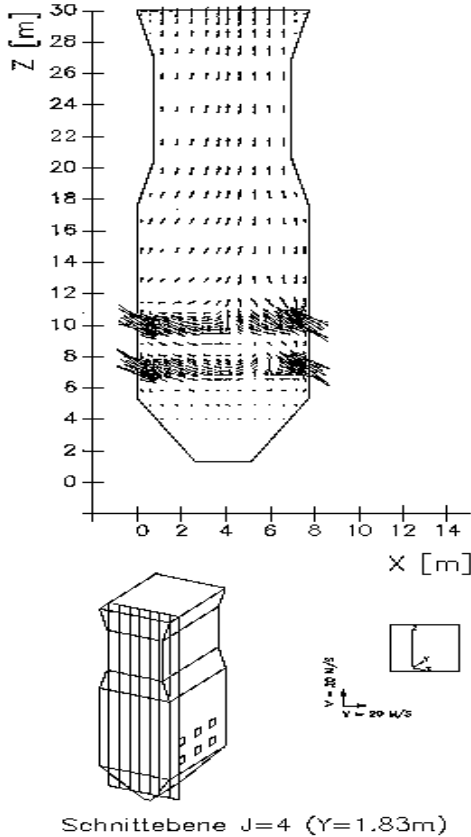
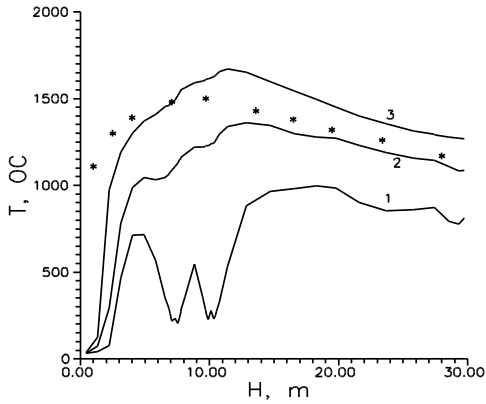


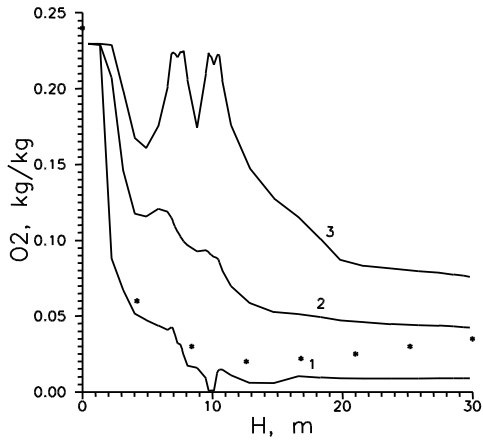
Figure 48 Full velocity vector field

Figure 49 shows distribution of the maximum, minimum and average temperature in the sections (X, Y) along the height of the boiler. Experimental data are also plotted here. The minima on all the curves have to do with the low temperature of the fuel air mixture (150°C) entering this area of combustion space through the burners.



1 - minimum, 2 - average, 3 - maximum values; line - calculation, *- experiment

Figure 49- Temperature distribution throughout combustion chamber height



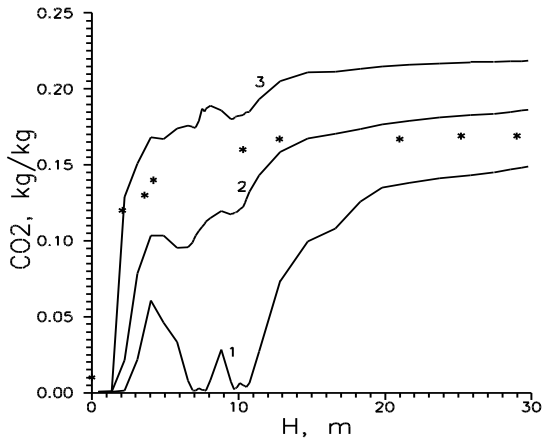
1 - minimum, 2 - average, 3 - maximum value; line - calculation, *- experiment

Figure 50 - Distribution of O₂ concentration along the combustion chamber

Large discrepancies in the calculated and experimental values for the temperature are observed in the region of ignition and damping. Excessive calculated values of the temperature in this region were also obtained in [61, 66-67, 77, 129].

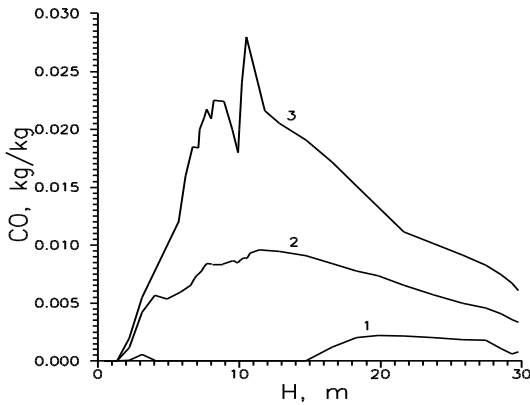
This can apparently be explained by the fact that increased heat release is established due to the assumption of complete combustion of carbon and neglecting the endothermic recovery of carbon dioxide in coke, which leads to an increase in temperature. At the same time, with the increase in temperature, the release of volatiles from coal is accelerated.

The burnout pattern is shown in Fig. 50-55 by curves of changes in the concentrations of oxygen, carbon dioxide CO_2 , carbon monoxide CO , methane CH_4 , coke, ash, H_2O . Analysis of these graphs shows that the main gas generation in the flare occurs in the burners' belt, which is typical for almost all types of combustion chambers. The minimum of CO_2 falls at the maximum of the velocities. It can be seen from Fig. 50 that the greatest discrepancy with experiment is observed in the region of ignition and combustion of volatile substances. One of the main reasons for this is determination of combustion rate of gases using a one-stage pyrolysis model, which uses a number of kinetic constants for the entire temperature range, in contrast to the two-stage pyrolysis model, where these constants have different values in the range of different temperatures.



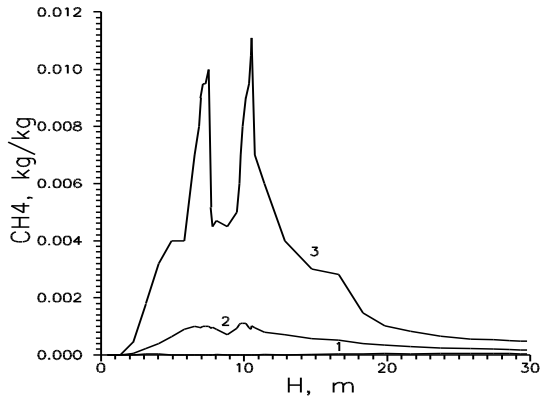
1 - minimum, 2 - average, 3 - maximum values; line - calculation, * - experiment

Figure 50a - Distribution of CO₂ concentration along combustion chamber



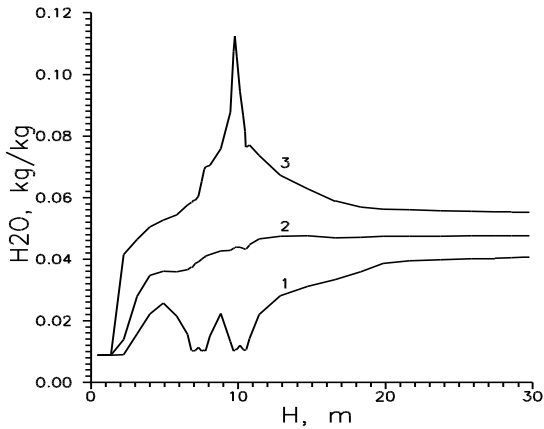
1 - minimum, 2 - average, 3 - maximum value;

Figure 51 - Distribution of CO concentration along combustion chamber



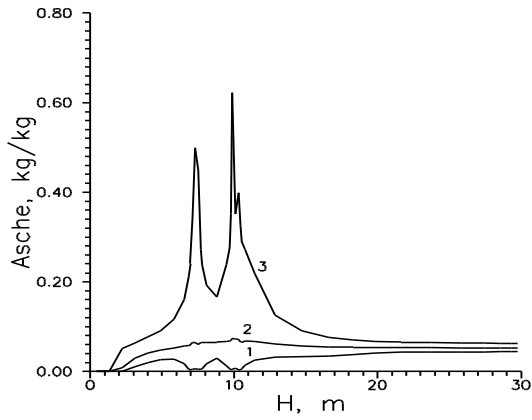
1 - minimum, 2 - average, 3 - maximum value;

Figure 52 - Distribution of CH₄ methane concentration along the combustion chamber



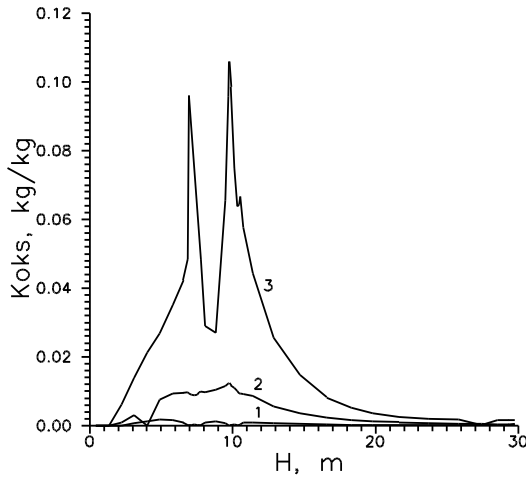
1 - minimum, 2 - average, 3 - maximum value;

Figure 53 - Distribution of H₂O concentration along the combustion chamber



1 - minimum, 2 - average, 3 - maximum value;

Figure 54 - Distribution of ash concentration along combustion chamber



1 - minimum, 2 - average, 3 - maximum value;

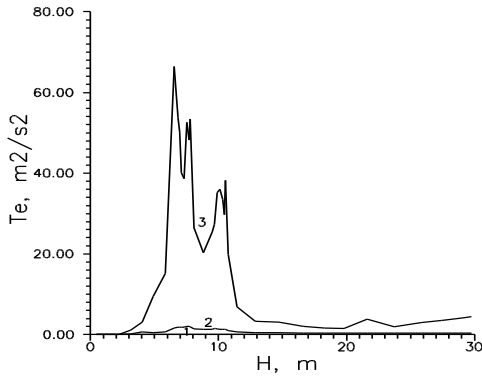
Figure 55 - Distribution of coke concentration along the combustion chamber

Analysis of the graphs in Fig. 50-55 shows that the burning rate decreases at the top of the camera. The distribution pattern of all the concentrations given in this section is modeled fairly well and coincides with those given in the literature. With the exception of the area of ignition and combustion of volatile substances, the discrepancy between the calculated and measured concentrations distribution is quite acceptable. It can be noted that regions with the greatest discrepancy coincide with areas of high concentrations of carbon monoxide (Figure 51). We note that experimental profiles correspond to the boundary condition at the furnace outlet, adopted in the model used in this paper.

The curves in Figs. 56 and 57 illustrate the nature of the change in kinetic energy of turbulence T_e and the energy Q_{chem} , which is released as a result of chemical processes occurring in the furnace. The nature of their changes along the furnace space presented in these figures is quite logical and is associated with the greatest intensity of all processes near the core flame. In the flare, distribution of turbulent velocity pulsations along the axis is complex. Near the nozzles of the burners, sharp intensity maxima of the turbulent velocity pulsations are observed in the distribution (Fig. 56), however, the subsequent removal from the nozzle in the region from the burners is accompanied by an abrupt drop in the intensity of pulsations and attenuation of chemical reactions.

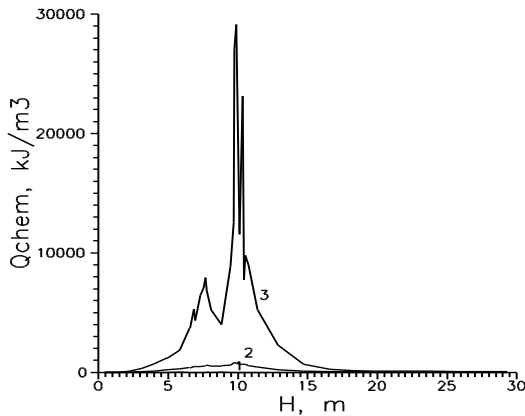
Fig. 58-61 gives distribution curves of quantities characterizing generation of NO_x from nitrogen-containing substances. Thus, Fig. 58 shows distribution of the maximum, minimum, and average values of NO_x concentrations, and Fig. 59 - the change in NH_3 ammonia concentration along the height of the boiler furnace. All these values have a maximum in the burner region. The conclusions of work [189] are confirmed that, the nitrogen of the fuel is released primarily at the initial section of the flare. This indicates the role of nitrogen fuel in the for-

mation of nitrogen oxides. At the output, only "traces" of NH_3 , and the corresponding MPC concentrations of NO_x are observed.



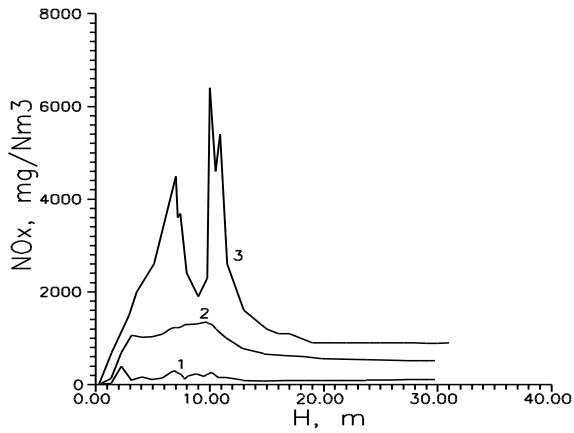
1 - minimum, 2 - average, 3 - maximum value;

Figure 56 - Distribution of kinetic energy turbulence along combustion chamber



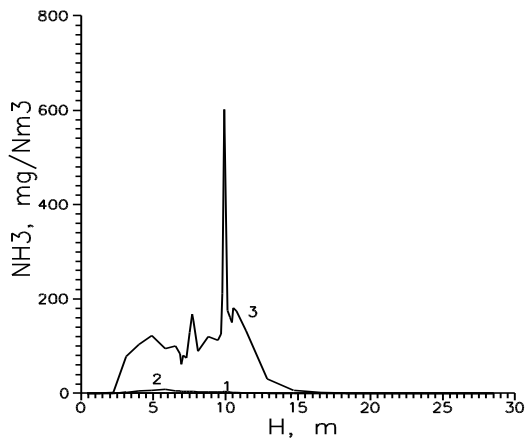
1 - minimum, 2 - average, 3 - maximum value;

Figure 57 - Q_{chem} distribution along combustion chamber



1 - minimum, 2 - average, 3 - maximum value;

Figure 58 - Distribution of NO_x concentration along combustion chamber



1 - minimum, 2 - average, 3 - maximum value;

Figure 59 - Distribution of concentration NH_3 along combustion chamber

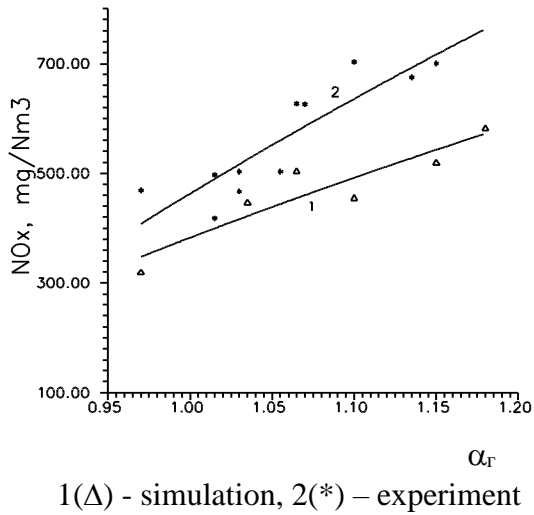


Figure 60 - Dependence of NO_x concentrations at the furnace outlet on the excess air factor in burners α_T

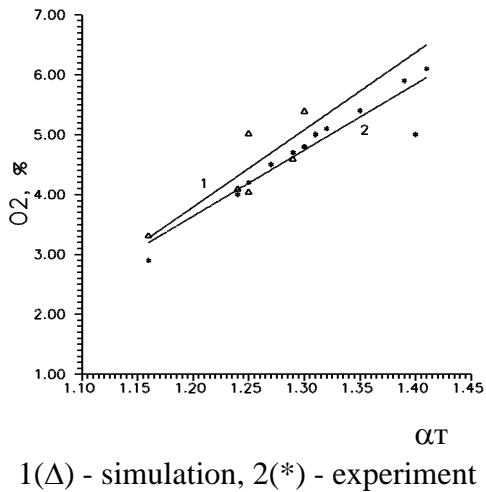


Figure 61 - Dependence of O₂ concentrations at the furnace outlet on the excess air factor in the furnace α_T

The change in the excess air factor significantly affects combustion process in the furnace volume. The level of nitrogen oxides at the furnace outlet basically depends on the excess air factor at the outlet of the operating burner. Figure 60 shows the dependencies of NO_x concentrations at the boiler plant output on the excess air factor in burners α_r , obtained as a result of numerical simulation (line 1 and triangles) and measurements made directly at the power plant (line 2 and asterisks). The level and dependence of NO_x concentration on α_r are of the usual form.

Dependence of oxygen concentration at the outlet from the combustion chamber on the excess air factor in the furnace α_T and comparison with the experimental data obtained at Erma-kovskaya GRES is illustrated in Fig. 61. Analysis of the presented graphs shows that the results of simulation and experiment are in a not-bad compliance, and distribution of nitrogen oxides along the length of the torch and the level of oxide emissions in it are close to industrial conditions.

Typically, in the combustion chambers, a small dilution is maintained to prevent gas puffing into the boiler room. In the following after the furnace flue gas boiler is set a vacuum, exceeding the vacuum in the furnace. Therefore, through leaks in the metal coating and boiler lining, there is a suction of atmospheric air through manholes and inspection holes into flues under negative pressure. Due to the suction cups, the volume of combustion products taking place in gas flues increases. The paper [167] lists the recommended air inflows in proportions of the theoretically required amount of air in the serviceable condition of coating and lining of boilers.

The role of the suction cups is shown in Fig. 62, where histograms of boiler outlet NO_x concentration values for the same values of excess air factor in burners α_r are given, but for different suction values in the furnace $\Delta\alpha$. It can be seen that an

increase in suction cups $\Delta\alpha$ increases the overall excess air in the furnace, and this in turn leads to an increase in the generation of nitrogen oxides.

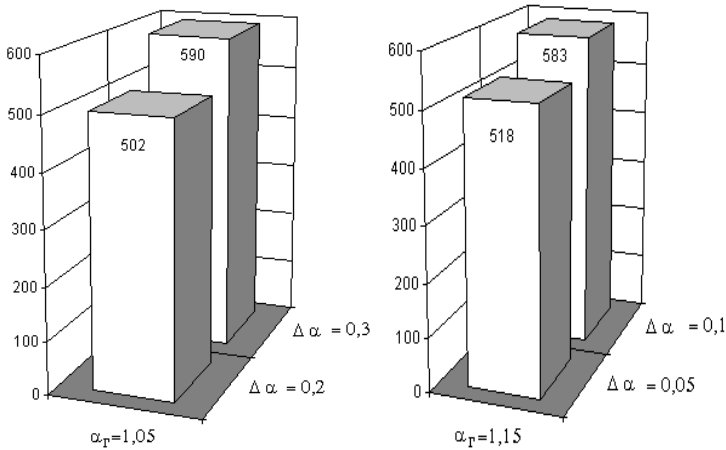


Figure 62 - Values of NO_x concentrations of (mg/mN^3) at combustion chamber outlet for various suction cups $\Delta\alpha$ in the furnace

Comparative analysis (in numbers) of the results of numerical simulation and experimental data for the concentrations NO_x [mg/Nm^3] at the outlet from the boiler plant for different values of the excess air factor in the burners α_T and the dependence of the O_2 concentration [%] on the air excess factor in the furnace α_T is shown in the form of histograms in Fig. 63-67.

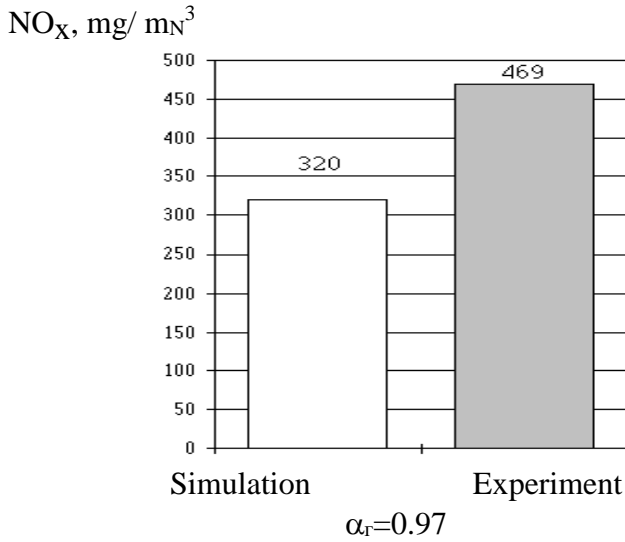


Figure 63 - Comparison of numerical simulation results with experimental data

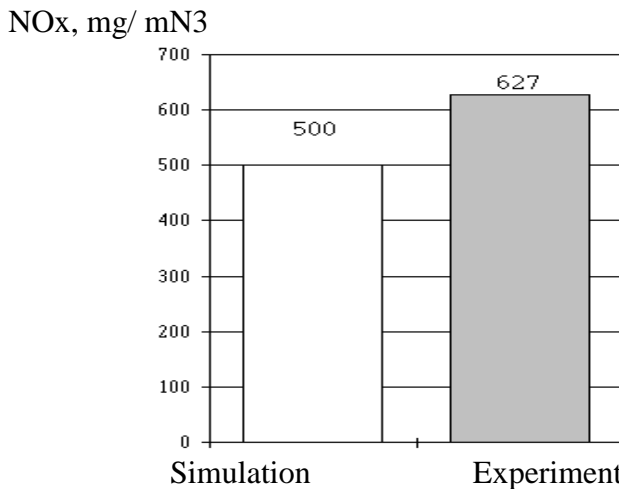


Figure 64 – Comparison of numerical simulation results with experimental data for $\alpha_r=1.06$

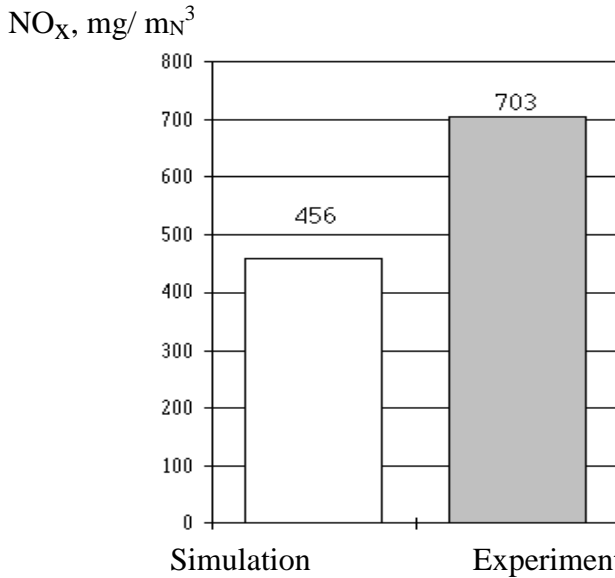


Figure 65 – Comparison of numerical simulation results with experimental data for $\alpha_r=1.1$

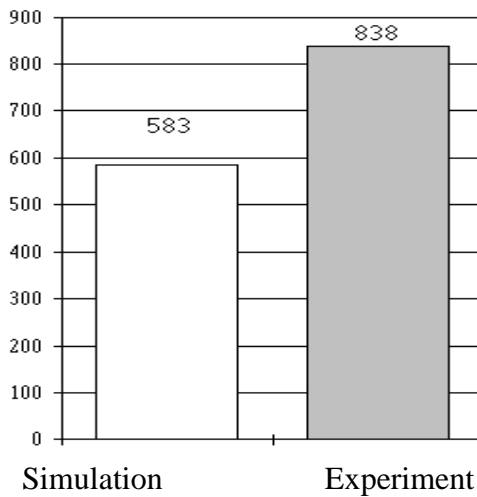


Figure 66 – Comparison of numerical simulation results with experimental data for $\alpha_r=1.18$

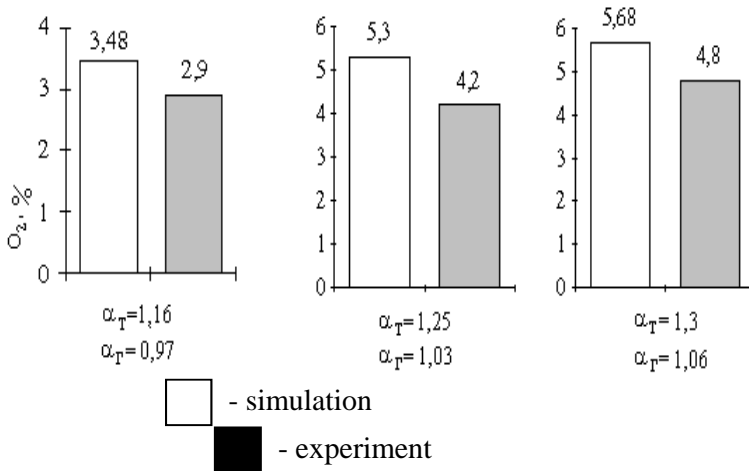
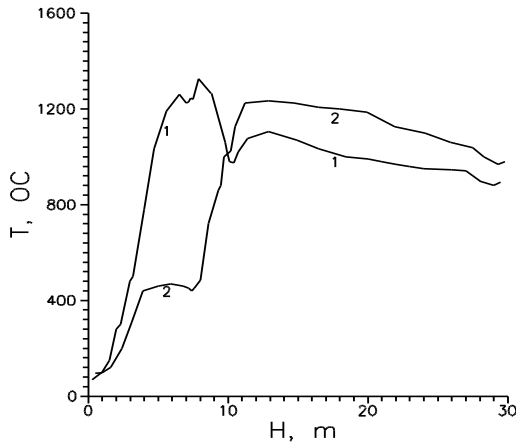


Figure 67 - Calculated and experimental values of O₂ concentrations at combustion chamber outlet

At the existing CHP plants there are sometimes situations of scheduled or emergency stopping of one of the pulverized-coal system, as a result of which some burners must be shut off. This situation has been simulated in the present work for the case of turn off of the upper or bottom tier burners. Figure 68 shows how temperature distribution along the furnace axis changes in case of its operation in "bottom tier mode" (all upper tier burners are off - line 1) and in "upper tier mode" (bottom tier burners are off - line 2).

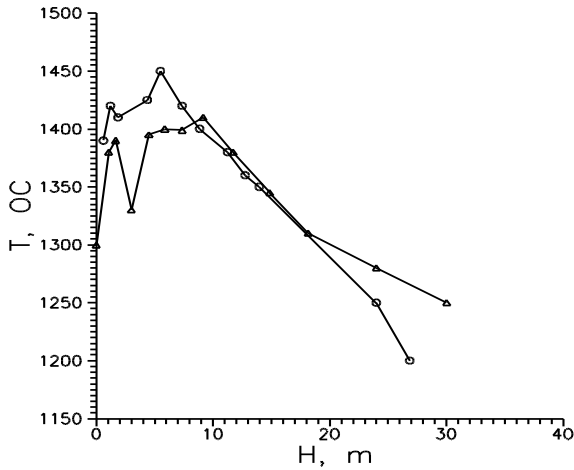


1 - bottom tier mode, 2 - upper tier mode

Figure 68 - Temperature distribution over combustion chamber height (simulation)

The nature of any change in the curves is completely consistent with the description given in [1] for these two furnace operating modes. Quote: "When the load decreases and all lower burners are turned off, the temperature in the lower part of the furnace drops, and the temperature level along the length of the flare somewhat decreases. However, at the furnace outlet, the temperature of the gases, despite the reduced load, remains approximately at the same level. This testifies to the sufficient effectiveness of such a method of maintaining the degree of superheating at reduced loads. This mode "results in delayed ignition and a decrease in the value of the maximum temperature in the core flame". In the case of the bottom tier mode, we have a faster rise in temperature at the initial flare section and earlier decrease in temperature in the core flame.

Since this work [1] describes an experiment on another boiler, we can speak of a good qualitative coincidence of the calculated curves with the experimental ones.



o - bottom tier mode, Δ - upper tier mode

Figure 69 - Temperature distribution over combustion chamber height (experiment [229])

Fig. 69 shows the results of experimental studies [229] of the bottom and upper tiers conducted on the fire model of the PK-39 boiler; however, for other burners and other coal characteristics. However, analyzing the course of the temperature curves in Fig. 68-69 we can note a good qualitative agreement between the calculated and experimental data.

All the experimental data used in this section are taken from works [1, 167, 228-230].

Thus, this section of the paper presented the results of numerical flow simulation and integral combustion reaction for

the PK-39 boiler at Ermakovskaya TPP and compared it with the published experimental data.

It was shown that the selected mathematical model allows to satisfactorily calculate flow parameters and thermo-technical characteristics of devices. Simulation of the generation of harmful substances (CO , NO_x) with the help of the model used in the work and the software package is quite possible. The results of the simulation allow us to conclude that in a furnace with a counter-position of swirl burners with strong flare twist favorable conditions are created that ensure steady ignition of the torch and intense burning of coal dust therein.

The results of the computing experiment allow optimizing the combustion of high-ash pulverized coal fuel in order to reduce emissions of harmful substances (NO_x , CO). All the results in this section are obtained in the framework of the international INTAS-KZ 95 project.

Control Questions:

1. Why are nitrogen oxides recognized to be the most toxic pollutants of the atmosphere?
2. What are the sources of generation of nitrogen oxides during combustion of hydrocarbon fuels?
3. Describe methods for suppressing generation of nitrogen oxides during fuel combustion.
4. What is the combustion chamber of the PK-39 boiler?
5. What is the distribution of carbon monoxide and carbon dioxide concentration in the combustion chamber of the PK-39 boiler?
6. How is the kinetic energy of turbulence distributed in the combustion chamber?
7. How does nitrogen oxides concentration depend on the excess air factor?

8. How does the switching off of the upper or bottom tier burners affect temperature distribution in the combustion chamber?

9. Compare the numerical calculation results with the experimental ones in case of switching off the upper or bottom tier burners. Please explain why there is a discrepancy between the results.

REFERENCES

- 1 Aliyarov B.K. Managing the burning of Ekibastuz coal in thermal power plants. - Almaty: Ghalym, 1996. – p. 272.
- 2 Shiryaev AA Physical aspects of the problem of numerical simulation of flows with combustion. - M.: Science, 1986. – p. 404.
- 3 Ekimtsov A.S., Kulachkova N.A. Numerical simulation of unstable combustion in rocket engines on solid fuel. - Moscow: Science, 1991. 4. 4. p. 144.
- 4 Polezhayev V.I., Bune A.V., Verezub N.A. and others. Mathematical simulation of convective heat and mass transfer on the basis of the Navier-Stokes equations. - Moscow: Science, 1987. – p. 256.
- 5 Oran E., Boris J. Numerical simulation of reactive flows. - M: The World. 1990. – p. 660.
- 6 Polak L.S., Goldenberg M.Ya., Levitsky A.A. Computational methods in chemical kinetics. - M: Science, 1984. – p. 280.
- 7 Lukyanov A.T., Artyukh L.Yu., Itskova P.G. Resonant equilibrium in combustion theory problems. - Alma-Ata: Science, 1989. – p. 180.
- 8 Lukyanov A.T., Artyukh L.Yu., Itskova P.G. Mathematical simulation of the problems of combustion theory. - Alma-Ata: Science, 1981. – p. 117.
- 9 Kompaniets V.Z., Ovsyannikov A.A., Polak L.S. Chemical reactions in turbulent gas and plasma flows. - M., 1979. – p. 124.
- 10 Grishin A.M., Fomin V.M. Conjugate and non-stationary problems in the reacting media mechanics. - Novosibirsk: Science, 1984. – p. 317.
- 11 Grishin A.M. Mathematical simulation of some non-stationary aerothermochemical phenomena. - Tomsk: TNU, 1973. – p. 282.

12 Ilyashenko S.M., Talantov A.V. Theory and calculation of straight-through combustion chambers. - M., 1964. – p. 506.

13 Ustimenko B.P., Dzhakupov K.B., Krol V.O. Numerical simulation of aerodynamics and combustion in combustion and technological devices. - Alma-Ata: Science, 1986. – p. 222.

14 Lilly D.G. Overview of works on combustion in swirling flows. // Rocket technology and astronautics, - 1977. - 15, 8. - p. 12-13.

15 Spalding, D.B. General theory of turbulent combustion. // Rocket technology and astronautics. - 1979. - 17, 8. – p. 185-201.

16 Oszherbi I.T. Review of the literature on the modeling of geometric dimensions and processes in combustion chambers of gas turbine engines. // Rocket technology and astronautics. - 1974. - 12, 6. - p. 9-23.

17 Lilly D.B. Calculation of inert swirling turbulent currents. // Missile technology and astronautics. - 1973, - 11, 7. - p. 75-82.

18 Mellor G.L., Herring H.Zh. Overview of models for closure of equations of the averaged turbulent flow. // Rocket technology and astronautics. - 1973.-1, 5. - p. 17-29.

19 Ustimenko B.P., Dzhakupov K.B., Krol V.O. Numerical study of aerodynamics of a polyhedral annular combustion chamber. // In: Convective heat transfer. - Kiev, 1983. - P. 134-143.

20 Ustimenko B.P., Tkatskaya O.S. Investigation of the regularities of motion and heat transfer in turbulent weakly swirling jets. - // In: Problems of heat power engineering and applied thermophysics. - Alma-Ata. - 1971.-7. - pp. 174-183.

21 Bayev V.K., Golovichev V.I., Yasakov V.A. Two-dimensional turbulent flows of reacting gases. - Novosibirsk: Science, 1976. – p. 264.

22 Ilyashenko S.M., Talantov A.V. Theory and calculation of straight-through combustion chambers. - M., 1964. – p. 506.

23 Lukyanov A.T., Artyukh L.Yu., Itskova P.G. Numerical study of non-stationary homogeneous combustion for various Lewis numbers. Numerical methods of continuum mechanics. - Novosibirsk, 1975. - 6. - C .94-100.

24 Young T.R., Boris J.P. A Numerical Technique for Solving Stiff Ordinary Differential Equations Associated with the Chemical Kinetics of Reactive Flow Problems // J. Phys.Chem. 1977. - 81. - p. 2427.

25 Ñkassia C., Kennedy A. Calculation of two-dimensional chemically reacting flows .- // Rocket technology and astronautics. - 1974. –12, 9. p. 130-136.

26 Kuskova T.V., Chudov L.A. On approximate boundary conditions for a vortex when calculating viscous incompressible fluid flows. // In: Computational methods and programming. M., 1986. - p. 27-31.

27 Patankar S.V. A calculation Procedure for Two-Dimensional Elliptic Situations. //Numer. Heat Transfer. 1981, 4. pp. 409-425.

28 Jakupov K.B. Numerical calculation of gas flows at small Mach numbers in the inlet section and the cooling chamber of combustion module.// Izv. SB AS USSR. -1985. -2, technical series. p. 27-33.

29 Messerle V.E., Sakipov Z.B., Ustimenko A.B. Mathematical simulation of electrothermochemical preparation of energy coals for combustion, taking into account generation of nitrogen oxides. // Mathematical simulation in power engineering.-Kiev.-1990. - 3. p. 137-140.

30 Grishin A.M. Mathematical simulation of some non-stationary aerothermochemical phenomena. - Tomsk: TSU, 1973. – p. 282.

31 Jaugashtin K.E., Yarin A.L. A flat torch of non-variable gases.- // FGV, 1981. - 3. P. 49-56.

32 Babiy V.I., Kuvayev Yu.F. Combustion of pulverized coal and calculation of a pulverized-coal flame.-M.: Energoizdat., 1986.- p. 209.

33 Artyukh L.Yu., Loktionova I.V. Turbulent diffusion flare on a plate surface with injection. // In the collection: Research of transfer processes. Alma-ata, 1986. - p. 23-26.

34 Artyukh L.Yu., Kashkarov V.P., Tyshkanbaeva M.B. Theoretical study of turbulent jets and diffusion flare using semiempirical models of turbulence. - // In: Mathematical simulation and optimal control. Alma-Ata, 1980. p. 39-46.

35 Artyukh L.Yu., Kashkarov V.P., Tyshkanbaeva M.B. Numerical study of combustion of turbulent gas jets. In: Thermal physics of gases and liquids. Alma-Ata, 1980. p. 62-68.

36 Vulis L.A., Yarin L.P. Aerodynamics of the flare. L., 1978. – p. 215.

37 Rotta I.K. Turbulent boundary layer in an incompressible fluid. L., 1967. – p. 233.

38 Glushko G.S. Turbulent boundary layer of an incompressible fluid on a plate. // Izv. AN SSSR. Ser. Mechanics, 1965. - 4. p. 13-23.

39 Lilly D.G. A simple method for calculating velocities and pressures in highly vortical flows. // Rocket technology and astronautics. - 1976. - 14, 6. p. 57-67.

40 Kusunlin M.L., Lockwood F. Calculation of axisymmetric turbulent swirling boundary layers. // Rocket technology and cosmonautics. - 1974. - 12, 4. p. 168-177.

41 Seffen P.G., Wilcox D.C. Model of turbulence for calculating the turbulent boundary layer. // Rocket technology and space exploration, -1974.-12.4.p.160-167.

42 Potankar S., Spolding D. Heat and mass transfer in boundary layers. M., 1971.- p. 215.

43 Artyukh L.Yu., Vulis L.A., Kashkarov V.P. Flow past a plate with gas burning on its surface with gas. // IFJ, -1961. - 4, 3.

44 Artyukh L.Yu., Vulis L.A., Kashkarov V.P. Some problems of the laminar boundary layer during combustion on the surface of a streamlined body. // *Physics of Combustion and Explosion*, - 1969. - 2.

45 Artyukh L.Yu., Vulis L.A., Zakarin E.A., Kashkarov V.P. Thermal mode of heterogeneous combustion in a laminar boundary layer. // *II All-Union Symposium on Combustion and Explosion*, Chernogolovka, 1969. - P. 83.

46 Artyukh L.Yu., Kashkarov V.P., Loktionova I.V. Numerical study of turbulent diffusion combustion on a vertical surface. // *FGV*, 1985, 21B ZU - p. 8-14.

47 Zakarin E.A. Numerical investigation of flows in a laminated boundary layer in the presence of chemical reactions. Author's abstract. Dis. cf.-m. n. Alma-Ata, 1972. – p. 22.

48 Finerman S.I. Numerical investigation of a laminar straight-jet flame. Author's abstract. Dis. Ph.D. Alma-Ata, 1977. – p. 18.

49 Volchkov E.P., Terekhov V.I. Heat and mass transfer in the boundary layer in the presence of chemical reactions. // *Transfer processes in high-temperature and chemically reacting streams*. -Novosibirsk, - 1982. - 2. p. 13-39.

50 Butner. Finite-difference methods for solving boundary-layer equations. // *Rocket technology and astronautics*. - 1970. - 2. p. 3-18.

51 Kramer M.A., Rabitz H., Calo J.M., Kee R.J., Sensitivity Analysis in Chemical Kinetics: Recent Developments and Computational Comparisons. // *Int. J. Chem. Kin.* - 1984. - 16. pp. 559-578.

52 Godunov S.K., Ryabenky V.S. Difference schemes. M., 1973. – p.439.

53 Miller D., Frenklach M. Sensitivity Analysis and Parameter Estimation in Dynamic Modeling of Chemical Kinetics. // *Int. J. Chem. Kin.* - 1983. - 15. pp. 677-697.

54 Roach P. Computational Fluid Dynamics. -M.: World, 1980, - p. 616.

55 Brailovskaya I.Yu., Kuskova T.V., Chudov L.A. Difference methods for solving the Navier-Stokes equations // In: Computational methods and programming. M., 1968. p. 3-8.

56 Oran E.S., Boris J.P. Detailed Modelling of combustion Systems. // Prog. Eneg. Comb. Sci. 1981. - 7. pp. 1-72.

57 75. Numerical methods in fluid mechanics, Ed. M. Belotserkovsky. M., 1972. – p. 304.

58 Jones W.D., Whitelaw J.H. Calculation Methods for Reacting turbulent Flows: A Review. - Combustion and Flame, 1982. - 48, 1. p.1-26.

59 A.Schiller, K.C. Fischer, M.Michel. On the Investigation of Slagging and Fouling of a Lignite Fired Boiler with a Three-Dimensional Computer Code // Proc. 8th Workshop on Two-Phase Flow Prediction. Merseburg, 1996. pp. 26-29.

60 Leithner R., Wang J. Eindimensionales Wirbelschichtmodell. // BWK. - 1990. - 42, 7/8. S. 436-439.

61 Vonderbank R., Schiewer S. Modellierung paralleler Calcinerung und Sulfatierung von CaCO_3 -Partikeln. // Chem. Ing. Nech. - 1993. - 65, 3. S.321-323.

62 Weisweiler W., Stein R. Modellversuche zur trockenen Rauchgasentschwefelung in der Wirbelschicht mit halbcalcinierten Dolomit. //CIT.-1988. -60, 4. S. 314-318.

63 Warnatz J. The Structure of Freely Propagating and Burner Stabilized Flames in the CO_2 - CO - O_2 System. Ber. Bunsensers. // Phys. Chem.- 1979. - 83. S. 950-957.

64 Warnatz J., Bockhorn Y., Möser A., Wentz H.W. Experimental Investigations and Computational Simulation of Acetylene-Oxygen Flames from near Stoichiometric to Sooting Conditions/19th Int. Symposium on Combustion, 1982.S.197-209.

65 Habisreuter P., Schmittel P., Idda P., Eickhoff H., Lenze B. Experimentelle und numerische Untersuchungen an einer

eingeschlossenen Drall-Diffusionsflamme//Verbrennung und Feuerungen. 18 Detscher Flamentag. VDI-Gesellschaft Energietechnik. Düsseldorf,1997,ISBN3-18-091313-4.S.127-132.

66 Fischer K., Schiller A., Leithner R., Müller H., Michel M. Dreidimensionale Simulation der Gas-Feststoff-Strömung in kohlegefeuerten Dampferzeugern. // Verbrennung und Feuerungen. 18 Detscher Flamentag. VDI-Gesellschaft Energietechnik. Düsseldorf, 1997,SBN3-18-091313-4.S.371-377.

67 Müller J. Dreidimensionale Simulation der NO-Kinetik und SO₂-Einbindung bei der Kohleverbrennung in zirkulierenden atmosphärischen Wirbelschichtfeuerungen. Fortschr.-Ber. VDI Reihe 6 Nr.323. Düsseldorf: VDI-Verlag. 1995. - 200 s

68 Holfeld T., Bernstein W., Hildebrand V., Ruttloff G. Experimentelle und numerische Modellierung der Strömungs-,Verbrennungs- und Emissionsvorgänge in Dampferzeugern. //Verbrennung und Feuerungen. 18 Detscher Flamentag. VDI-Gesellschaft Energietechnik. Düsseldorf, 1997, ISBN 3-18-091313-4. - S. 377-383.

69 Lange M., Riedel U., Warnatz J. Direct Numerical Simulation of Turbulent Using Detailed Chemistry. //Verbrennung und Feuerungen. 18 Detscher Flamentag. VDI-Gesellschaft Energietechnik. Düsseldorf, 1997, ISBN 3-18-091313-4. S. 431-436.

70 Deuflhard P., Bader G., Novak U. A Software Package for the Numerical Simulation of Large Systems Arsing in Chemical Reaction Kinetics, in: Modelling of Chemical Reaction Systems, Springer-Verlag, New York, 1981.

71 Karasina E.S., Shrago Z.Kh., Aleksandrova T.S., Torevskaya E.S. Algorithm and program of zonal calculation of heat exchange in furnace chambers of steam boilers. - M.: Heat power engineering. - 1982. - 7. p. 42-44.

72 Sergejev P.V., Slynko L.E., Trusov G.B. A method, a universal algorithm for thermodynamic calculation of multi-component heterogeneous systems. M.: MVTU, 1978. - 268.

73 Sinyarev G.B., Vatolin N.A., Trusov G.K. Use of computers for the thermodynamic calculations of metallurgical processes. - M.: 1982. – p. 363.

74 Karpenko E.N., Messerle V.E., Ustimenko A.B. Mathematical model of the processes of ignition, combustion and gasification of pulverized coal fuel in devices with an electric arc. // Thermophysics and aeromechanics.-195b.-2. p.173-187

75 Messerle V.E., Zhukov M.F., Engelsht V.S., Peregudov V.S., Solonenko O.P. Thermal plasma Technology of Rational cool Combustion with simulations Improvement of Ecological Characteristics. // Proceedings of Japanese Symposium on Plasma Chemistry. -1992. - 5. pp. 283-290.

76 Kachesheva V.A., Kaschiyev M.S., Kochin V.N., Fedoseyev A.I. MULTIMODE Software package for calculating the frequency spectra of axisymmetric and longitudinally homogeneous electromagnetic resonators by the finite element method: Prep. IHEP 82-92. Serpukhov, 1982.- p. 32.

77 Muller H. Numerische Berechnung dreidimensionaler turbulenter Stromungen in Dampferzeugern mit Wärmeübergang und chemischen Reaktionen am Beispiel des SNCR-Verfahrens und der Kohleverbrennung. Fortschr.-Ber. VDI Düsseldorf: VDI-Verlag. 1992. - 6, 268. - 158 s.

78 Blasius H. Grenzschichten in Flüssigkeiten mit kleinen Reibung. // Z. Math. und Phys. - 1908. - 56, 1. s.1-37.

79 Hanna O.T., Myers J.E. Laminar boundary layer flow and heat transfer past a flat plate for a liquid of variable viscosity // A.I. Ch. E. Jornal. - 1961. - 7, 3.

80 Pohehausen E. Zur näherungsweise Integration der Differentialgleichung der laminaren Reibungsschicht. // ZAMM. -1921. - 1. S. 252-268.

81 Vulis L. A., Kashkarov V.P., Lukjanov A.T. Numerical solution of some problem of boundary -layer theory. //Int. J. Heat and Mass Transfer. - 1966. - 9. pp.1095-1102.

82 Kashkarov V.P., Michael B.M. Heat and mass transfer in jets of dropping liquids with variable properties. // In volume Heat and mass-transfer.-M.: Energia.-1968.-1.p.397-401.

83 Lyakhov V.K. Calculation of heat transfer and hydraulic resistance of wall-adjacent one-dimensional turbulent flows under variable thermophysical properties. // Thermal physics of high temperatures, - 1976.-14, 3. P. 553-558.

84 Brandt F Brennstoffe und Verbrennungsrechnung FDBR - Fachbuchreihe Bd. 1, Vulkan Verlag Essen, 1981.

85 Zinser W. Zur Entwicklung mathematischer Flammenmodelle für die Verfeuerung technischer Brennstoffe//Fortschritt-Berichte VDI-Verlag GmbH, Düsseldorf.-1984.-171, 6.

86 Westeuberd A., Fristrom. Methan-Oxygen Flame Structure IV. Chemical kinetic considerations. - // J. Phys. Chem. - 1961. - 4. C. 65.

87 Pesnyakov A.B., Ustimenko B.P. Thermotechnical foundations of cyclone combustion and technological processes. - Alma-Ata, 1974. – p. 373.

88 Smoot L. D. Pulverized Coal Diffusion Flames: A perspective Through Modelling // 18 Symposium (International) on Combustion, The Combustion Institute. - 1981. pp. 1185 – 1202.

89 Bauersfeld G. Weiterentwicklung des Zonenverfahrens zur Berechnung des Strahlungsaustausches in technischen Feuerungen. Dissertation Universität Stuttgart , 1978.

90 Viskanta R. Mengüç M.P. Radiation heat transfer in combustion systems. // Progr. Energy Combustion Science. - 1987. - 13. pp. 97-160.

91 Klose W., Lent M. Berechnung der Wärmestrahlung in athermen Medien mittels einer verallgemeinerten n - Flußmethode. // Wärme - und Stoffübertragung. - 1985. - 19. S. 73 - 84.

92 Smoot L.D., Modeling of Coal-Combustion Processes //Prog. Energy Comb. Sci. - 1987. - 10. pp. 229 - 272.

93 Görner K., Dietz U. Strahlungsaustauschrechnungen mit der Monte - Carlo - Methode , 1990. - 62, 1. S. 23 – 33.

94 Richter W. Anwendungen von Berechnungsmodellen für Feuerräume. // VGB Kraftwerkstechnik. - 1982. - 62, 10. S. 845 - 852.

95 Ström B. A simple heat transfer model for furnaces based on zoning metod. // Wärme - und Stoffübertragung. - 1980. - 13. S. 47 – 52.

96 Sidall R.G., Selcuk N. Two - Flux modelling of two-dimensional radiative transfer in axisymmetrical furnaces. // Journal of the Institute of Fuel. - 1976. pp. 10 – 20.

97 Richter W., Anwendungen von Berechnungsmodellen für Feuerdume // VGB Kraftwerkstechnik. - 1982. - 62, 10. S. 845 – 852.

98 Lowes T.H. Prediction of Radiant Heat Flux Distributions // Heat Transfer in Flames, Scripta Book Comp., Wash. - 1974. S. 179 - 190.

99 Filla M., Maresa. G. A Flux Method Approach to the Radiative Transfer in a Cracking Furnace // Riv. Combust. - 1975. - 7, 8. pp. 321 - 328.

100 De Marco A.G., Lockwood F.C. A New Flux Model for the Calculation of Radiation in Furnaces // La rivista dei combustibili Giornate Italiane delle Filamme. - 1975. pp. 184 – 196.

101 Docherty P., Fairwater M. Prediction of Radiative Transfer from Nonhomogeneous Combustion Products Using the Discrete Transfer Method. // Combustion and Flame - 1988. - 71. pp.79 - 87.

102 Lockwood F.C., Shah N.G. A new radiation solution method for incorporation in general combustion predication procedures // 18 Symposium (International) on Combustion, The Combustion Institute. - 1981. pp.1405 – 1414.

103 Johnson T.R., Beer J. M. The Zone Method Analysis of Radiant Heat Transfer: A model of Luminous Radiation // J. Inst. Fuel. - 1973. pp.301 - 309.

104 Hein K., Lowes T. Beitrag zum Strahlungswärmeübergang in feststoffbeladenen Gasströmen // Brennstoff - Wärme Kraft - 1972. - 24. S. 1 - 6.

105 Patankar S. Numerical methods for solving heat exchange problems and fluid dynamics. - M.: Energoatomizdat, 1984. - p. 150.

106 Patankar S.V., Spalding D.B. A Calculation Procedure for Heat, Mass and Momentum Transfer in Three-Dimensional Parabolic Flows. // Int. J. Heat Mass Transfer, 1972. - 15. pp. 1787-1806.

107 Leithner R. Wärme-und Stoffübertrager Vorlesungsmannuskript. Institut für Wärme-und Brennstofftechnik, TU Braunschweig. - 1989.

108 Rubin S.G., Khosla P.K. Polynomial Interpolation Methods for Viscous Flow Calculations // Journal of Computational Physics. - 1977. - 24. pp.217 - 244.

109 Benim, A.C. Finite Elemente zur Berechnung turbulenter Diffusionsflammen //Fortschritt-Berichte VDI-Verlag GmbH, Düsseldorf. - 1988. - 6, 222. - 167 s.

110 Leschziner M.A. Practical evaluation of three finite difference schemes for the computation of steady-state recirculation flows // Computer Methods in Applied Mechanics and Engineering - 1980. - 23. pp.293 - 312.

111 Raithby G.D., Torrance K.E. Upstream-Weighted Differencing Schemes and their Application to Elliptic Problems involving Fluid Flow // Computers and Fluid Vol. - 1974. - 2. pp.191 - 206.

112 Leonhard B.P. A Stable and accurate convective modeling procedure based on quadratic upstream interpolation // Computer Methods in Applied Mechanics And Engineering - 1979. - 19. pp.59 - 98.

113 Leonhard B.P. Locally modified QUICK scheme for highly convective 2 - D and 3 - D Flows // Proceedings of 5th International Conference on Numerical Methods in Laminar and Turbulent Flow, Monreal. - 1987. pp. 35 - 47.

114 Raithby G.D. Skew Upstream Differencing Schemes For Problems involving Fluid Flow // Computer Methods in Applied Mechanics and Engineering - 1976. - 9. pp.153 - 164.

115 Vulis L.A. Thermal combustion mode - M.: Gosenergoizdat, 1954. – p. 288.

116 Shlanchauskas A.A., Uliskas R.V., Zhukauskas A.A. Turbulent heat transfer of a fin in various liquids flows with variable viscosity // Proceedings of AN Lit. SSR. - 1969. - 11, 59. p. 163-178.

117 Shlanchauskas A.A., Pyadyshyus A.A., Zhukauskas A.A. Universal temperature profiles and turbulent Prandtl number in the boundary layer on the plate in the flow of liquids. // Tr. AN Lit. SSR. - 1969. - 11, 59. – p. 32.

118 Zeldovich Ya.B., Sadovnikov P.Ya., Frank-Kamenetsky D.A. Oxidation of nitrogen during combustion. - M.: USSR Academy of Sciences Publishing House, 1947. – p. 317.

119 Miller J.A., Branch M., Kee R.J. A chemical kinetic Model for the Selective Reduction of Nitric Oxide by Ammonia // Combustion and Flame -1981. -43. pp. 81-98.

120 Silver J.A. The Effect of Sulfur on the Thermal DeNO_x Process // Combustion and Flame. - 1983. - 53. pp.17.

121 Kimball-Linne M.A, Hanson R.K. Combustion Driven Flow Reactor Studies of the Thermal DENO_x reaction Kinetics. // Combustion and Flame. - 1986. - 64. pp.337.

122 Salimian S., Hanson R.K. A kinetic study of NO removal from combustion gas by injection of NH_i containing compounds // Combustion Science and Technology. - 1980. - 23. pp. 225-230.

123 Lyon R.K., Hardy J.E. Discovery and Development of the Thermal DeNO_x Process // Industrial Engineering and Chemical Fundamentals. - 1986. - 25, 1. pp. 19-24.

124 Lyon R. K. Thermal DeNO_x Controlling nitrogen oxides emissions by a noncatalytic process. // Environmental Science Technology. 1987. - 21, 3 - pp.231-236.

125 Lyon R.K. Kinetics and Mechanism of Thermal DeNO_x : //A Review Preprints of papers; Am. // Chem. Soc Division of Fuel Chemistry. - 1987. - 32, 4 - pp. 433-444.

126 Fujii, Nobuyuki; Sato, Hisaaki, Fujimoto, Shiro et al. Determination of the rate Constant for the Reaction $\text{NH}_3 + \text{O} \leftrightarrow \text{NH}_2 + \text{O}$ // Bulletin of The Chemical Society of Japan. - 1984. - 57. pp.277.

127 Seidle J.P., Branch M.C. Hydroxyl Concentration Measurements in the NH_3 -NO-O₂ Reaction in postflame gases // Combustion and Flame, 1983. - 52. p. 47.

128 Vockrodt S "3-Dimensionale Simulation der Kohleverbrennung in zirkulierenden atmosphärischen Wirbelschichtfeuerungen", // VDI-Fortschrittberichte, VDI-Verlag GmbH, Düsseldorf. - 1995. - 6, 334s.

129 Mitchel J.W., Tarbell J.M. A Kinetic Model of Nitric Oxide Formation During Pulverized Coal // Combustion AICHE Journal. -1982. - 28, 2. S. 302-311.

130 VanHeek , K.H., Mühlen H.J. Heterogene Reationen bei der Verbrennung von Kohle // Brennstoff-Wärme Kraft. - 1985.- 37. S.20-28.

131 Reidelbach H., Algermissen J. Berechnung der thermischen Zersetzung von Gasflammkohlen Berechnung der thermischen Zersetzung von Gasflammkohlen Brennstoff // Wärme Kraft. - 1981. - 33, 6. S. 273-281.

132 Anthony D.B., Howard J.B. Coal Devolatilization and Hydrogasification // AICHE Journal. - 1976. -22, 4. pp. 625-656.

133 Anthony D.B., Howard J.B., Sarofim A.F. Rapid Devolatilization of Pulverized Coal //15th Sysmpos. (Int.) on Combustion, 1975. pp. 1303-1317.

134 Kobayashi H., Howard J.B., Sarofim A.F. Coal Devolatilization of High Temperatures // 16th. Symposium on Combustion, 1976. pp.411-426.

135 Lockwood F.C., Salooja A.P. Syed S.A. A Prediction Method for Coal Fired Furnaces // Combustion and Flame. - 1980. - 38. p.1-15.

136 Vasenin I.M., Kozlobrodov A.N., Shrager G.R. Calculation of the flow of a viscous incompressible fluid with a free surface. // Tr. V All-Union Seminar on numerical methods of viscous fluid mechanics. -Novosibirsk, 1975. - P. 58-69.

137 Riley N. Radial jets with swirl. Part I. Incompressible flow. // The Quart. J. Mech and Appl. Math. 1962. - 15, 2. pp. 435-458.

138 Kozlobrodov A.N., Shifanov A.V. Calculation of the unsteady velocity field and the shape of the free surface when a high-viscosity incompressible liquid flows out of the hole to a horizontal plane. // Materials of the 5th Scientific conference on mathematics and mechanics – Tomsk University, - 1975. - 2. p. 94-95.

139 Spalding D.B. Mixing and Chemical Reaction Steady Confined Turbulent Flames //13. Inter. Symposium on Combustion, The Combustion Institute.-1971.pp.649-657.

140 Magnussen B.F., Hjertager B.H. On Mathematical Modelling of Turbulent Combustion with Special Emphasis on Soot Formation and Combustion, 1976.-pp.719-729.

141 Leithner R. Wärmetechnische Anlagen I Vorlesungsmanuskript Institut für Wärme-und Brennstofftechnik, TU Braunschweig. 1988

142 Görner K. Simulation turbulenter Strömungs - und Wärmeübertragungsvorgänge in Großfeuerungsanlagen // Fort-

schrift-Berichte VDI-Verlag GmbH, Düsseldorf - 1987. - 6, 201. - 198 s.

143 Klebanoff P.S., Tidstrom K.D., Sargent L.M. The three-dimensional nature of boundary-layer instability. // J. Fluid Mech. - 1962. - 12, 1. pp. 1-34.

144 Kutateladze S.S. Wall-Adjacent Turbulence. - M.: Science, 1973. - p. 227.

145 Nichols B.D., Hirt C.W. Improved Free Surface Boundary Conditions for Numerical Incompressible-Flow Calculations // Journal of Computational Physics.-1971.-8.pp.434 - 448

146 Launder B.E, G.J. Reece, Rodi W. Progress in the development of a Reynolds-stress turbulence closure // J. Fluid Mech. - 1975. - 68, 3. pp. 537-566.

147 Launder B.E, Spalding D.B. The numerical computation of turbulent flows Comp. Maths. //Appl. Mech. Eng.: - 1974.- 3. pp. 269-289.

148 Monin A.S., Yaglom A.M. Statistical hydromechanics. Mechanics of turbulence. - Moscow: Science, 1965. - p. 639.

149 Zhukauskas A.A. Convective transfer in heat exchangers. - Moscow: Science, 1982. - p. 472.

150 Askarova A.S. Strongly whirled radial liquid jet. // Questions of heat and mass transfer, 1989. P. 82-85.

151 Jischa M. Konvektiver Impuls-, Wärme- und Stoffaustausch. Braunschweig, 1982, - 367 s.

152 Antonopoulos K.A. Heat Transfer in Tube Banks under Conditions of Turbulent Inclined Flow // Int. J.Heat Mass Transfer, Vol. - 1985. - 28, 9. pp.1645 - 1656.

153 Ustimenko B.P., Aliyarov B.K., Abubakirov B.K., Doromin G.A., Nasibova T.I., Tuganbaev K. Burning of various coals in the fire model of the BKZ-320boiler furnace. // Model studies of furnace units. M., 1979.- p. 3-8.

154 Kurmangaliyev M.R., Akhmetov E.S. Research on fire models of the furnace and the influence of operating factors on

the level of emissions of nitrogen oxides. // Model studies of furnace devices. M., 1979. - p. 16-25.

155 Aliyarov B.K., Doroshin G.A., Ustimenko B.K. Influence of the air mixture temperature on the burning of a vortex flame of Ekibastuz coal. // Model studies of furnace arrangements. M., 1979. p. 26-35.

156 Aubakirov E.K., Aliyarov B.K., Aziyev Zh., Nasibova T.I. Study of the effect of fineness of grinding and shutdown of a part of burners on the progress of the combustion process in the fire model. // Model studies of combustion devices. M., 1979. p.36-42.

157 Aliyarov B.K., Doroshin G.A., Investigation of the effect of twisting of flows on aerodynamics and burning of a pulverized-coal flame of a vortex burner. // Pulverized coal fire and burners (operational testing). M., 1983. p.12-18.

158 Vdovenko M.I., Chursina N.Ya., Kogai VS, Mikhalskaya L.O. Thermal technical characteristics of coal in the Orel field of Turgai brown coal basin. // Combustion of energy fuel and furnace processes. M., 1981. p.15-27.

159 Doroshin G.A., Nasibova T.I. Experimental study of the burning of Ekibastuz coal of different grinding fineness. // Combustion of energy fuel and furnace processes. M., 1981.- P. 40-46.

160 Ustimenko B.P., Zmeikov V.N., Serant F.A., Ivanov V.P., Ivanov E.M., Viatchennikov A.M., Tochilkin V.N., Strizhko Yu.V. Investigation of the circular furnace on the large-sized fire model. // Combustion of energy fuel and furnace processes. M., 1981. p. 46-57.

161 Reznyakov A.B., Ustimenko B.P. Modeling of combustion devices of powerful power units. Report No. GR 6844, B447167, KazNI-IE, Alma-Ata, 1975, p. 339.

162 Shagalova S.L., Yuriev L.P., Parparov D.I., Schnitzer I.N. Regulation of aerodynamics in combustion chambers with

tangential arrangement of tilting burners. // Heat power engineering. 1979. - 2.

163 Jaugashtin K.E., Yarin A.L. A flat torch of non-variable gases // Physics of Combustion and Explosion, 1976. - 3. p. 49 - 56.

164 Study of the physical foundations of the working process of furnaces and combustion chambers. // Edited by Doctor of Technical Sciences, Professor Vulis L.A. Publishing House of the Academy of Sciences of the Kazakh SSR., Alma-Ata, 1954. – p. 471.

165 Khzmalyan D.M .Theory of furnace processes. M.: Energo-atomizdat, 1990-p. 352.

166 Ustimenko B.P., Aliyarov B.K., Doroshin G.A., Shishkin A.A. Research and reconstruction of the PK-39 boiler furnace for tangential configuration of the direct-injection burners. Scientific report of the Kazakh Energy Research Institute, Almaty. - 1989. - No. 0187006172. –p. 80.

167 Askarova A.S. , Auelbekova E.V., Baidullayeva G.E. Optimization of combustion processes of radiation-treated solid fuel in a pulverized state // Vestnik KazGU, Ecological Series. - 1997. - 2. p.25-30

168 Askarova A.S. Materials of the symposium "Contemporary problems of environmentally friendly technologies and materials", Almaty. 1996. - P. 23

169 Artyukh L.Yu., Askarova A.S., Loktionova I.V. Approximate analysis of the stability of burning problems as planning of a numerical experiment. // Materials of the international scientific conference "Mathematical simulation in natural sciences", Almaty, 1997. - P. 54.

170 Artyukh L.Yu., Askarova A.S., Loktionova I.V. Computer simulation of diffusion combustion in combustion chambers. // Materials of the symposium "Problems of applied aerodynamics, heat and mass transfer and combustion", Almaty, 1997.-p.38-39.

171 Askarova A.S., Artyukh L.Yu., Loktionova I.V. On stability of combustion in the light of the works of L.A. Vulis. // Materials of the symposium "Problems of applied aerodynamics, heat and mass transfer and combustion", Almaty, 1997. - P. 36-37.

172 Askarova A.S., Auelbekova E.V. Modeling heat and mass transfer processes when burning solid fuel in a boiler plant. // Materials of the symposium "Problems of applied aerodynamics, heat and mass transfer and combustion. Almaty, 1997. p. 44.

173 Askarova A.S., Baidullaeva G.E. Combustion of radiation-treated fuel in the steam boilers furnaces // Materials of symposium "Problems of applied aerodynamics, heat and mass transfer and combustion. Almaty, 1997.-p.45-46.

174 Ivanov A.G., Goncharov L.K. Effect of the design of burners and their configuration on heat loss with combustible loss. // Heat-power engineering, 1963. – p. 10.

175 Aliyarov B.K. Research of combustion chamber models with a rectangular shape. Part II "Fire tests". Report. No. GR 7233, B64269, Kaz-NIIE, Alma-Ata, 1974. – p. 104.

176 Aliyarov B.K., Doroshin G.A. Research of combustion at the power plant of the gross excavation at the operating power stations with the development of recommendations and feasibility studies for the reconstruction of equipment. Section III experiments on the BKZ-420 boiler. Report No. 028800756. KazNIIE, Asma-Ata, 1987. – p. 152.

177 Kurmangaliyev M.R., Naiburger N.V. Participation in the tests of the BKZ-420 boiler. Report 02870033863, Kaz-NIIE. A-A: 1986.- p. 27.

178 Palatnik B.B., Lavrov B.E. Development of recommendations for the use of a modeled memory system for BKZ-420-140 boilers. Report №02900005523. KazNIIE Karaganda. CHP with a purification degree of at least 99%. Publishers Energy and Electric power of the USSR. A-Ata. 1989. – p. 30.

179 Khmyrov V.I. Processing and introduction of technology of staged combustion of fuel with a decrease in yields of nitrogen oxides by 30-40%, for PTVM-100 boilers, BKZ-420, BKZ-160, Report No. 287942. KazNIIIE-A-Ata. 1990. – p. 42.

180 Askarova A.C., Buchmann A. Über Struktur der Flamme von Wirbel-brenneren und Verbrennungsvorgänge der aschenreichen Kohle. //Verbrennung und Feuerungen. 18 Deutsch-Niederländischer Flammentag. VDI-Gesellschaft Energietechnik. Düsseldorf, VDI Verl. ISBN3-18-091313-4. 1997, S. 241-244.

181 Askarova A.S. Auyelbekova E., Baidulaeva G.E. Simulation der Verrennungsvorgänge der aschenreichen Kohle in den Feuerungen eines Dampfkessels. // Inbetriebnahme und Betriebserfahrungen neuer und modernisierter Kraftwerksanlagen-XXIX Kraftwerkstechnisches kolloquium. Dresden, P.18a-b, 1997.-4s.

182 Askarova A.S. Auyelbekova E., Loktionova I. Optimisation of Solid Fuel Combustion for Decreasing Harmful Substances. // International Symposium “Chemistry of Flame Front”, Almaty, Kazakstan, 1997.- P. 88-89.

183 Askarova A.S., Mazhrenova N.R. Ecological problems of the fuel and energy industry in Kazakhstan and unconventional ways to solve them. // Monograph, "Kazakh University" Almaty, 1997.-ISBN 5 7667-7, 1981.- p.202.

184 Artyukh L.Yu., Askarova A.S. On diffusion combustion of a coal particle under conditions of natural convection. // IZv.NAN RK, ser. Physics and mathematics -1994.-2. p.69-74.

185 Leithner R., Lendt B., Müller H. Reduction of N_x emission in coal-fired boilers // Int. Symp. Coal Combustion, Peking, Sept. 1987.

186 Askarova A.S., Auelbekova E.A., Baidullaeva G.E., Loktionova I.V., Leitner R., Fokrodt S., Schiller A. Modeling of heat-mass transfer processes during solid fuel combustion in

boiler units. // Bulletin of KazGU physics series, Almaty; Kazakh University, 1998.-5. p. 73-79.

187 Akhmetov E.S., Kurmangaliyev M.R. Study of reduction of nitrogen oxides emissions in two-stage combustion of coal dust from Ekibastuz coal. // In: Pulverized furnace units and burners. M., 1983.- p.45-51.

188 Kurmangaliyev M.R., Akhmetov E.S. Investigation of the effect of operating factors on the level of nitrogen oxide emissions on fire models of furnace units and burners. // In: Model studies of furnace devices. -M., 1979.- P. 16-25.

189 Ustimenko B.P., Zmeiko V.N., Tkatskaya O.S., Vyatchennikov A.N., Ivanov E.M., Arzyukov S.V., Serant F.A., Tochilkin V.N., Strizhko Yu.V. Study of the generation of nitrogen oxides in the combustion of Ekibastuz coal of different ash content in the fire model of the circular furnace. // In: Pulverized furnace units and burners. M., 1983. - p.24-31.

190 Maximov I.A., Tkatskaya O.S., Kulatov U.T., Zhandozov M.Zh. Suppression of nitrogen oxides during burning of brown coal in a furnace with liquid slag removal. // In: Pulverized coal furnace and burner devices. M., 1983. - p.36-39.

191 Doroshchuk V.E., Rubin V.B. Boiler and turbine units of power units with a capacity of 500 and 800 MW. -M.: Energy, 1979.- p. 680.

192 Ustimenko B.P., Zmeikov V.N. et al. Study of the generation of nitrogen oxides in the combustion of Ekibastuz coal of different ash content in the fire model of a circular furnace. // In: Pulverized coal fire and burners. M., 1983. - p. 24-31.

193 Smart J.P., Weber R. Reduction of NO_x and Optimisation of Burnout With an Aerodynamically AirStaged Burner and an Air-Staged Precombustor Burner. // J. Inst. Energy. 1989. pp.237-345.

194 Freihaut J.D., Proscia W.M., Seery D.J. Fuel Bound Nitrogen Evolution During Coal Devolatilization/Pyrolysis: Simi-

larities and Differences With Coal Rank Characteristics. // 6th Int' Pittsburgh Coal Conf. Pittsburgh. 1989. pp.1184-1193.

195 Leithner R., Lendt B. Messungen über feuerungstechnische Maßnahmen zur NO_x-Minderung an einen Schmelzkammerkessel // 15. DVV-Kolloquium, Clausthal 1986

196 Messerle V.E., Sakipov Z.B., Ustimenko A.B., Kalinenko R.A., Levitsky A.A. Mathematical simulation of combustion of solid fuels taking into account generation of nitrogen-containing compounds, Plasmokhimiya-90 M., INHS ANSSSR 1990, - 1, 5. - p.41-68.

197 Messerle V.E., Ibrayev Sh.Sh. Problem of effective use of low-grade solid fuels with minimal negative impact on the environment // Energy and fuel resources. -1992.-2, 0.3 - p. 21-25.

198 Messerle V.E., Sakipov Z.B., Ustimenko A.B. Modeling of thermochemical interaction of plasma oxidizer. Stream with fine-dispersed coal with account generation sulphur and nitrogen oxides // Proceeding of the International Symposium on Electrical Contacts, Theory and Applications. June 21-25, 1993. ISECTA '93 Almaty, Kazakhstan. 7 s.

199 Nilsson M., Mauss F., Straged Lund/S. Combustion of Nitrogen Doped Fuels. //VDI -Gesellschaft energietechnik Verbrennung und feuerungen 18. Deutsch-niederländischer flammentag. Taugung Delft, 28. und. August 1997.-pp.413-418.

200 Riedel U., Maas U., Warnatz J. Simulation of Nonequilibrium Hypersonic Flows. // Computers and Fluids. - 1993. - 22. pp.285-294.

201 Klaus P., Warnatz J., Heidelberg A. Further Contribution Towards a Complete Mechanism for the Formation of NO in Flames. // VDI -Gesellschaft energietechnik Verbrennung und feuerungen 18. Deutsch-niederländischer flammentag. Taugung Delft, 28. und. August 1997.-pp.425-430.

202 Thevenin D., Behrendt F., Maas U., Przywara B., Warnatz J.: Development of a parallel direct simulation code to investigate reactive flows. // Computers and Fluids. - 1996. - 25, 5. pp. 485-496.

203 Maas U., Warnatz J.: Simulation of chemically reacting flows in two-dimensional geometries // Impact Comput. Science Eng. 1, 1989. pp. 394-420.

204 Rabl H. -P., Gifhorn A, Meyer-Pittroff R. Freising. Vergleichende Untersuchungen an Dreiwegekatalysatoren auf NO₂ -Emissionen. // VDI -Gesellschaft energietechnik Verbrennung und Feuerungen 18. Deutsch-niederländischer Flammentag. Taugung Delft, 28. und. August 1997.-pp.437-442.

205 Hahn, Th.; Lintz, H. -G.: Die Kinetik der Reaktion zwischen Distickstoffoxid und Kohlenmonoxid an polykristallinem Platin, Palladium und Rhodium bei niedrigen Drücken. // Zeitschrift für Physikalische Chemie, Band. - 1994. - 280. s. 195-213.

206 Oser H., Thanner R., Grotheer H. -H., Stuttgart, Richers U., Walter R., Merz A., Karlsruhe. Continuous Process Monitoring by Jet -REMPI First Application in an Experimental Incinerator. // VDI -Gesellschaft energietechnik Verbrennung und Feuerungen 18. Deutsch-niederländischer Flammentag. Taugung Delft, 28. und August 1997.-pp.503-508.

207 Lange M., Dioxin -Emissionsquellen und Emissionsbegrenzung. Übersicht und Ausblick. VDI-Bericht 1298, Düsseldorf 1996.- pp. 161-190.

208 Meyer-Wulf C.. Dioxinmissionen bei der Kupfergewinnung und Maßnahmen zu ihrer Minderung. // VDI -Bericht 1298, Düsseldorf 1996.- pp.319-336.

209 Ritter B., Keller H. -J.. Dioxinminderung bei der Herstellung von Sekundäraluminium. // VDI -Bericht 1298, Düsseldorf 1996.- pp.301-317.

210 Petek J., Univ O., Staudinger G., Graz/A. Thermische Umsetzung eines Eizelpartikels in inerter und reaktiver Umgebung. // VDI -Gesellschaft energietechnik Verbrennung und feuerungen 18. Deutsch-niederländischer flammentag. Tagung Delft, 28. und. August 1997.-pp.591-596.

211 Rummer B., Petek J., Staudinger G.: Trocknung und Pyrolyse eines Einzelpartikels-Modellrechnung und experimentelle Verifikation; VDI Berichte 1314, 1997.- pp.265-279.

212 Scholz, F. Schulenburg, M. Beckmann. Modellierung und Vergleich verschiedener Feuerungsführungen in Rostsystemen. // VDI -Gesellschaft energietechnik Verbrennung und feuerungen 18. Deutsch-niederländischer flammentag. Tagung Delft, 28. und. August 1997.-pp.597-602.

213 Biollaz S., Nussbaumer Th., Onder Ch. Messen des Verweilzeitspektrums in Nachbrennkammern von Holzfeuerungen zur Modellierung der Kohlenmonoxid - Oxidation.//VDI-Gesellschaft energietechnik Verbrennung und feuerungen 18. Deutschniederländischer flammentag. Tagung Delft, 28. und. August 1997.-pp.603-608.

214 Nasserzadeh V., Swihenbank J., Lawrence D., Garrod N., Jones. B.: Nmeasuring gas-residence times in large municipal incinerators, by means of pseudo-random binary signal tracer technique. // Journal of the Institute of Energy, September. - 1995. - 68.-pp.106-120.

215 Zuberbühler U., Baumbach G. Möglichkeiten der Holzreste-und Abfallholzverbrennung in gewerblichen Feuerungsanlagen bis 1 MW_{th} . // VDI -Gesellschaft energietechnik Verbrennung und feuerungen 18. Deutsch-niederländischer flammentag. Tagung Delft, 28. und. August 1997.- pp.609-614.

216 Zuberbühler U., Baumbach G. Emissionsarme Verbrennung von problematischen gewerblichen und industriellen Rest- und Abfallhölzern in Pilotanlagen unter 1 MW Feuerungsleistung, insbesondere in der Bauindustrie.//12 Statuskol-

loquium des PFF am 12. und 13. März 1996 im Forschungszentrum Karlsruhe, FZKA -PEF 142, S.347-356.

217 Nakoryakov V.E., Burdukov A.P., Salamatov V.V. Effective environmentally friendly solid fuel TPPs. - Novosibirsk: Science, Siberian Branch of USSR Academy of Sciences, 1990.

218 Yavorsky I.A. Energy efficiency of plasma-chemical processing of organic solid fuels. // Physical and Technical Journal of the SB RAS. - 1993. - 1. p. 93-97.

219 Yavorsky I.A. Characteristics of the mechanism of generation of sulfur-containing compounds in the combustion of coal and the prospects for the creation of technologies that exclude their release of the surrounding gas environment. // Physical and Technical Journal of the SB RAS. - 1993. - 1. p. 123-131.

220 Messerle V.E., Sakipov Z.B., Ustimenko A.B. Thermochemical preparation of low-grade coals at various excesses of an oxidizer // Chemistry of high energies. - 1990. - 1, 24. p. 80-83.

221 Messerle V.E., Sakipov Z.B., Ustimenko A.B., Kalinenko R.A., Levitsky A.A., Kuznetsov A.P. Mathematical simulation of electrothermochemical preparation of energy coals for combustion with regard to generation of nitrogen oxides. Proceedings of the All-Union Scientific and Technical Conference "Mathematical Simulation in Power Engineering" - Kiev: IPME of the Academy of Sciences of the Ukrainian SSR, 1990. - 3. P. 137-140.

222 Messerle V.E., Sakipov Z.B., Ibrayev Sh.Sh. Electrothermal and chemical preparation of coal for incineration. - Almaty: Ghylym, 1993. - p. 258.

223 Messerle V.E. Integrated electrothermal chemical processing of low-grade solid fuels. // In: Plasma Activation of Coal Burning. -Alma-Ata: KazNIIIE. 1989. p. 106-119.

224 Nakoryakov V.E., Burdukov A.P., Salamatov V.V. Effective environmentally friendly solid fuel TPPs. -Novosibirsk: Science, Siberian Branch of USSR Academy of Sciences, 1990.

225 Yavorsky I.A Energy efficiency of plasma-chemical processing of organic solid fuels. // Physical and Technical Journal of the SB RAS. - 1993. - 1. p. 93-97.

226 Askarova A.S. Auyelbekova E. Convection Heat and Mass Transfer and Combustion of Solid Fuel to Decrease Harmful Discharge. // 4-th Combustion Symposium., Gorukle-Bursa, Turkey, 1995.-pp.89-98.

227 Askarova A.S. Mathematical simulation of optimal combustion modes for solid fuel in order to increase the efficiency of power plants and reduce emissions of harmful substances. // Heat and mass transfer MMF-96 Minsk, 1996.- XI. p.p. 72-76.

228 Spalding D. Burning and mass exchange. -M.: Mechanical Engineering, 1985. – p. 240.

229 Aliyarov B.K., Ustimenko B.P., Buchman M.A. // Report 01910010550. KazNIIIE. Development and introduction of vortex three-channel burners on P-39-2 boilers of Ermakovskaya GRES. Alma-Ata. 1991. – p. 59.

230 Aliyarov B.K., Ustimenko B.P., Dedovets V.A. // Report 76074275. KazNIIIE. Investigation of the operation of the boiler furnace PK-39-II EGRES on the fire model. Alma-Ata. 1979. – p.127.

231 Aliyarov B.K., Abubakirov E., Ustimenko B.P., // Report 76073843. KazNIIIE. Investigation of the interaction of burners with their various layouts on a semi-industrial fire model of a combustion chamber during combustion of Kansk-Achinsk and Ekibastuz coals. Alma-Ata. 1979 .- p. 67.